NTNU – Trondheim
Norwegian University of
Science and Technology

Evaluation of Shale Formations as Barrier Element for Permanent Plug and Abandonment of Wells

Kristian Moum Skjerve

Petroleum Geoscience and Engineering
Submission date: June 2013
Supervisor: Sigbjørn Sangesland, IPT

Norwegian University of Science and Technology
Department of Petroleum Engineering and Applied Geophysics

NTNU
Norges teknisk-naturvitenskapelige universitet **Fakultet for ingeniørvitenskap og teknologi**
Faculty of Engineering and Technology
Studieprogram i Petroleumsfag
Study Programme in Petroleum Geosciences and Engineering

Institutt for petroleumsteknologi og anvendt geofysikk
Department of Petroleum Engineering and Applied Geophysics

HOVEDOPPGAVE/DIPLOMA THESIS/MASTER OF SCIENCE THESIS

Kandidatens navn/The candidate's name:	Kristian Moum Skjerve
Oppgavens tittel, norsk/Title of Thesis, Norwegian:	Evaluering av skiferformasjoner som barriere element for permanent plugging og forlating av brønner
Oppgavens tittel, engelsk/Title of Thesis, English	Evaluation of Shale Formations as Barrier Element for Permanent Plug and Abandonment of Wells

Utfyllende tekst/Extended text:

Background:

Many of the large producing fields on the Norwegian Continental Shelf are approaching the end of their lifetime. As a consequence a large number of permanent plug and abandonment (PP&A) operations will take place. The requirements for a permanent barrier state that the barrier must cover the entire cross-section of the wellbore, including all annuli. This thesis evaluates the potential of using shale formations alone or in combination with other sealing materials to provide the required annular barrier.

Tasks:

1) Discuss existing regulations regarding PP&A, how a PP&A operation can be performed and challenges that may arise during a PP&A job.
2) Discuss conventional, new and future technologies, materials and procedures to solve challenges related to lack of annular seal.
3) Perform laboratory tests to evaluate the potential of settled barite as the annular seal.
4) Compare the use of formation as a barrier vs. alternative solutions for providing the required annular seal.

Supervisor	*Sigbjørn Sangesland*
Co-supervisor	
Studieretning/Area of specialization:	*Petroleum Engineering, Drilling Technology*
Fagområde/Combination of subject:	*Drilling*
Tidsrom/Time interval:	*January 14 – June 10, 2013*

……

Sigbjørn Sangesland

Acknowledgement

This report is made in accordance with my master thesis during the 10th semester of a five-year master's degree program in Petroleum Engineering at the Norwegian University of Science and Technology (NTNU) in Trondheim.

First of all I would like to thank my supervisor professor Sigbjørn Sangesland for guidance and support throughout the work conducted on this thesis. I'm also grateful towards Rune Martin Holt and Pål Skalle at NTNU for sharing their knowledge as well as providing me with valuable papers related to the topic.

A special thanks goes to SINTEF Petroleum Research in Trondheim, for providing me with access to their formation mechanics laboratory. Also, I would like to thank PhD student Mohammed Bhuiyan and Samir Rashid for helping me with my experiments conducted at SINTEF. Without their valuable contributions the experiments would not have been possible.

Finally, I would like to thank MI Swaco for providing me with micro-barite on short notice.

Trondheim
June 2013

Kristian Skjerve

Summary

In a similar fashion to the commonly used saying "that the only thing certain in life is death", the only thing certain for petroleum wells is that sooner or later the wells will have to be permanently plugged and abandoned. Permanent plug and abandonment (PP&A) is ideally performed by setting a number of cement plugs inside the casing strings. This technique is however only allowed if the casing strings are supported on the outside by a sealing material with sufficient quality over a required interval. When planning PP&A operations several operators have discovered that the annular seal, traditionally provided by annular cement, does not fulfil the abandonment requirements. The operators are thus left with a shortage of annular barriers and costly remedial cementing, milling or cut and pull of casing has to be performed in order to plug and abandon the well.

Traditionally, PP&A has been seen as sunk cost with little possible economic upside. However, today as many of the large producing fields on the Norwegian Continental Shelf (NCS) are simultaneously approaching the end of their lifetime, a large wave of PP&A jobs is imminent. As a consequence of the increased relevance, to improve the efficiency and reduce the cost of the operation several new methods, materials and procedures related to all parts of the PP&A operation have been developed.

One of these newly developed methods is to use inward moving shale formations as the annular sealing material in cases where the casing cement has failed. Up to now the presence of such barriers has been quite sporadic and their usefulness merely limited to some locations. This thesis has evaluated the potential of these barriers alone or in combination with other sealing materials to create the desired annular seal on a larger scale.

The main conclusion is that most shales at least have the potential to seal off parts of the annular gap between the formation and casing within the time frame of PP&A. Whether or not the full gap is closed is dependent on the shales flexibility and creep rates. In general Smectite rich shales found between 2000-3000meters appears to be the most suitable for becoming annular barriers. Useful indicators of a shales creep potential are clay content and stiffness. The two most efficient ways in increasing the chance for shales providing an annular barrier is exposing the formation to cations with small hydrated diameter or reducing the annular gap. The latter could be obtained through increasing the casing size or through an annular fill material. Laboratory test shows that compressed barite in combination with only water does not constitute a good sealing material. Thus, unless some additives are added, settled barite could not make up the above-mentioned fill material. Compressed micro-barite on the other hand appears to form a practically impermeable seal and the material could therefore in combination with inward moving formations make up the required annular barrier element. However, the material has challenges when it comes to placement. Further work should therefore be focused on how this could be performed or alternatively on identifying other more ideal fill materials. Barite in combination with oil-water emulsions, diesel or barite mixed with small, soft and non-degradable particles may provide good solutions.

Sammendrag

På samme måte som det ofte brukte ordtaket ” det eneste som er sikkert med livet er døden”, er det eneste som er sikkert for en petroleums-brønn at før eller siden vil brønnen bli permanent plugget og forlatt. Permanent plugging for forlating blir ideelt sett utført ved å sette en serie med sement plugger inne i et par av fôringsrørene i borehullet. Denne metoden er imidlertid bare tillatt i tilfeller hvor fôringsrørene har støtte på utsiden av et tetningsmateriale med tilstrekkelig kvalitet over en påbudt minimums lengde. Under planleggingen av permanente plugging og forlatings-operasjoner, har flere operatører oppdaget at tetningsmaterialet i ringrommet, tradisjonelt sement, ikke tilfredsstiller kravene for forlating. Operatørene har da en mangel på ringroms-barrierer og kostbare helbredende tiltak som re-sementering, seksjons-milling eller kutt og løft av fôringsrør må utføres før man kan plugge og forlate brønnen.

Tradisjonelt har plugging og forlating av brønner blitt sett på som en kostnad med liten økonomisk oppside, men i dag på grunn av at levetiden på mange av de store produserende feltene på norsk kontinental-sokkel nærmer seg slutten, har området fått økt fokus. Som en konsekvens av den økte relevansen, for å øke effektiviteten og redusere kostnadene, har flere nye metoder, materialer og prosedyrer relatert til alle delene av en forlatings-operasjon blitt utviklet.

En av de nylig utviklede metodene er å bruke innsigende skiferformasjoner som ringroms barriere i tilfeller hvor fôringsrør-sementen har sviktet. Hittil har tilstedeværelsen av slike barrierer vært ganske sporadisk, og deres nytte har vært begrenset til noen brønner. Denne masteroppgaven har evaluert potensialet for slike barrierer alene eller i kombinasjon med andre tetningsmaterialer for å danne ringroms barrierer i en større skala.

Hovedkonklusjonen er at de fleste skifertyper har potensial til å dekke i alle fall deler av ringrommet mellom formasjon og fôringsrør innen tidsperspektivet for forlating. Om hele eller bare deler av ringrommet avstenges, er avhengig av skiferens fleksibilitet og kryp-rater. Generelt virker smektitt-rike skifrer funnet mellom 2000 og 3000 meter å være de best egnede for å forme den ønskede barrieren. Nyttige indikatorer på en skifers kryp-potensiale, er leirinnhold og stivhet. De to mest effektive måtene å øke sjansen for dannelsen av skiferbarrierer, er å eksponere skiferen for kationer med liten hydrert diameter eller redusere den effektive størrelsen på ringrommet. Sistnevnte kan oppnås ved å øke foringsrørstørrelsen eller gjennom et ringroms fyllmateriale. Laboratorietester viser at komprimert barytt i kombinasjon med bare vann ikke er et godt tetningsmateriale. Derfor, med mindre noen tilsetningsstoffer er involvert, kan ikke utfelt barytt utgjøre det nevnte fyllmaterialet. Komprimert mikro-barytt derimot, ser ut til å være praktisk talt impermeabelt og materialet kan derfor i kombinasjon med innover-bevegende skiferformasjoner utgjøre den påkrevede ringroms-barrieren. Et problem med materialet er imidlertid å få ønsket plassering i ringrommet da det ikke feller ut som vanlig barytt. Videre arbeid bør derfor fokusere på hvordan nevnte plassering kan oppnås eller alternativt på å identifisere andre mer ideale fyllmaterialer. Barytt i kombinasjon med olje/vann-emulsjoner, diesel eller barytt mikset med små, myke og ikke nedbrytbare partikler, kan være potensielle løsninger.

Table of Content

List of Figures

List of tables

1. Introduction

1.1 Background

Since the Norwegian oil adventure started with the Ekofisk field in 1969, many fields have been discovered and numerous wells has been drilled. Today there are 70 fields in production on the Norwegian Continental Shelf (NCS), but on many of these the production is declining (1). As a consequence in the near future many wells will either have to be permanently plugged and abandoned for slot recovery or decommissioning purposes.

Traditionally permanent plug and abandonment (PP&A) is done by setting a number of cement plugs inside the casing strings, however this is only adequate if the quality of the sealing material behind the casing is of sufficient quality. When planning PP&A operations the diagnostic logs often reveal that the annular seal, traditionally provided by the casing cement, does not fulfil the requirements. The operators are thus left with a shortage of annular barriers and costly remedial cementing, milling or cut and pull of casing has to be performed in order to plug and abandon the well in a satisfactory manner.

With the currently used technology the above-mentioned operations are quite time consuming and expensive, but due to the so far relatively low number of jobs PP&A has traditionally been seen as sunk cost with little possible upside. As a consequence little effort have been made to improve the procedures. However, today as many of the major oil producing fields on the NCS is almost simultaneously approaching the end of their lives, and decommissioning is likely to happen in a not too distant future, the area is receiving more and more attention.

According to OLF approximately 2000 wells will have to be abandoned on the NCS alone between 2012 and 2040 (2). As a consequence of the increased relevance, as well as an enhanced awareness of the cost saving potential related to PP&A, the operating companies on the NCS established a P&A forum in 2009. The purpose of this forum is to "develop robust and cost efficient solutions to the current & upcoming P&A challenges on the NCS" (2). As a direct result of the increased focus new methods and procedures with the goal of achieving safe and secure abandonment at lower cost, using less time and yielding better total results are constantly being developed.

The new methods are related to all parts of the PP&A operation and among other new cutting technology, techniques to increase the applicability of light weight intervention (LWI) vessels, alternatives to section milling, new sealing materials and techniques for verifying displaced formations as annular barrier elements has been developed.

1.2 Approach

This master thesis will discuss and evaluate the newly developed methods with respect to creating an annular seal. To get a better understanding of the problem a rapid description of the whole PP&A procedure and some common problems and solutions will also be briefly discussed. As much of the new technology has already been thoroughly described in recent master's theses, e.g. (3), (4), (5),(6), the focus here will be on the possibility of using the formation as barrier element. Since this is a fairly new topic, relatively little research is done on subject. As a consequence a quite thorough description of the theory behind will be presented.

Formation as a barrier element is based on the fact that when drilling through certain extremely low permeable formations, such as shale and salt, the rock will sometimes move inward and begin to close of the well. During drilling this phenomena is undesirable, but after the casing is set, such behaviour is ideal and can provide a much needed and economically very beneficial barrier. Compared to other sealing materials using the formation as an annular barrier stands out since it provides a natural and free barrier. Moreover, as shale and salt formations act as cap rocks for many reservoirs, they have proven their sealing ability over millions of years and are thus likely to be unbeatable with respect to long-term integrity. However, for instance shale movement is in addition to being poorly understood, often also a slow and uncertain process. The presence of formation barriers is therefore quite sporadic and their usefulness merely limited to sometimes offering the operator with a contingency plan is cases where the casing cement fails.

This thesis aims to give a better understanding of the mechanisms thought to be responsible for formation displacement. To figure out in what kind of formations and on what time-scale the creation of such barriers are likely. Moreover, it will look at ways to speed up or at least increase the chance of the formation sealing of the annulus outside the casing, hence possibly increasing its application area to more than only a contingency plan for PP&A. Furthermore, it will look into the possibility of combining formations with other sealing materials to provide the required barrier and describe the procedure for qualification of formations as barrier element. The main focus will be on shale/clay barriers, but much of the theory presented could also be applied on for instance salt formations.

2. Introduction to permanent plug and abandonment

After the lifetime of a well is over as a last operation the well has to be plugged for permanent abandonment. The purpose of all PP&A operations is to re-establish the barriers broken during drilling so that the well can no longer be used as a flow path for fluids. This chapter will give a brief introduction into the governing regulations for PP&A on the NCS. Furthermore, it will describe how a PP&A operation is conventionally performed and discuss some typical problems that may arise and make the operation more complex, such as lack of annular seal. The main part of this thesis is devoted to an alternative solution to solving the latter. To demonstrate the usefulness of this alternative solution, some traditional as well as some newly developed techniques and materials to solve the problem, their strengths and weaknesses, will also be presented here.

2.1 PP&A regulations

As with all other drilling and intervention work the requirements for permanent plug and abandonment (PP&A) on the NCS is governed by the regulations issued by the Petroleum Safety Authority Norway (PSA). Although international standards such as ISO and EN form the basis of all petroleum related activities, the Norwegian safety framework and climate conditions require amendments. Until the new and revised version, expected released in august 2013 come into force, the prevailing regulations regarding PP&A can be found in the NORSOK standard D-010, rev 3 from 2004 (7). To encourage innovation the standard only contains minimum requirements and alternative standards and solutions can be used as long as they can be proven equally good or better.

The NORSOK standard D-010 describes requirements for well barriers during all stages of drilling and well operations and chapter 9 of the document is devoted to requirements for permanent well barriers during sidetracks, suspension and abandonment operations. This section gives a brief introduction into the most important rules and regulations regarding PP&A as described by the standard. As mentioned the standard is planned replaced by a new one in a not too distant future. The author has obtained a draft of this new standard, and where the two standard show discrepancy this will be mentioned. It must be emphasized that since it is only a draft it cannot yet be considered a steering document, but as it does show possible future changes it is still of interest. For further insight and a more detailed description of the topic the reader is recommended to read the prevailing document itself.

2.1.1 General Principle

According to the NORSOK-D010 the definition of permanent abandonment is: “well, status where the well or part of the well, will be plugged and abandoned permanently, and with the intention of never being used or re-entered again”(8). Thus, the well shall be abandoned with an eternal perspective and the barriers shall be designed to withstand the load/environmental conditions it may be exposed to.

Generally during all operations on a well it is required that the well always has two verified well barriers when drilling through a potential source of inflow. A well barrier is defined by NORSOK as " an envelope of one or several dependent WBE's (Well Barrier Elements) preventing fluids or gases from flowing unintentionally from a formation into another formation or to surface"(8) .
Since permanently plugged wells have to be abandoned with an eternal perspective the usual two well barrier approach does no longer suffice. In addition to the two, often referred to as primary and secondary barriers, an open hole to surface well barrier and well barriers between reservoir zones of different pressure regimes is required. The purpose of the latter is to prevent crossflow between the zones, while the purpose of the open hole to surface barrier is to isolate the hole from the surface after the casing has been cut and to act as a final barrier against flow. The functions of a well barrier can be combined if it fulfils more than one objective, with the exemption that a secondary well barrier can never be a primary well barrier for the same reservoir. Thus, for instance the primary barrier for a shallow reservoir can be used as a secondary barrier for a deeper reservoir if they are within the same pressure regime. An illustration of the PP&A requirements for a well drilled through two-reservoirs with different pressure regime can be found in figure 2.1. As seen the open hole to surface barrier is only required in cases where the intermediate casing string is not cemented into the surface casing.

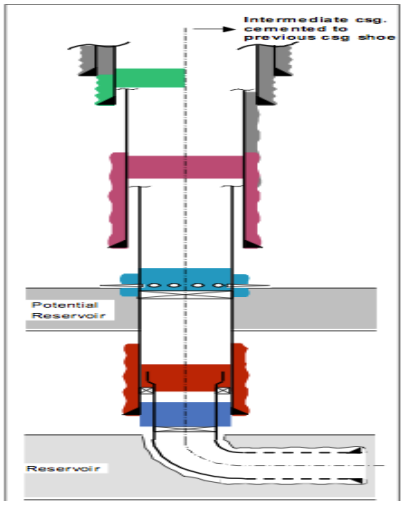

Figure 2.1 Permanent abandonment requirement for a well drilled through two different pressure regime reservoirs, with and without the intermediate casing being cemented into the surface casing. After (8).

As a general rule the installed barriers shall be located as close to the potential source of inflow as possible and cover all possible leak paths. Moreover, they shall be placed adjacent to an impermeable formation and "extend across the full cross section of the well, include all annuli and seal both vertically and horizontally"(8). Thus, for a casing plug to provide a permanent barrier, it has to be set in areas with verified sealing in the annulus as illustrated in figure 2.2. Furthermore, according to the current NORSOK standard a well barrier shall be placed at a depth where the formation fracture pressure

is larger than the worst anticipated pressure it may be exposed to. It shall have a minimum length of 100m MD and extend a minimum distance of 50m MD above any source of inflow/leakage point, unless the plug is set inside a casing with a mechanical plug as foundation, then the minimum length is 50m MD (8).

The worst anticipated pressure is dependent on type of well. In production wells it is typically found by subtracting the hydrostatic pressure to the barrier depth from the initial reservoir pressure, while in injection wells the reservoir pressure is exchanged with the maximum injection pressure. Contrary to the worst anticipated pressure, the fracture pressure is a more loosely defined term. When drilling, to avoid fracturing the formation, the critical upper mud weight pressure is typically defined as the minimum formation stress (σ_h) plus an empirical factor ΔP_{exp}. Where the empirical factor is found through operational experience and margins (9). According to the regulations this pressure could be used as the fracture pressure. However, many operators, such as for instance Statoil, choose to be more conservative. According to their company standard, APOS, the fracture pressure is defined as the minimum formation stress, which can be found through extended leak off tests. This is in accordance with the new standard which states that for new wells drilled after 01.06.2013 the minimum formation stress shall exceed the maximum expected wellbore pressure, while for existing wells drilled before 01.06.2013 the old regulations suffice (10). Another discrepancy between the new and old standard is the requirements for annular barrier elements. In the new standard if the casing cement is verified through logging a minimum of 30m cumulative interval, where the minimum accepted bonding interval is 3m, is required for the barrier to act a permanent WBE (10). If the barrier is not verified, 50m of cross-section seal, as in the current standard is required.

After a well barrier element is placed, its location, strength and quality shall be verified. This can be done through various combinations of the following procedures: logging, tagging, job assessments and pressure tests (either inflow or leak test).

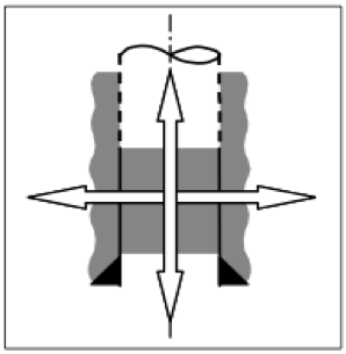

Figure 2.2 Requirements for a permanent barrier. It has to extend across the full cross section of the well, include all annuli and seal both vertically and horizontally. After (8).

2.1.2 Material requirements

Since the permanently plugged wells shall be abandoned with an eternal perspective there are several requirements for the materials used in permanent well barriers.

According to NORSOK D-010 a material used in a permanent well barrier should have the following properties (8):

a) Impermeable
b) Long term integrity
c) Non Shrinking
d) Ductile-(non Brittle)- able to withstand mechanical loads/impact
e) Resistance to different chemicals/substances (H_2S, CO_2 and hydrocarbons).
f) Wetting, to ensure bonding to steel

An additional requirement of the material not being harmful to the steel tubulars integrity is added in the draft for the new standard (10).

The only material explicitly mentioned as accepted for PP&A in the prevailing version is cement. However, the new draft through the statement "the suitability of the selected plugging materials shall be verified and documented" make it clear that all materials that meet the above mentioned requirements can be used as barrier elements. Although, only cement is mentioned in the current standard, due to the fact that the standard only contains minimum requirements, the operators are still free to choose other materials as long as the selected material can be proven equal or better than cement.

Even though the present standard is vague when describing accepted materials it does however mention some materials that are never accepted as part of a permanent well barrier. For instance, mechanical and elastomeric sealing elements are never allowed used alone as part of a well barrier as they can degrade over time. Moreover, steel tubulars are only accepted as permanent WBE's when they are supported by cement or other accepted sealing materials. As a consequence of these requirements, bridge plugs frequently used for temporary abandonment cannot be used alone for PP&A. They can however be used as a solid foundation for placement of plugs of other sealing materials such as for instance cement.

2.1.3 Removal of equipment above seabed

In general after an offshore well has been permanently plugged and abandoned there shall be no traces of the well ever existing. To obtain this "the wellhead and the following casings shall be removed so that no part of the well will ever protrude the seabed" (8).Required cutting depth below seabed should be considered in each case, and be based on prevailing local conditions such as soil, seabed scouring, sea current erosion, etc. The cutting depth should be 5m below seabed. No other obstructions related to drilling and well activities shall be left behind on the seafloor" (8).

Removal of platforms and other fixed equipment on the NCS is called decommissioning and is governed by the OSPAR commission decision 98/3. It states that everything in principle shall be removed, but extremely large structures such as gravity based concrete installations, steel structures weighing more than 10 000 tonnes in air and

floating concrete can be subject to an issue of permit to be left partly or wholly in place (11). However, going more into detail on this topic is out of the scope of this thesis, which is mainly focused on annular barriers, thus the interested readers are therefore encouraged to read the document themselves.

2.2 Ideally performed permanent plug and abandonment

In the previous section the regulations regarding PP&A of a well on the NCS was discussed. For a well to go from being a production well to permanently plugged and abandoned, as illustrated in figure 2.3, a comprehensive operation has to be performed. The procedure will of course vary from well to well, but here the main steps of the current operational procedure for an ideally performed PP&A job is presented.

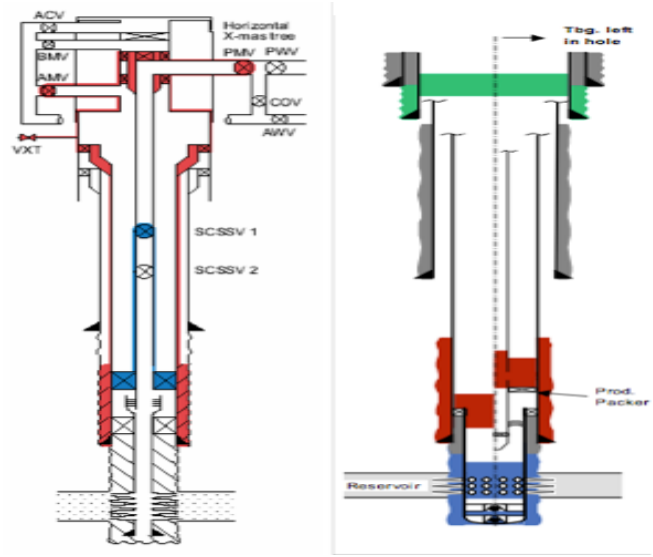

Figure 2.3 Well before and after PP&A. Illustration to the left show typical well configuration for a production well with horizontal x-mas tree. Illustration to the right show plugged and abandoned well with and without pulled tubing respectively. Free after (8)

2.2.1 Get rig/vessel in place and ready to execute the operation

The first step of every PP&A-operation is to get the vessel needed to perform the PP&A-operation in place. For wells drilled from fixed platforms the "vessel" is already in place, but for subsea wells the vessel may have to travel a long distance to get in site. Since this part of the operation is a logistics problem, the main challenge is good planning.

2.2.2 Kill the well

When the vessel is in place, before the well can be entered for PP&A purposes, the well has to be killed. In practice this is done by replacing the fluid in the wellbore with heavier mud to create overbalance. After overbalance is obtained the X-mas tree is nippled down and the BOP nippled up.

2.2.3 Pull the tubing

Once the well is killed the next step commonly executed is to pull the tubing. In theory, according to the prevailing regulations, the tubing is allowed to stay in the hole as long as permanent plugs can be installed inside and around it. However, this is often difficult

in practice because control cables and lines, frequently clamped to the production tubing, have to be removed before a well barrier can be placed. Due to a lack of alternative solutions to remove these control cables and lines, the conventional method of solving this problem is to pull the tubing. Figure 2.4 shows an illustration of control lines and clamped to the production tubing.

Figure 2.4 Control cables and lines clamped to production tubing. After (5).

2.2.4 Diagnostic logging run

After the tubing is pulled a diagnostic logging run, usually performed with a CBL (Cement Bond Log) and a USIT (Ultrasonic Imaging Tool), is executed to assess the downhole conditions. Typically the logs provide the operators with crucial information such as casing integrity and quality and length of the annular sealing. Thus, for the rest of the PP&A operation the quality of the logging and the subsequent interpretation of the logs is of utmost importance. A brief description of the logging tools can be found appendix C.

2.2.5 Set permanent plugs

When the tubing is pulled in the ideal case of good casing integrity and sufficient annular sealing the next step is setting the required plugs. There are several ways of placing a permanent plug, but the most common method used when setting a cement plug is the balanced plug method. Other techniques involve modifications of the balanced plug method, use of dump bailer, inflatable packer or umbrella shaped membranes(12). The procedure for the balanced plug is as follows (13):

1. Create a foundation for the plug at desired depth. The foundation is usually either a viscous pill (e.g. thixotropic bentonite suspensions or a cross-linked polymer pill) or a mechanical plug (bridge plug), but also dense drilling mud may be used.
2. Run stinger or drillpipe to desired depth for the plug foundation.
3. Pump predetermined amounts of spacer, cement and displacement fluid. To avoid U-tubing effects the volumes should be such that they correspond to the same heights in the annulus and in the pipe. This is illustrated in figure 2.5.
4. Once the plug is balanced the pipe is slowly pulled out of the cement and the plug is left to settle.

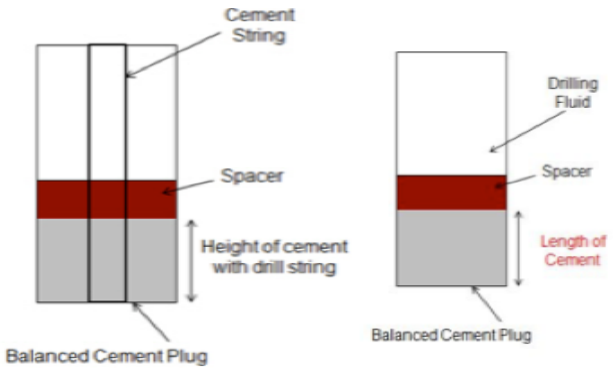

Figure 2.5 Balanced plug (14).

2.2.6 Removal of upper parts of well

The last operation on a PP&A job is to remove the upper parts of the surface casing, conductor and wellhead. This is done to fulfil the requirement that no part of the well will ever protrude the seabed. As discussed previously in the regulation section, NORSOK requires that all casings shall be cut at least 5m below seabed. To achieve this several techniques can be used. The conventional way to perform the operation is by using cutting knives, but also explosives are acceptable as long as directed/shaped charges and upward protection are used to reduce the risk to surrounding environment to the same level as other means of cutting the casing (8).

2.3 Causes for increased PP&A complexity

The previous section described how PP&A jobs are ideally performed. However, in many cases due to various reasons the PP&A operations becomes more complex. Here some of the most common reasons for increased complexity are discussed.

2.3.1 Lack of sufficient annular seal

One of the main reasons for the increased complexity of the PP&A operations is lack of annular barriers. Traditionally these barriers are supposed to be provided by the casing cement, but in many cases when the operators plan PP&A jobs the logs (section 2.2.4) reveal a shortage of annular barriers (15). The shortage is typically either due to the annular sealing column being to short or the formation at the base not being strong enough. The former is typically a result of the placed cement failing to fulfil its purpose, while bad planning and subsequent misplacement of the casing string cause the latter. In the following a both of these reasons for lack of annular seal will be discussed.

2.3.1.1 Casing cement failure

As mentioned, according to the prevailing regulations for the annular sealing material to provide a permanent barrier it need at least 50m of sealing, otherwise the seal cannot be approved as a barrier element and alternative means of obtaining the needed barrier have to be initiated. As typically more than 200m of cement is pumped to initially fulfil the requirement for the production stage, cement failure and not too small cement volumes is commonly the reason for lack of annular barriers.

In general there are many ways in which the casing cement can fail and some of these are illustrated in figure 2.6. The reasons for these failures have several causes but are mainly related to the shortcomings of cement as sealing material when exposed to changes in downhole conditions. A more comprehensive description of the causes for the failure modes seen in figure 2.6 and some ways to reduce the chances of them occurring can be found in Appendix A.

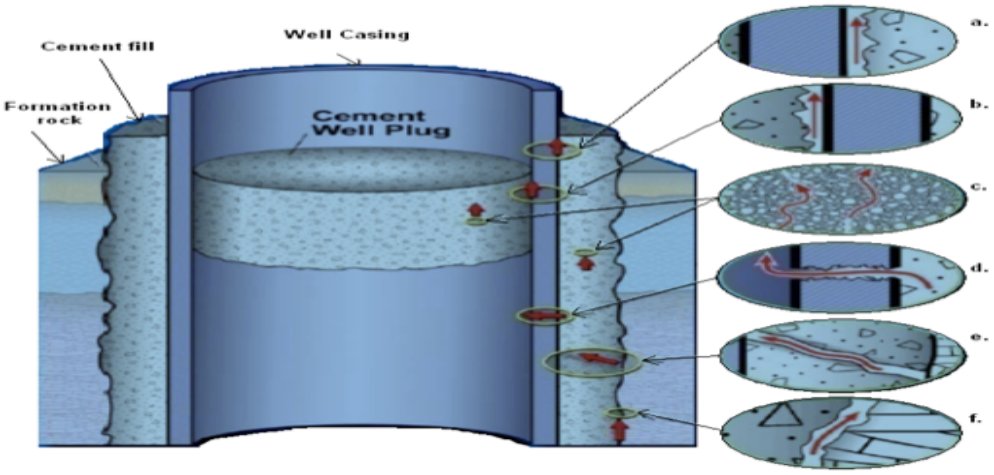

Figure 2.6 Well barrier failure modes. Case a, b and f illustrates how poor bonding between casing/ casing cement, cement plug/casing and casing cement/ formation respectively can lead to a possible leak paths (microannulus). Case c and e shows how fluids (e.g. hydrocarbons) can mitigate through a permeable cement, while case D illustrates well barrier failure due to casing wear. After (5).

A well integrity study performed by the PSA in Norway in 2006 showed that 2% of the 406 selected active wells in the survey had well integrity issues related to cement. Although this is a relatively small number, the fact that few subsea wells are adequately monitored and therefore reported few failures/issues, gives reason to believe that the real number could be significantly higher (16). Moreover, the wells with cement issues where all less than 14 years old when the survey was conducted, meaning that they where drilled in the period 1992-2006. A possible explanation for this is that due to technological advances newer wells can be drilled into more hostile environments than before. As a consequence, the problems with cement as annular barrier could be expected to further increase in the future. Another concern is that the survey was conducted on active wells in the production phase, there could however be many more that don't have sufficient cement for the abandonment phase.

2.3.1.2 Unsuitable adjacent formation at casing cement depth

Another reason for lack of annular barrier is that the casing cement is set at depth where the adjacent formation is too weak or otherwise unsuitable to be part of the barrier envelope. As mentioned earlier for the adjacent formation to be part of a barrier envelope it has to be practically vertically impermeable and have sufficient strength so that it will not fracture when subjected to pressure from below. The former requirement is typically only fulfilled in certain formations such as shales and salts, while knowledge about whether or not the latter is fulfilled can be obtained through strength calculations. The latter will be further discussed in chapter 3.

2.3.2 Tubular deformations

Another reason for increased PP&A complexity is severe tubular deformations. Tubular deformations can, as illustrated in fig.2.7, be caused by tensional, lateral or compressional, shear or bending forces respectively. Although a comprehensive explanation of the different mechanisms is out of the scope of this thesis, in general the tubular deformations are caused by loadings from the formation rocks as a response to stress changes when depleting the reservoir. Tubular deformation problems can occur both in the overburden and in the reservoir, and especially fields with significant subsidence or tectonic activity are often vulnerable. On the NCS especially Ekofisk and Valhall have reported many problems with casing deformation (17)and(18).

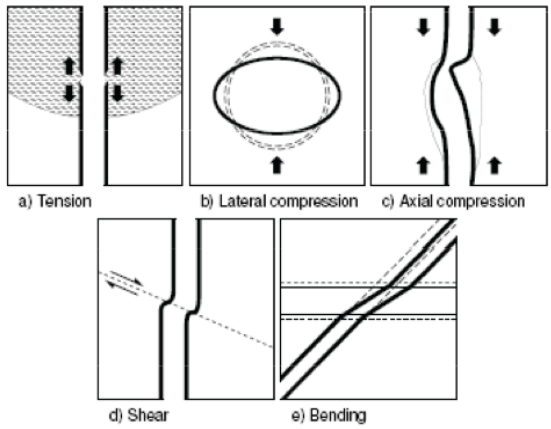

Figure 2.7 Casing deformation mechanisms. After (19).

With respect to PP&A the problems with casing deformation appear when the operator, due to restricted well access, is no longer able to set the plugs deep enough for the formation to provide a barrier. The simplest solution would of course be to avoid the problem with casing deformation altogether. However, a major problem when trying to mitigate the risk of casing deformation is that the factors causing the deformations are interrelated. Thus a mitigation action against one type of failure may promote another. For instance problems with buckling can be reduced by putting the casing in tension, however this makes the casing more susceptible to collapse due to lateral compression, shear and bending (17). As a consequence, problems with casing deformation can in some areas be difficult to avoid altogether, and plugging wells drilled in these regions often represent a real challenge. Going into detail on methods for PP&A with casing deformations is out of the scope of this thesis, but some suggested solutions to solve such problems are (6):

- Milling through restriction
- Pumping expanding cement through restriction
- Sidetracking and re-entering the wellbore, similar to a relief well
- Casing and Tubing opening tool
- Abrasive technology

2.4 Traditional solutions to lack of annular barrier

As seen in the previous section, there are many reasons that can lead to lack of annular seal and problems with this are therefore rather common when abandoning wells. In order to fulfil the requirement that the placed permanent abandonment plugs seal the wellbore in all directions, including all annuli, several solutions have developed during the years. Here some of the traditional solutions are presented.

2.4.1 Remedial cementing

The maybe most natural solution to a problem with lack of annular seal is to try to re-cement the annulus in an operation called remedial cementing. Remedial cementing in PP&A operations involves perforating the casing, at least at one spot, and pump cement into the perforation to repair the problem. Although the method is quite fast and cheap it suffers from low success ratios. Nevertheless, several techniques have been developed for remedial cementing operations, and here two of the most common ones are presented.

2.4.1.1 Standard squeeze

This method is sometimes used when cement is needed at a certain spot. The spot where the cement is needed has to be perforated and to make sure that the cement goes into the perforation; the spot is typically isolated with a mechanical plug below and packer (or retainer) above. Alternatively, sometimes the BOP is used as the above barrier and the technique is then often referred to as a Bradenhead squeeze. Bradenhead squeezes has the obvious advantage of not needing a packer, but it also pressurizes the hole string during the squeeze and can therefore only be used if strong casings are used(12). The two methods are depicted in figure 2.8.

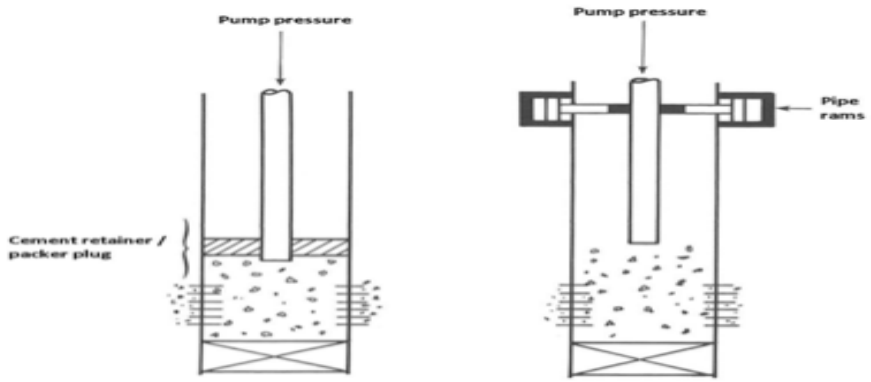

Figure 2.8 Standard squeeze and Bradenhead squeeze. Free after(3).

2.4.1.2 Circulation squeeze

Another remedial cementing method often used is the circulation squeeze. In a circulation squeeze the casing is perforated at 2 points in the well. Circulation through the perforations is obtained by setting a bridge plug right below the lower perforation and a retainer (or packer) between the perforations as illustrated in figure 2.9. When cement is pumped through the pipe it will be forced to go behind the casing through the lower perforation and back inside at the upper perforation. Since the method enables

circulation behind the casing it is often used to repair channels in the casing cement. Due to the risk of the pipe getting stuck between the perforation by the setting cement, this method is also frequently referred to as the suicide squeeze (12).

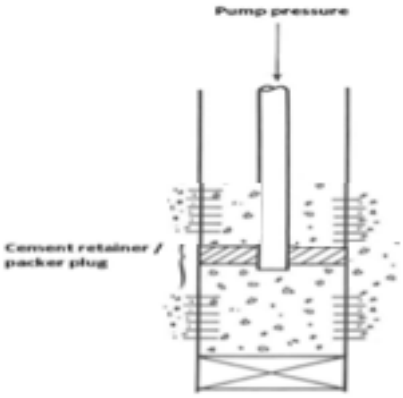

Figure 2.9 Circulation/ suicide squeeze. Free after (3).

2.4.1.3 Advantages and disadvantages with remedial cementing

Table 2.1 Advantages and disadvantages with remedial cementing to solve problems with lack of annular seal.

Advantages	Disadvantages
• Relatively cheap • Fast to perform • Vast experience	• Low success ratio • Many remedial runs may required, and still no guarantee for success. • Logging is needed after each run.

2.4.2 Section milling

Due to the low success ratio with remedial cementing the most common method to solve problems with lack of annular barrier is to perform an operation called “section milling”. Section milling is usually conducted in 4 main steps (20):

1. Section mill desired interval
2. Clean the created open hole
3. Underream the section
4. Set balanced plug

The aim of the first step is to get communication from the wellbore to the annulus. This is obtained by removing a desired section of casing. The principle of casing removal by section milling and a typical milling tool is illustrated in figure 2.10. The purpose of the second step is to remove swarf (metal filings or shavings removed by the cutting tool) and other debris from the hole. While, the objective of the third and fourth step is to expose the well to new formation and fulfil the abandonment requirements respectively.

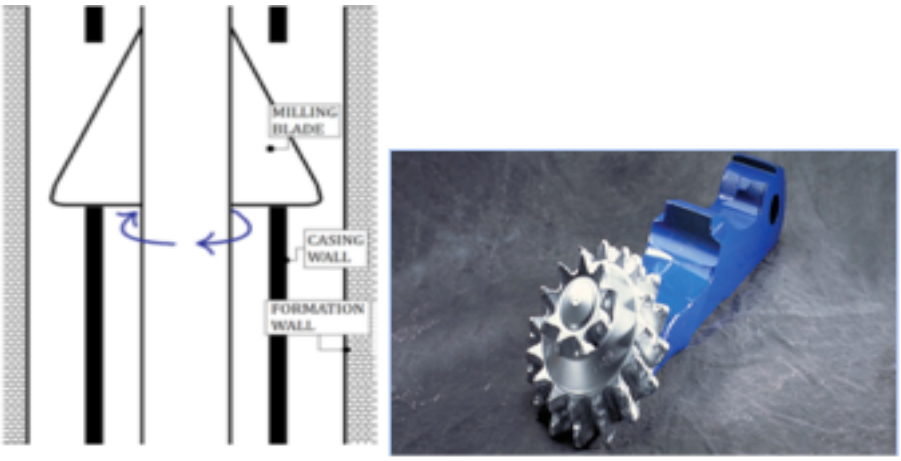

Figure 2.10 Principle of section milling and Lockomatic milling tool. After (4) and (21).

Although section milling, if applicable, has high success ratios when it comes to obtaining the goal of fulfilling the PP&A requirements, there are also several challenges related to the method. For instance the fluid used must both be able to keep the open-hole section stable and transport swarf and debris to surface. To obtain both these objectives the fluid has to have a certain density and a relatively high viscosity. The latter requirement can generate high Equivalent Circulating Densities (ECD) values, and if the values exceed the fracture gradient of the exposed open hole it can lead to losses while circulating. Other issues are swabbing, well control issues, poor hole cleaning, and packing off around the Bottom Hole Assembly (BHA)(20). Moreover, due to the sharp nature of the swarf particles they can do serious damage to critical downhole equipment, such as the BOP, when being transported out of the hole and thus jeopardise the well integrity.
In addition to the previously mentioned challenges the operation is also quite time consuming (the 4 step procedure explained above typically takes 10.47 days) and verification of the sealing capability is often difficult to asses (20).

2.4.2.1 Advantages and disadvantages with section milling

Table 2.2 Advantages and disadvantages with section milling to solve problems with lack of annular seal

Advantages	Disadvantages
• High success ratios • Traditional method (vast experience)	• Time consuming (several runs required) • HSE risk related to swarf removal • Cleaning may require high ECD values, thus risks for fracturing of the formation • Not possible to use in wells with small drilling window. • Difficult to verify sealing capability of annular part of the plug.

2.4.3 The cut and pull method

Another method frequently used in cases with no or insufficient cement in the annulus is the cut and pull method. When applying this method one typically tries to find a free point (point where the annulus lack cement), cut the casing above this point and pull the

casing out of the hole. The free point may be found in several ways. The most common one being cement logs, but also stretch tests, similar to finding the free point for a stuck drill pipe is frequently used (3).
The cut and pull method is most effective in cases where the annulus contains no cement, but can also be used in cemented annuluses. Although, the latter case significantly reduces the length of casing pulled at each run and therefore also leads a more time consuming and costly operation.

2.4.3.1 Advantages and disadvantages with the cut and pull method

Table 2.3 Advantages and disadvantages with the cut and pull method

Advantages	Disadvantages
• Well known technology	• Time consuming if cemented casing has to be pulled • Time consuming if deteriorated casing • Requires large rig with much pulling capacity

2.5 New technology to solve problems with lack of annular seal

So far only the traditional methods solve situations with lack of annular barriers have been discussed. However, due to the increasing number of PP&A jobs there has been several recent developments within the area and more are likely to come in the near future. Here some of these recently developed methods will be discussed.

2.5.1 New technology to enhance performance of section milling

As mentioned in a previous discussion about section milling the method is unpopular because it is quite time consuming, involves HSE risks related to swarf removal and has ECD issues. However, as shown by ConocoPhillips and Baker Hughes during a P&A campaign in 2009, by applying state of the art cutters combined with a downhole optimization sub many of these problems can be significantly reduced(22).Here these two improvements will be discussed individually before the combined effect of using them during the mentioned campaign are briefly presented.

2.5.1.1 Improvements from new cutter technology

Traditionally cutters are made of randomly crushed, sintered tungsten carbide particles suspended in a special cobber-base brazing-type alloy with high nickel content. The newest cutters are however made from powder carbide and although the inserts are designed to act much like crushed carbide, instead of being randomly shaped the cutters have identical geometry making the inserts more effective. Moreover, the newest cutters also typically have longer cutting edge, hence making them less susceptible to single point loading. Combined these two effects gives the new cutters an considerably improved impact resistance, thus reducing the number of runs required to mill a section significantly (22).

The other main problem, swarf removal and high ECD, is furthermore also reduced with the newest cutters. This is due to them having a chip breaker incorporated into each insert that leads to significant reductions in cutting length (22).The new and old cutters are depicted in figure 2.11.

Figure 2.11Milling blade with traditional cutter and milling blade with new P-Cutter. After (22).

2.5.1.2 improvement from downhole optimization sub

A downhole optimization sub is a tool that gathers downhole data, such as Weight on Tool, Torque, RPM, Bending Moment, Vibrations, Pressure and Temperature. Moreover, simultaneously to being gathered the data could also be transferred real-time to surface through mud pulse telemetry. Such tools therefore give the operator a clearer picture of what is happening downhole and can therefore contribute to improved decision making as well as facilitating learning from previous jobs. On the above-mentioned P&A campaign the technology was found especially useful in deep section milling operations because close monitoring of real-time ECD and pressure data reduced problems with unintentional fracturing of the formation. Such problems are typically solved with time-consuming circulation of lost circulation material (LCM) and mud pills, thus by avoiding this considerable amount of time could be saved.

2.5.1.3 Combined effect of new technologies

The combination of the new cutter technology and downhole optimization sub described above increased the section milling efficiency on the mentioned P&A campaign from an average number of 65 days to an average of 46 days, hence reducing the number of days needed to P&A a well with over 40% (22). In addition to being more cost effective, the technology is also better with respect to health, safety and environment (HSE), and has a wider application area than previous techniques. The latter is due to the fact that ECD can be monitored closer. Figure 2.12 illustrates the section milling performance before and after the introduction of the new technology.

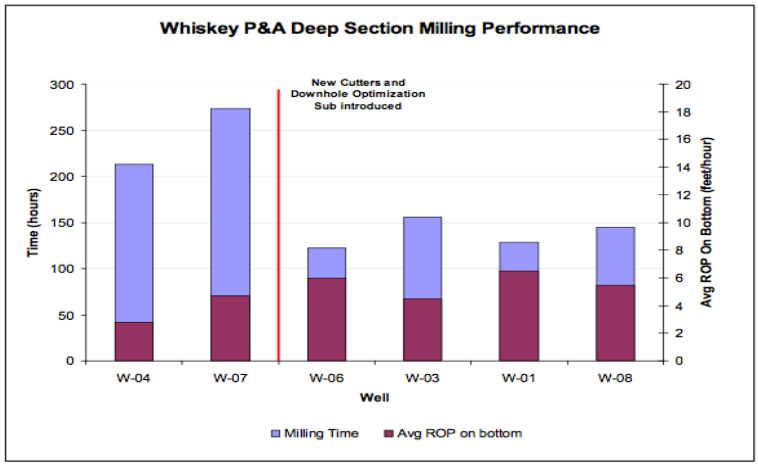

Figure 2.12 Deep section milling performance before and after introduction of new section milling technology. After (22).

2.5.2 Perforate, wash and cement system from Hydrawell Intervention

So far the new methods for obtaining the required annular seal has been improvements of traditional techniques. However, a relatively new product on the market, HydraWash from Hydrawell Intervention, is based on a completely new perforate, wash and cement (PWC) system. The system enables plugging of wells with insufficient annular barriers without removing casing, and its usefulness has already been recognized by NORSOK as an alternative to section milling (10).

HydraWash itself is tool run on drillpipe and consists of a jetting tool and a cement stinger with a Tubing Conveyed Perforation (TCP) gun attached below (23). To enhance the quality of the set plug often also a tool called HydraArchimedes is connected directly above the HydraWash tool. The HydraArchimedes tool looks similar to Archimedes screw and is designed to optimize cement plug placement by mechanically pushing the cement through the perforations when the tool is rotated (24). The upper and lower part of the HydraWash tool with HydraArchimedes and TCP gun respectively attached is illustrated in figure 2.13.

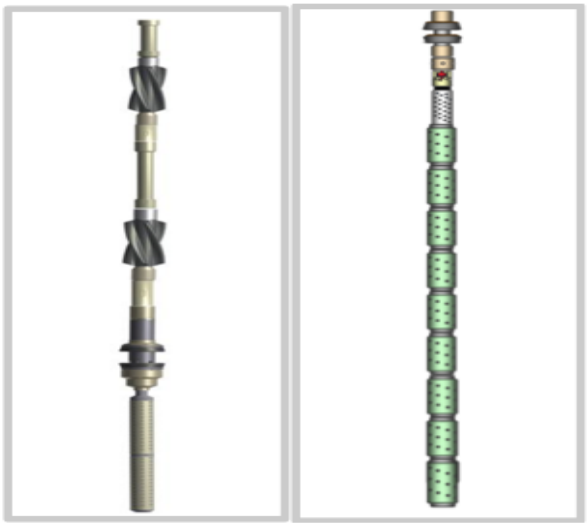

Figure 2.13 Hydrawash tool with HydraArchimedes and TCP guns attached. Upper and lower part of the tool respectively. After (4).

2.5.2.1 Operational Procedure

After a logging operation has been conducted, and the location of where the permanent plug should be placed has been determined, the tool is run in hole to the desired depth. When the tool is at this depth a ball is dropped from surface and the gun fires and perforates the casing. After firing, the TCP gun assembly will automatically drop and a new ball is released from surface. This ball activates the washing assembly by shifting flow channels from the bypass mode used during tripping to circulation mode for washing. The perforated interval is washed and cleaned by the jetting tool until desired pump rate (friction pressure equal theoretical clean annulus) is achieved, before the spacer is pumped down. Next, the workstring is run past the lower perforation and a new ball is dropped. This activates a hydraulic release system that separates the HydraWash jetting tool from the cement stinger and HydraArchimedes tool. The swab cups of the released jetting tool act as a foundation and plugging material is pumped down and a plug is placed in a similar fashion to the balanced plug method described earlier. To improve the quality of the plug and utilize the HydraArchimedes tool the string is usually rotated while the plug is being placed.

After the plug is set verification of the annular integrity of the cement can be obtained by drilling out the plug and run cement evaluation tools. To regain cross sectional integrity the internal casing plug has to be replaced. In general this verification procedure is only conducted during system qualification tests or if an operational problem has been encountered which could affect the integrity of the plug (4).

The whole operational procedure, including verification of the annular seal is illustrated in figure 2.14.

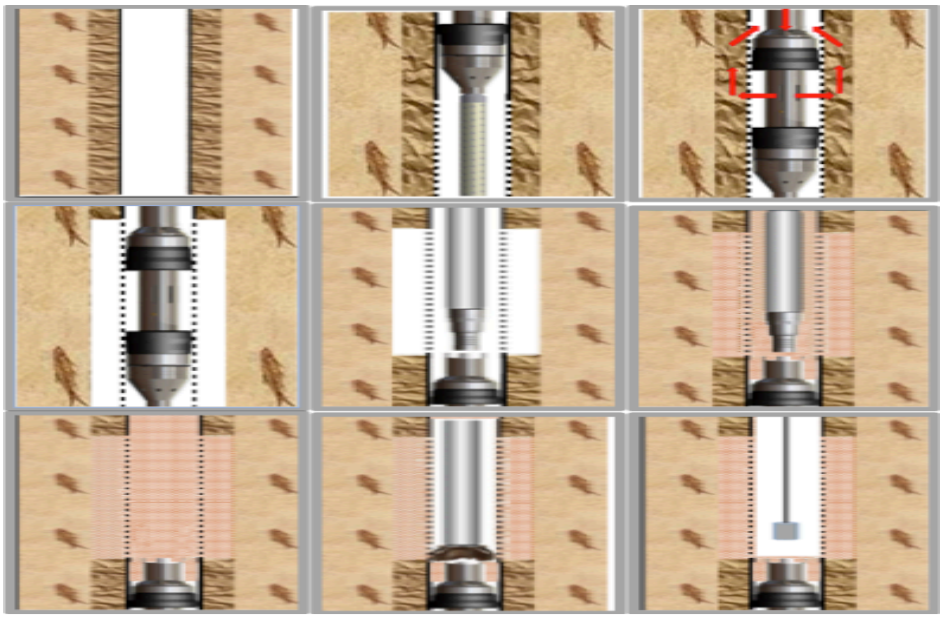

Figure 2.14 Operational procedure for Hydrawash system: From the upper left corner the illustration shows; uncemented section, perforation of casing, cleaning of uncemented section, clean section, release of cement stinger from jetting tool, cementation of section, cemented section, internal plug re-drilled and logging respectively. Free after (25).

2.5.2.2 Hydrawash vs. Section milling

As mentioned earlier HydraWash is developed to fulfil the same purpose as section milling, i.e. create an annular barrier so that the PP&A requirements can be satisfied. However, since the techniques are very different the application area will also be a bit different. As discussed, section milling crushes the casing string in such a way that full access to the annulus is obtained, so that the annular material can be reamed out. In contrary PWC techniques only perforate the casing, and removal of annular material is dependent upon hydraulic jetting. The latter technique is considerably less effective in removing set solid material, such as casing cement. As a consequence, although the PWC systems may tolerate a certain amount of aged unsealing cement in the annulus, the system is preferably applied to completely uncemented annulus.

Nevertheless, in areas where the method can be used, minimum setting depth and annular material conditions taken into consideration, the method is a significant improvement over section milling in many ways. First of all the method is significantly faster than conventional section milling. In a field study ConocoPhillips reported that the average time to accomplish each conventionally set plug using section milling was 10.5 days, while it only took 2.6 days to set a single run PWC plug (20). Moreover, the method gives a safer work environment and reduces the material disposal costs by limiting the production of swarf and other milling debris. Another benefit with the method compared to section milling is that it enables verification of the annular seal. With the PWC method this can be achieved by drilling out the internal plug and run wireline logs to evaluate the quality. However, for section milled wells such an evaluation becomes more difficult. In general, the top of the plug set after section milling operation could either end up inside the cased hole or below, in the open hole. In the first case, the plug can be tagged and pressure tested, but these test only assess the quality of the cement inside the casing and cannot be used to determine the quality of the cement in the

annulus. In the latter case the plug can be tagged, but since a pressure test may fracture the formation to perform an actual pressure test may be impossible. In both cases, attempts to drill out the internal plug as during verification with the PWC method, will only lead to sidetracking and logging tools run into such a hole will be of marginal use in assessing the plug (20). A list over advantages with Hydrawash vs. section milling can be found in table 2.4.

Table 2.4 Advantages and disadvantages with HydraWash vs. section milling.

Advantages	Disadvantages
• Time and cost saving compared to section milling techniques • Improved verification of plug • Swarf handling, transport and disposal are eliminated • No viscous milling fluid • Enhanced well control • Less chance of fracturing the wellbore • Recognised in the draft for the new NORSOK standard as alternative to section milling	• Primarily a solution in areas with free pipe • Cleaning more difficult in deviated and eccentric casing strings. • Less experience • Placement of plug may require squeeze cementing

2.6 New sealing materials

As seen many of the problems with PP&A operations are related to the shortcomings of traditional cement as a sealing material. Due to the increased focus on PP&A and well integrity, several new cement systems and completely new sealing materials have been developed with the purpose to improve this the last decades. Here some of them will be briefly discussed. Although several other alternatives, such as for instance compressed sodium bentonite and geopolymers exists, these have been deemed less applicable and are therefore for simplicity omitted here (13).

2.6.1 New cement systems

As seen in section earlier in this chapter there are many ways in which the casing cement can fail to fulfil its purpose. To improve future cement jobs, much research has been conducted on understanding the causes of cement failure to provide a lasting seal. The general findings are that many of the problems seen can be traced back to cements stiff and brittle nature, and especially in areas where the cement will be exposed to high stress concentrations a more ductile behaviour would be beneficial (26) and (27). Moreover a high tensile strength to Young's modulus ratio is often advantageous and it is deemed unlikely that the cement will fail due to lack of compressive strength (27). As a consequence of these findings several new cement systems have been developed to improve cement's flexibility and thus also in many cases long-term durability.

The simplest way of achieving more flexible cement is to reduce the slurry density by adding more water. However, as this technique has detrimental effects on the

compressive strength and permeability of the set cement, as well the obvious limited usefulness in areas where dense cement is needed, it is normally not considered a good option (12).
Another alternative sometimes used for this purpose is foam cement. Foam cement consists of base cement slurry, a gas (usually nitrogen), a foaming surfactant as well as materials to provide stability. It was originally developed to reduce the density of the cement slurry, but due to the fact it also have other advantageous properties such as relatively high compressive strength, reduced problems with gas migration and fluid loss as well as low permeability, it has become rather popular. Moreover, with respect to long-term sealing capability the material also provide higher ductility and tensile strength than conventional cement. Although there are several advantages there also some disadvantages with the material, making it a less obvious choice. The most prominent of these are the fact that it requires additional equipment (e.g. nitrogen pump) for placement, have alternating properties during circulation as well being hard to identify on logs due to its low density (12).
In addition to the two systems mentioned above also some other systems to make the material more durable has been suggested and sometimes used. These include for instance to incorporate flexible particles (e.g. rubber balls) or elastomeric polymers, such as latex styrene butadiene into the slurry. However, since such systems are more complex and thus more costly than conventional cement the operators are generally reluctant in using them unless it can be proved that the cement will fail otherwise(13).

Table 2.5 presents some general advantages and disadvantages with cement as a sealing material.

Table 2.5 Advantages and disadvantages with cement as a sealing material. After (13).

Advantages	Disadvantages
• Conventional cement is cheap • Much experience • High compressive strength • Easy to modify behaviour • Provide casing support • Can be produced with a wide range of densities • Well established procedures for use • Well established logging tools • Is considered to be the material of choice	• Generally shrinks • Brittle • Low tensile strength • Generally low flexibility • Generally weak to corrosive fluids • Systems often include many additives

2.6.2 ThermaSet®

One of the new sealing materials on the market is Thermaset produced by Wellcem AS. Thermaset is a low viscosity resin product based on non-reactive polymers. In its purest form Thermaset is a 100% particle free liquid with low density and viscosity. However, by adding filler particles the material can be tailored and densities and viscosities in the

region of 700-2500kg/m^3 and 10-2000cP respectively can be obtained (28). Since the material behaves like a liquid it can be pumped downhole using conventional cementing techniques and equipment. Moreover, due to the fact that it can be produced with very low viscosities, it is pumpable through narrow channels and can therefore be used for for instance "fixing" failed annular cement (28).

The main difference with the placement procedure, compared to cement, is how the material sets. As opposed to cement where the curing is based on a hydration process that starts from the moment the cement-powder is mixed with water, Thermaset is thermally activated. This means that the material sets when exposed to a certain temperature over a given time. The fact that both the temperature and time can be predetermined, gives the product a great advantage over cement, because by setting the temperature to the downhole temperature the risk of early set vanish. Moreover, as the setting occurs through a phase transfer (liquid to complete solid) the behaviour can be seen as perfectly right angle set (e.g. no transition period) (28). An illustration of Thermaset in liquid and set form can be found figure 2.15.

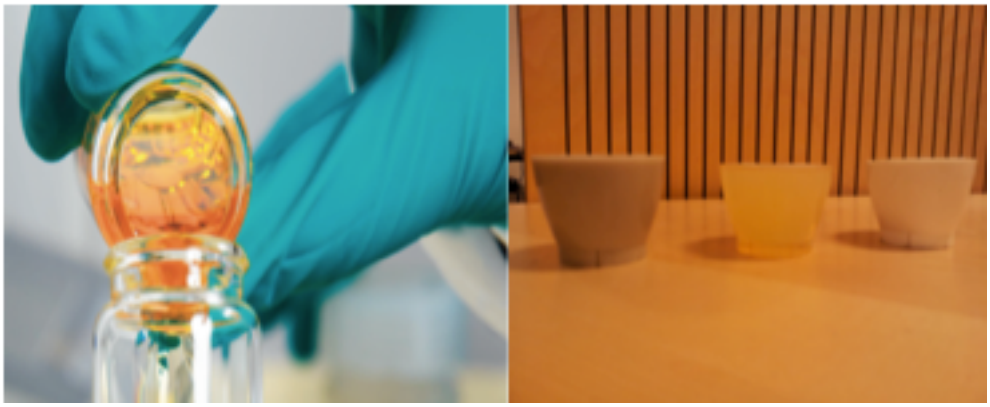

Figure 2.15 Thermaset in liquid and set state. After (28) and(6).

Although the curing process is advantageous, the main benefit with the material is its, compared to cement, superior properties when set. Thermaset has 60 times the tensile strength of cement and this combined with a lower Young's modulus and slightly higher compressive strength makes the material far better suited to high stress concentrations than normal cement. Moreover the material is practically impermeable, can be operated in temperatures from -9°C to 150°C and after it sets it can handle pressures and temperatures up to 320°C and 500 bar respectively, as well as being corrosion resistant (28) and (6).

Table 2.6 Upper and lower limits for density and Young's modulus for Thermaset. After (29).

	Upper (kg/m3)	Lower (kg/m3)
Density	2500	700
Young's modulus	2310	2170

Although, property wise the material may look like an obvious choice, it also has some disadvantages, the most prominent being high cost and little experience. Another issue is verification. If used as a replacement for casing cement the only way to evaluate the quality of the seal over the entire sealed interval, without perforating the casing, is logging. Conventional logging tools, such as USIT and CBL, are based on differences in acoustic impedance (defined as the product of the density and the compressional velocity of the material). Since typical values for mud and Portland cement are very different (e.g. 2.14MRayl and 5.68MRayl, for a 1510kg/m3 WBM and neat class G cement respectively), they are normally quite easy to separate (12). Although, the exact acoustic impedance of Thermaset is uncertain, and will vary depending on the density used, a rough upper and lower limit estimate can be obtained by assuming a constant Poisson ratio of 0.35, and inserting the values from table 2.5 into the following equation for compressional velocity in a linear elastic material, V_p (12):

$$v_p = \left[\frac{E(1-\nu)}{\rho(1+\nu)(1-2\nu)} \right]^{\frac{1}{2}} \quad (2.1)$$

The velocities become 1217.8 m/s and 2230.5m/s, which gives acoustic impedances of 3.04MPa and 1.56 respectively. These values as significantly lower than for class G cement, in fact for low density Thermaset the values are even lower than WBM mud. Nevertheless, the calculations show that, although maybe still possible, it is likely that separating mud and Thermaset with conventional logs becomes difficult.
A comprehensive summary of some advantages and disadvantages with Thermaset as a sealing material can be found in table 2.7.

Table 2.7 Advantages and Disadvantages with ThermaSet. Based on(28) and(30).

Advantages	Disadvantage
• More elastic, flexible and ductile than cement • Higher tensile and compressive strength than cement • Mechanical properties does not diminish with time • Right angle set • Possible to regulate setting time • No radial Shrinkage • Can be prepared in cement mixer days in advance • Extremely low permeability • Can be used to reinforce formation • Durable • Provide good bond to steel • Compatible with most fluids and tolerable to contamination • Less environmental impact than cement	• Very expensive compared to cement • Relatively new product (i.e. little experience) • May be more difficult to verify quality through USIT/CBL logs than cement due to lower acoustic impedance.

• ISO 13310V3 certified (liquid penetration test) • Product gas tight tested (API Spec 10)	

2.6.3 Sandaband

Another quite new sealing material on the market is Sandaband produced by Sandaband Well Plugging AS. Sandaband consist of about 70-80% by volume of quartz with grain size distribution varying from couple of millimetres to less than a micron. The rest of the volume consists of water and fluidising additives, such dispersants and viscosifier, making the mixture pumpable (31). Although it requires some extra wellsite equipment, such as purpose built tanks and a high-pressure pump, the material can be displaced much in the same manner as cement.

The main difference with Sandaband compared to the previously mentioned sealing materials is that is does not cure and set into a solid material. Instead, its behaviour can be seen as that of a Bingham plastic fluid (e.g. toothpaste). Bingham plastic fluids are characterized by the fact that they need a certain shear stress (yield point) to start behaving like a liquid, but before this yield point is reached they behave like a solid material. Thus, during pumping as the material is exposed to high shear stress it will behave like liquid, but as soon as the pumping stops and the shear stress is removed, the material will rapidly start behaving like solid. This behaviour gives the material a great advantage over brittle solid materials because independent of stress the material cannot fracture. If exposed to high enough stresses the material will instead float and deform until the shearing forces are once again below the yield stress so the material can return to its “solid“ state. Moreover, as this is purely a mechanical process the transition between solid and fluid phase can be repeated forever without the material experiencing detrimental effects, such as fatigue (31). In addition, since no chemical reaction is involved there is no shrinkage or wait on setting time. Thus, problems such as the formation of microannulus and gas coming through the sealing material during transition phase are avoided. An illustration of Sandaband and its Bingham plastic properties can be found in figure 2.16.

Figure 2.16 Sandaband a Bingham plastic material. After (32).

Sandabands sealing ability is due its unique particle size distribution, where small particles fill the void between the larger, and the void between these smaller particles is further reduced by adding even smaller particles, and so on, until micron-sized particles are reached, hence creating a very low permeable matrix. Moreover, the permeability is even further reduced due to the fact that flow in the pore space is hampered by the existence of electrostatic binding forces between the water molecules that initially occupy the pore space and the smallest micro silica grains (33).
Furthermore, in addition to initially being low permeable the material is likely to stay that way because quartz and water are chemically stable and will not degrade with time. Although strictly speaking the material contains other additives, these are just added to make the material pumpable, hence an eventual degradation of them will not affect the materials sealing capability. The particle size distribution in Sandaband is illustrated in figure 2.17.

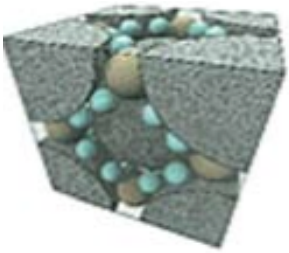

Figure 2.17 Particle size distribution in Sandaband. After (33).

As discussed Sandaband have several advantageous properties, but there are also some disadvantages associated with the material. As with Thermaset its popularity is hampered by high costs and the limited experience using the material. The former is made even worse by the fact that Sandaband plugs is typically required to be several times longer than solid sealing material plugs (e.g. cement and Thermaset) in order to control the same pressure. This is because, as opposed to solid sealing materials where the pressure control ability is obtained through high friction (shear stress) between the material and its surroundings, Sandaband is a Bingham fluid, hence the pressure it can withstand is dependent on 3 factors (32):

1. Hydrostatic pressure exerted by water column.
2. Hydrostatic pressure exerted by the plug itself ($\rho_{Sandaband} \approx 2150 kg/m3$).
3. Yield point*Surrounding contact area with the Sandaband plug.

Another operational issue caused by the Bingham plastic behaviour of Sandaband is that the material needs a solid foundation to rest upon. Moreover, as opposed to the other sealing materials for PP&A this foundation has to be permanent, hence it can only be provided by other permanent sealing materials or for instance the well floor

Although maybe not a disadvantage another difference with Sandaband compared to cement is how it has to be verified. For cement the standard way of verifying a plug is tagging and pressure testing, while annular cement is verified through CBL or USIT logs (12). However, since Sandaband is in a liquid state downhole and consist of poorly

sorted solid materials suspended in a suitable carry fluid, these techniques cannot be applied.
For plugs the conventional way is run a pipe slightly into the plug, and circulate bottoms up from below the calculated top of the Sandaband plug. If sand is observed over the shakers, it indicates that the Sandaband plug is present at the given depth (31).
Moreover, to verify the sealing ability of the plug it can be inflow tested, and in cases where solid sealing material plugs are used as foundation, pressure tested. The latter will however only test the foundation and does not say anything about the quality of the Sandaband plug itself.
To verify Sandaband in the annulus, the preferred logging method is based on using a pulsed neutron tool. The tool bombards the formation with neutrons, which responds by sending out gamma rays. Because the different materials interact with the incoming neutrons in different ways, it is possible to say something about the material behind the casing. Since Sandaband consist primarily of quartz the presence of silicon, which make up large parts of the quartz minerals, would indicate that Sandaband is present behind the casing (3).

A comprehensive summary of some advantages and disadvantages with Sandaband as a sealing material can be found in table 2.8.

Table 2.8 Advantages and disadvantages with Sandaband. After (13).

Advantages	Disadvantages
• Incompressible • Infinite durability and cannot fracture • Not affected by changes in well conditions • Gas tight • Non degradable • If used as annular integrity medium, cut and pull of casing becomes very efficient. • Thermodynamically stable and chemically inert • Ductile • Extremely low permeability • Environmentally friendly • Low loss to formation • Efficient as LCM material • No microannulus • No Shrinkage • Premixed onshore, no mixing offshore • Reduced deformation of casing • Little if any formations damage • Time efficient compared to setting a cement plug • Plugs can be washed out, no need to re drill if the well has to be re-entered	• Expensive compared to cement • Need a solid foundation • Not suitable behind load bearing casing string because of relatively low shear strength • Have to be premixed onshore • Relatively high density • Little experience • Need extra wellsite equipment

2.7 Future technology

So far mainly the available technology today to improve PP&A operations have been discussed. However, there are some future improvements on the present methods that are just around the corner. Here two of these are presented

2.7.1 Hydrawash run on coiled tubing

Currently, at least to the author's knowledge, the HydraWash tool has not been deployed on coiled tubing (CT). However, such technology is under development and since CT can be run on significantly smaller vessels than full sizes rigs, it can be a major contributor to reducing PP&A cost in wells with lack of annular seal. However, as discussed in a previous master thesis, there are some challenges with running the PWC system on coiled tubing (4).

First of all the 60 meter long TCP gun assembly will be difficult to run into a live well with regular coiled tubing surface equipment as the lubricator length is not sufficient. Secondly, obtaining rotation of the coiled tubing to utilize the HydraArchimedes tool may be an issue. Normally rotation with coiled tubing is achieved with a powered motor that uses fluid flow through the tubing as a power source. However, such a motor cannot be turned off and since it will induce high frictional pressure drops, it may result in large operational problems during washing and cementing. As a consequence alternative means of obtaining the required rotation has to be developed. A possible solution is to use a eternally mounted turbine for rotation, similar to those used for liner drilling (4). Finally, a third problem with using coiled tubing is that fact the tubing has significantly less radius than conventional drill pipe, thus in sections with large casing inner diameter the velocity needed to clean out particles during washing could be difficult to achieve. A possible solution could be to leave the debris downhole instead of lifting it all the way to surface (4).

2.7.2 SwarfPak from Westgroup

SwarfPak is new and ambitious milling tool specially made for PP&A and slot recovery operations with the purpose of reducing rig time and environmental footprint. According to the developer, Westgroup, the tool should be able to increase the milling speed from today's 3m/hr to 18-30m/hr, and thus contribute significantly to reduced cost with a milling operation. Another benefit with the tool with respect to PP&A is that it is able to do milling and cementing in one operation. Moreover, the tool mills upward, in contrary to the traditional downward, and this will according to Westgroup give lower vibrations and therefore result in less wear and prolonged lifetime of the cutters. Furthermore, the tool uses reverse flow circulation and combined with the upward milling this makes it possible for the tool to leave the swarf down-hole instead of transporting it to surface, thus contributing to increased safety of the operation (34). Although the tool sounds promising, it is still only a prototype and it is yet to be known if it lives up the expectations created by Westgroup. Currently, Westgroup together with their partners, among others Statoil and ConocoPhillips, is running field test on the tool

and if everything goes as planned the tool should be ready for the market during the second quarter of 2013 (35). An illustration of the tool can be found in figure 2.18.

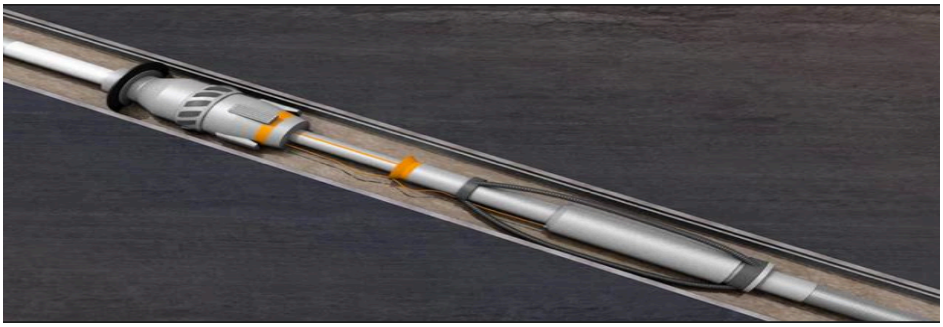

Figure 2.18 SwarfPak tool. After (34).

3. Introduction to shale as annular barrier element

In the previous chapter lack of annular sealing, mainly due to casing cement failure, was identified as one of the primary reasons for increased PP&A complexity and thus also cost. Several newly developed materials to avoid the problem as well some traditional and new technical solutions, all based on some sort of well intervention work, to solve the problem were discussed. However, in cases where the casing cement has failed a relatively new approach is to look for the possibility of inward moving shale formations providing a barrier and thus avoiding the complex remedial work.
Here the governing regulations regarding them, some of their properties as well as the identification and verification procedure for such barrier will be discussed.
In the following chapters the displacement mechanism thought to be responsible for the radial movement, possible ways to increase the movement as well as other alternatives with moving shales in combination with other sealing materials will be presented.

3.1 Regulations regarding formation as annular barrier

As described in the section 2.1.2, defining the material requirements for permanent well barriers on the NCS, the operators are free to choose barrier elements as long as they can be proven to be (8):

a) Impermeable
b) Long term integrity
c) Non Shrinking
d) Ductile-(non Brittle)- able to withstand mechanical loads/impact
e) Resistance to different chemicals/substances (H_2S, CO_2 and hydrocarbons).
f) Wetting, to ensure bonding to steel

Certain rocks types, for instance shale and salt, satisfies all these requirements and can therefore be used as well barrier elements as long as they can be proven to have the required strength and seal around the complete circumference of the casing over a sufficient interval. However, since the concept of formation barriers is newer than the last edition of the current prevailing regulation, they are not explicitly mentioned there, and no specific requirements for formation barriers are given. Nevertheless, after the current regulating document was written, the PSA of Norway has approved a procedure for the acceptance of formation as barrier element (15).Furthermore, a WBEAC for formation barriers is included in the draft for the newest edition of the governing document and can be found in appendix B.

The WBEAC includes both the requirements for the barrier to be accepted for PP&A as well as a procedure for how it can be verified. In general the requirements are that for a formation to provide a barrier element it needs at least 50 meters with good continuous bonding of a element that has the ability to withstand the maximum differential pressure the formation may be exposed to. Moreover, as with all other annular barriers the minimum formation stress at the base of the element shall be sufficient to withstand

the maximum pressure that could be applied. A detailed description of the verification procedure and how formation barriers can be found will be presented later in this chapter. Although, as mentioned salt formation could provide a barrier in a similar way to shales, due to the high frequency of shale zones on the NCS, procedures for verifying shale zones as barrier element will be the main focus here.

3.2 Shale

As mentioned, one of the accepted formation barrier rocks is shale. Shales make up over 75% of the drilled formations and can be defined as fissile fine-grained, clastic sedimentary rocks, composed of at least 40% clay minerals in addition to other tiny fragment minerals, such as quartz and calcite (36). The exact ratio of clay to other minerals is variable and the chemical and mechanical properties of the shale are highly dependent of the amounts and types of clay mineral.

3.2.1 Clay structure

Clay minerals are composed of layers of sheet shaped crystals. In general the different clay minerals are based on 2 basic units a tetrahedral and an octahedral sheet. The tetrahedral sheet is built from silica tetrahedrons (SiO_4-^{4}) linked together into a hexagonal structure with chemical formula $Si_4O_6(OH)_4$. The second type, the octahedral sheets, are sheets in which the silicon is replaced by cations like Al^{3+}, Mg^{2+} and linked together into octahedral structures, such as $Al_2(OH)_6$ and $Mg_3(OH)_6$, named gibbsite and brucite respectively (37).The basic sheets are furthermore combined by sharing oxygen's to form unit layers (clay minerals) and hundreds of these unit layers stacked up like in a deck of cards make up a clay particle.
The most common groups of clay minerals in sedimentary rocks are kaolinite, smectite illite and chlorite (38). The main difference is that they are made up of different combinations of the 2-basic structures and this gives rise to very different properties. This will be discussed further later in this chapter.

3.2.2 Isomorphic substitutions and Cation Exchange Capacity (CEC)

An ideal combination of the tetrahedral and octahedral layers gives a structure with balanced charges. However, in many cases, during the creation of the mineral, cations in the lattice structure is replaced with ions with a lower charge in a process know as isomorphic substitution, hence giving the lattice a negative surface charge. This can occur for instance if Si^{4+} ions in the tetrahedral structure is exchanged with $Fe^{3+,}$, or Al^{3+} ions in the octahedral structure is replaced by a Mg^{2+}ion (37).

The negative charges that are created in the unit layers generate strong attractive forces for polar molecules such water, which can be drawn in between the unit layers, known as bound water. Furthermore the charges created by the substitutions can be fully or partly neutralized by the absorption of cations from the surrounding water onto the lattice surface. Moreover, these loosely held cations could be exchanged with other cations present in the surrounding water, thus giving rise to a property known as the cation exchange capacity (CEC). The CEC is independent of pH, but varies from mineral

to mineral due to differences in where the substitutions occur (tetrahedral or octahedral layer) and the degree of substitutions (37).

The ability of one type of cation to replace another depends on the nature of the involved cations and their relative concentrations. When present in equal concentration the absorbed cations will replace each other in the following order(38):
$Al^{3+}>Mg^{2+}>Ca^{2+}>H^{+}>K^{+}>Na^{+}$
This is important because type of cations in the exchange positions of the clay has significant impact its ability to attract and store water in between its unit's layers, which furthermore have large impact on its physical properties. In general the higher the charge of the cations (electron valence) the less water will be attracted between the units layers. This is because multivalent cations (e.g. Al^{3+}, Ca^{2+},Mg^{2+}) will associate themselves with a number of unit layers equal to their charge, hence creating bonds between the layers limiting the maximum spacing between them. Monovalent cations, on the other hand, can only associate themselves with one unit layer and therefore not contribute to bonding. As a consequence, when monovalent ions are present more free water can be attracted in between the unit layers. This is especially true for smectite clays, because the layers are only bonded through weak Wan der Waals forces originally, thus the "extra" bonds obtained due to the cations have large impact (38). The effect of multivalent vs. monovalent cations is illustrated for a sodium montmorillonite and calcium montmorillonite in figure 3.1.

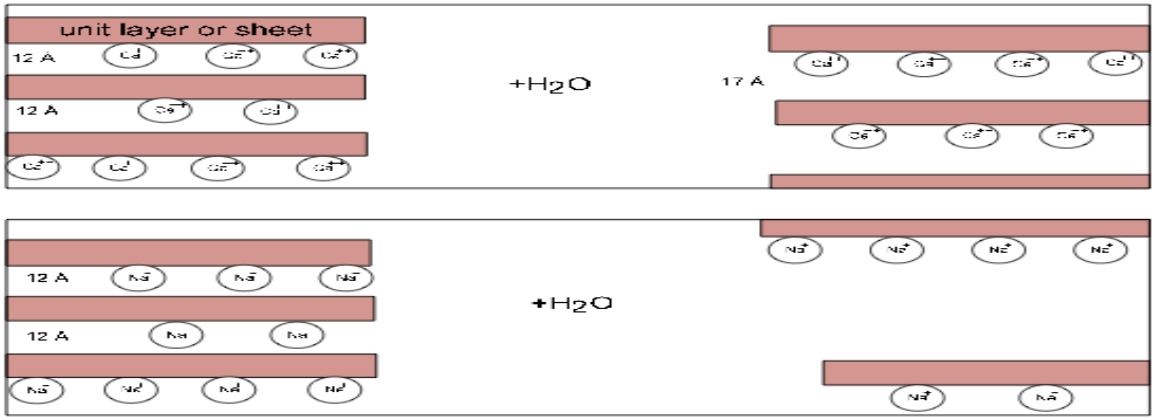

Figure 3.1 Schematic of hydration between unit layers for Calcium Montmorillonite (upper) and Sodium Montmorillonite (lower). After (38).

In addition to the charge of the cation the ability it has to attract water in between the unit layers is also dependent on the charge density (i.e. charge/ dehydrated ion volume) of the cation. This will be further discussed in chapter 6.

3.2.3 Clay minerals

As mentioned, there are several types of clay minerals and the main difference between them is that they are build up from different combinations of the 2 basic units. However, as this gives rise to very different properties the most important clay minerals will be discussed here.

3.2.3.1 Smectite

Smectite is a 2:1 layer mineral, consisting of a central gibbsite sheet embedded between two silicon tetrahedron sheets, with a combined thickness of about 1nm.The most common mineral within this group is montmorillonite, which again is the main mineral in bentonite frequently used as a viscosifier in drilling mud.

Smectites most prominent characteristic is their ability to absorb water and swell. The reason for this ability is two-fold. First of all the isomorphic substitutions in the mineral occurs mainly in the centrally placed octahedral layer. Because of this the associated cations are prevented from getting close the negative charge and are therefore less effective in neutralizing the charge. As a consequence, the mineral retain some of its ionic characteristics, which as mentioned creates very strong attractive forces for polar molecules, such as water, which readily force themselves in between the unit layers. Moreover, because the unit layers on smectite (assuming monovalent cations) are only weakly connected through van der walls forces the individual layers can separate as more water is attracted in between unit layers. This is a unique feature with smectites, because in the other clay minerals the bond formed between the unit layers are much stronger, hence preventing separation (37).

3.2.3.2 Kaolinite

Kaolinite is a 1:1, two-layered mineral composed of alternating layers of gibbsite and silicon tetrahedron sheet. A unit layer is 0.7nm thick and the successive layers are strongly bonded to each other with hydrogen bonds that effectively prevents water to enter in between the layers (36). Moreover, as there in general are few isomorphic substitutions within the mineral the attractive forces for polar molecules are much less than in smectites.

3.2.3.3 Illite

Illite or mica is 2:1, layer clay mineral, formed by weathering of feldspars, degradation of muscovite, and transformation of smectite to illite at depth (36). In Illite the isomorphic mainly occurs in the tetrahedral sheet causing a negative charge, which is balanced by potassium ions providing bonding between the silica tetrahedron sheets. This bond is much stronger than in smectite, hence preventing hydration, but is a lot weaker than in kaolinite (36).

3.2.3.4 Chlorite

Chlorite is a 2:1:1 layer consisting of alternating layers of illite, but with an additional brucite-like layer embedded between the tetrahedral layers. As in kaolinite the bonds between the layers are very strong and the mineral does not swell (37).

3.2.4 Physical properties

As mentioned shales are defined as rocks that consist of at least 40% clay minerals and both type and amounts of clay minerals have large effect on the physical properties of the rock. This is illustrated in table 3.1, which shows typical mechanical properties for

shales and clays. As seen the mechanical properties for both materials vary across a wide range and no "typical" shale or clay exist. Moreover, shales are in general stiffer and have higher strength than clays; this is mainly due to higher degree of cementation as well as the impact from non-clay minerals. As a consequence of this, strength and stiffness of shales normally decrease with increasing clay content, but also the type of clay is extremely important.
Clays properties are very much dependent on the type of mineral (kaolinite, smectite, illite or chlorite), which is dominant within the clay. In particular the amount of adsorbed or bound water present within the mineral or on the mineral surfaces is important (36). As previously seen, smectite clays have a larger ability to swell (store water within it structure) than the other clay minerals, they are therefore normally less stiff. Moreover, due to smectites ability to store water, shales with high smectite content are normally less brittle and have a more plastic behaviour than shales with low smectite content (39).

Table 3.1 Mechanical properties for shales and clay. Free after (36) and (39).

Material	Young's modulus (GPa)	Poisson ratio	Shear modulus (GPA)	Unconfined compressive strength Co (MPA
Shale	0.4-70	0-0.30	4-10	2-250
Clay	0.06-0.15	~0.40	0.02-4	0.2-0.5

3.2.5 Capillary effects

A prominent characteristic with shales is their extremely narrow pores, typically in the 5 to 25 nm range. With respect to shales sealing ability this gives rise to a very beneficial property known as the capillary effect.
Capillary effects or capillary forces occurs whenever the pore space is filled with at least two immiscible fluids and arises because it is energetically favourable that one of these fluids stay in contact with the solid (wetting fluid), while the other (non-wetting fluid) is somewhat shielded. Due to this effect, if the rock is initially saturated with the wetting fluid and then brought into contact with the non-wetting fluid, for the non-wetting fluid to enter the pore space of the rock it needs to have a overpressure equal to the threshold capillary pressure compared to the wetting fluid. The difference in pressure between the two fluids is known as the capillary pressure and is defined as (36):

$$p_{cp} = p_{nw} - p_{we} \quad (3.1)$$

where p_{nw} is the pressure in the non-wetting fluid, p_{we} is the pressure in the wetting fluid and P_{wc} is the capillary pressure.
The magnitude of the capillary threshold pressure depends on the type of fluids, the condition of the solid surface (determines degree of wettability for various fluids) and the size of the pores at the point where the fluids meet. Assuming full wettability capillary threshold pressure can be given as (36):

$$p_{cpt} = \frac{2\gamma}{r} \quad (3.2)$$

where γ is the surface tension between the fluids and r is the pore size. Typical values for the surface tension is $50 \bullet 10^{-3}$ N/m for oil-water and $40 \bullet 10^{-3}$ N/m for natural gas-water (36)and (40). Hence, since shales are usually water wet, assuming a pore size of 5nm, for the oil to penetrate the intact shale its needs a overpressure of 20MPa, while 16MPa would be required for gas to enter the same shale.

Another characteristics of shales are their extremely low permeability, typically in the nanoDarcy range. Moreover, since this is also caused by the narrow pore space, the permeability remain low even though the porosity of the shales could be quite high (up to 70%) (36). As a consequence, most shales satisfy the low permeability requirement for permanent annular barriers. For instance using Darcy's law assuming a permeability of 5 nanoDarcy, a fluid with a viscosity of 100cP would penetrate a 200m shale zone with a differential pressure of 100 bar at rate of $7.9 \bullet 10^{-9}$ m/year. Hence it would take over 25 billion years to penetrate through the complete shale zone.
Moreover, assuming similar pore size as for the previously performed capillary pressure calculations, a 100bar pressure differential wouldn't even be high enough for the fluid (oil) to penetrate the shale. Thus, as a consequence due to capillary effects and the extremely low permeability along with other beneficial qualities such as being self - healing and non-brittle, shales are very good sealing materials. This statement, as well as they're long-term sealing ability is furthermore confirmed through the many reservoirs where shales functions as the caprock.

3.3 Procedure for verification of shale annular barriers

As mentioned, in some wells the shale formation has been found to move radially inward and seal off the complete annular space between the formation and casing. Since shales, as seen in the previous section, can be an efficient sealing material, these displaced formations can sometimes be used as an annular barrier. However, for the barriers to fulfil the requirements they have to be identified and their sealing ability qualified. Here the necessary steps in the verification procedure for such annular barriers will be presented.

3.3.1 Define interval where formation can be

The first step in every shale barrier element verification procedure is to identify where the annular barrier can be located. As mentioned in section 2.1.1, NORSOK requires that permanent well barriers is set at depths where the potential pressure that the formation may be exposed to from the reservoir is less than its fracture pressure. Moreover, many operators, such as Statoil, choose to be more conservative and use the minimum formation stress, σ_h, instead of the fracture pressure. This requirement indirectly determines the interval where the formation barrier may be found in order to provide an annular barrier for PP&A.
Typically the fracture pressure gradients or σ_h gradients are taken from earth stress models of the actual field where the well is located (15). The models are created through

formation integrity tests (FIT), leak off tests (LOT) or extended leak off tests (XLOT), which are normally conducted at each casing setting depth.
By knowing the initial reservoir pressure, depth and fluid density as well as the discussed fracture or σ_h gradients for the formation, the minimum plug setting depth (i.e. upper limit for the formation barrier interval) can be estimated in the following manner:
The well pressure, P_x, at a given point x along the well trajectory can be calculated as

$$p_x = p_{res} - p_{hydrostatic} \quad (3.3)$$

Where

$$p_{hydrostatic} = \rho_{res.fluid} \cdot g \cdot (D_{res} - D_x) \quad (3.4)$$

P_{res} is the pressure at the source of inflow, $P_{hydrostatic}$ is the hydrostatic pressure of the fluid column with density $\rho_{res.fluid}$, from reservoir depth D_{res}, to depth at the given point x, D_x. As a worst case scenario P_{res} is often set equal to initial reservoir pressure, while $\rho_{res.fluid}$ is often set close to zero, thus assuming gas to be the fluid.

The formation fracture pressure, P_{frac} at depth x is given by

$$p_{frac} = \rho_{frac} g D_x \quad (3.5)$$

Where ρ_{frac} is the fracture gradient found from previously conducted formation strength tests, i.e. FIT, LOT or XLOT.
The requirement for a plugs/barriers setting depth is that

$$p_{frac} > p_x \quad (3.6)$$

Inserting equation 3.3, 3.4 and 3.5 into equation 3.6 and solving for D_x, yields the criteria for the upper limit depth for the formation barrier interval (minimum plug setting depth):

$$D_x > \frac{p_{res} - \rho_{res.fluid} \cdot g \cdot D_{res}}{g(\rho_{frac} - \rho_{res.fluid})} \quad (3.7)$$

If the displaced formation is found shallower than the depth found from equation 3.7, the worst anticipated pressure that the formation may be exposed to exceeds the strength of the formation. Consequently, the requirements are not satisfied and the barrier cannot be accepted as a barrier element. A graphical illustration of the method applied above is illustrated in figure 3.2.

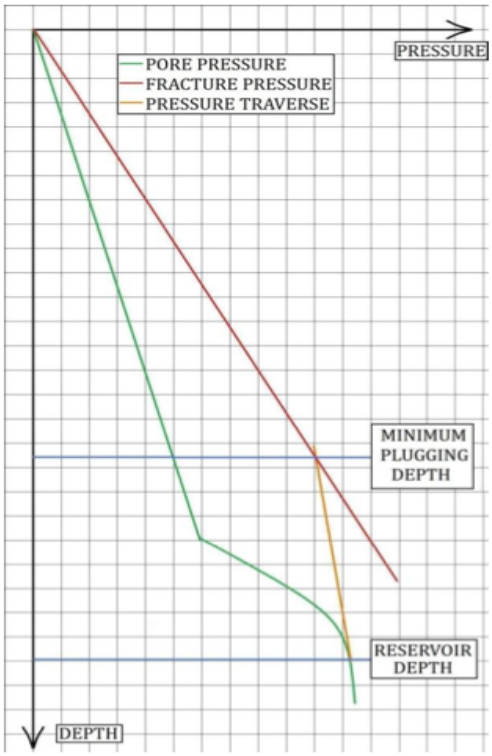

Figure 3.2 Minimum plug setting depth for permanent barriers. After (4).

3.3.2 Logging to Identify possible barriers

For a barrier to possibly provide an annular seal it has to be practically impermeable, extend over a minimum of 50 meters and have full azimuthal coverage. Thus, after the interval where the formation barriers can be found has been identified the next step is to log the interval and see if any such barriers are present.

Logging is typically conducted using either sonic or ultrasonic acoustical logging tools. Although, several different tools exist, they are all based on the fact that when sound waves travel across boundaries between two materials, a portion of the wave is transmitted through to the next medium, while the rest is reflected back into the first medium. The amount reflected vs. transmitted is determined by the acoustic impedance difference between the two mediums defined as (12):

$$Z = \rho v_p \quad (3.8)$$

Where Z is the acoustic impedance, ρ is the density and v_p is the compressional velocity of the material.

As a rule of thumb the greater the difference between the acoustic impedances of the two mediums, the larger the reflected portion will be compared to the transmitted. The sum of the amplitudes of the reflected and transmitted waves is equal to the amplitude of the original wave. Hence, since different materials tend to have different acoustical properties by measuring the received amplitudes, travel time and possible paths is it possible to determine what kind of mediums the waves have been travelling through. A

list of typical acoustic properties for common rocks and materials can be found in table 3.2.

Table 3.2 Important acoustic properties for common rocks and materials found downhole. Based on several tables found in (12)and values found in (36).

Material type	Δt (μs/ft.)	Sound velocity (m/s)	Acoustic impedance (MRayl)
Steel (compression wave	51.4	5,930	46.00
Plate wave in casing (CBL)	57	5.334	41.60
Dolomite	43.5	7,010	20.19
Sandstone(5-20% porosity)	62.5 to 86.9	4,877 to 3,505	12.58 to 8.20
Limestone (5-20% porosity	54.0 to 76.9	5,639 to 3,962	14.83 to 9.43
Shale(2.3-2.8 g/cm3)		1,600-4,500	3.68-12.6
Neat Glass G cement (1.89g/cm3)		3,000	5.68
36% quality foam cement (1.2g/cm3		2,300	2.76
Water (0.998g/cm3)	206	1,482	1.48
Seawater (1.025g/cm3)	199	1,531	1.57
Diesel (850g/cm3)	221	1,380	1.17
WBM (1.510g/cm3)	215	1,420	2.14(low frequency)
OBM (1.510 g/cm3)	245	1,240	1.87(low frequency)
Gas			<0.1

For a barrier to be identified two independent logging measurements shall be applied. The most common is to use the CBL/VDL and the USIT log. A comprehensive description of these tools can be found in Appendix C.

As seen from table 3.2 the acoustic difference between shales and fluids is quite high and they are therefore quite easy to separate. However as seen, the acoustic impedance of shales could be somewhat similar to other non-sealing rocks, such as Sandstone and Limestone. Moreover, if impinged onto the casing these formations would also show typical chevron patterns on VDL log implying geological beds. Thus, an important task is in the verification of shale barriers is to prove that the localised solid material is in fact shale. This can typically be demonstrated through electrical logs or cutting description logs made during or after drilling (15).
To make sure that the interpreted good seal is in fact is a 360° full coverage seal it is often wise to run the sonic and ultrasonic tools in combination. Although, the sonic tools have the obvious shortcoming of only using single average amplitude values, and therefore has no azimuthal coverage, due to the fact that low frequency waves are less attenuated than high frequency waves they are less affected by high density drilling fluids and dry-microannulus. Thus, for interpretation purposes the combination of the

two tools provides a coherent picture, which compensates for individual limitations of the two tools.
The following guidelines have been suggested when interpreting the different logs in shale zones to qualify them as annular barriers.

Table 3.3 Recommended guidelines for log interpretation with respect to identifying a shale barrier (15)

	Cement bond log amplitude	Variable Density log	Ultrasonic acoustic impedance scanner
Good Barrier	CBL less than 20 mV over 80% of interval	Low contrast casing signal and clear formation arrivals	AI reading greater than 3 MRayl on all azimuthal readings
No Barrier	CBL reading within 20% of free pipe reading	High contrast casing signal and weak formation arrivals	Reading less than 2 MRayl on some azimuthal readings

Although, the two tools when ran in combination is quite effective in separating solids from fluids both of them have limitations when come to logging through several layers of steel. As a consequence, in areas where the barriers have to be set at depths where there are multiple casing strings, with today's technology, all but the largest casing string has to be pulled in order to identify shale or other solid materials behind this casing (41). Since annular barriers are usually created months or years after the casing is set, this is one of the main disadvantages with the method compared other sealing materials where the seal can be verified immediately.

3.3.3 Verification of possible barrier

After a possible barrier in the correct interval has been identified the next and final step in the verification procedure is to prove that the barrier has the required physical properties, such as extremely low permeability and ability to withstand the maximum differential pressure it can be exposed to. This confirmation is done through pressure testing. For the pressure tests to be valid they have to be conducted from below or near the base of the potential barrier and exceed the maximum anticipated pressure that the reservoir fluids may expose the barrier to. To avoid the chance of possible leakage being missed when applying lower pressures, the pressure test are often performed as leak-off tests (LOT).

There are several ways to perform such pressure test in practice. Some of those methods are (15):

- Perforate the casing at the base of the potential barrier identified from logs. Apply pressure in the well until either a pressure response is seen in the casing annulus at surface, or a leak-off response is observed.
- Perforate the casing at the top and base of the potential barrier identified from logs. Then run a test string with a packer and set a packer between the perforations. Apply pressure in the test string until either a pressure response is seen at the test string annulus, or a leak-off response is observed.

- Run a cased hole formation tester with pump-in capability. Make a hole in the casing at the base of the potential barrier. Monitor formation pressure to ensure no connectivity to other pressured zones. Pump into the hole until leak-off pressure is reached. Repeat the measurement to ensure good quality.

After a pressure test is successfully executed, the bond log response associated with the now proven barrier is assumed to indicate the required minimum acceptable bond log response for barrier confirmation in subsequent wells (15). Thus, the next time the bond log alone is qualified to identify and annular barrier in that particular shale horizon without performing pressure tests.

3.4 Advantages and disadvantages with shale as sealing material

Table 3.4 presents some general advantages and disadvantages with shale formations as sealing materials.

Table 3.4 Advantages and disadvantages with shale as a sealing material

Advantages	Disadvantages
• Proven to seal over millions of years • Self healing • Chemically inert • Capillary effects • Free natural barrier • Extremely low permeability	• Unless casing strings are removed only applicable as annular barrier element • Creation uncertain and time consuming • Likely only to be applicable for PP&A in some wells • In areas with multiple casing strings, all but the largest have to be pulled in order to identify shale barriers.

4. Behaviour models and downhole stress states

As mentioned in the previous chapter a relatively new approach when it comes to annular sealing materials is to use radially inward moving impermeable rocks that close of the annular space of the wellbore. The behaviour occurs as a response to the change in stress state around the wellbore during and after drilling and is furthermore dependent on the material properties as well as the initial stress situation. In this chapter behaviour models, ways to determine the initial downhole stress state in addition to the different mechanisms responsible for the change in stress and their contributions to the final stress state will be presented.

4.1 Behaviour models

To be able to predict the behaviour of a material, the stress state has to be calculated. To calculate the stress state one must furthermore assume deformation behaviour. For shales this is further complicated by the fact that shales falls into a category that lies at the boundary between weak rocks and stiff or hard soils. Their lithology is typically similar to that of clay soil, but their strength characteristics is often more comparable to those of rocks (39). Due to the latter, shales will in this thesis manly be threated as rocks, but for completeness and better understanding of the behaviour of soft shales, also behaviour theories used to describe soils will be presented.

4.1.1 Shale as a rock

All solid materials, such as rocks will deform when subjected to stress. The exact behaviour may often be difficult to predict, however there are many different theories trying to explain the relationship between applied stress and the resulting deformation (strain). Here some of the most common theories are discussed.

4.1.1.1 Elastic behaviour

Most solid materials have an ability to resist and recover from deformations produced by forces. This ability is called elasticity. When an elastic material is deformed due to an external force, it experiences internal forces that try to counteract the deformation. The more the material is deformed the higher these forces gets until equilibrium condition is reached. If the external force is later on removed the material will return to its original shape due to the internal counteracting forces being larger than the external forces.

The simplest possible model to explain elastic behaviour is when there is a linear and unique relationship between the applied stress, σ, and the resulting strain, ε. In one dimension the relationship is given by an equation known as Hooke's law:

$$\sigma = E \cdot \varepsilon \quad (4.1)$$

Where E is called Young's modulus and is a measure of the rocks stiffness, i.e. the resistance against being compressed by a uniaxial stress. Strain is defined as a change of relative positions of particles within the material and can occur either as elongation

$$\varepsilon = -\frac{\Delta L}{L} \quad (4.2)$$

or shear strain

$$\gamma = \frac{1}{2}\tan\psi \quad (4.3)$$

Where L is the original distance between two particles, ΔL is the change in distance between the two particles and ψ is the change in angle between two initially orthogonal directions.

In three dimension the relationship can be written as (36):

$$\varepsilon_X = \frac{\sigma_x}{E} - \frac{\nu}{E}(\sigma_y + \sigma_z) \qquad \gamma_{yz} = \frac{\tau_{yz}}{2G}$$

$$\varepsilon_y = \frac{\sigma_y}{E} - \frac{\nu}{E}(\sigma_x + \sigma_z) \qquad \gamma_{xz} = \frac{\tau_{xz}}{2G} \qquad (4.4 - 4.9)$$

$$\varepsilon_z = \frac{\sigma_z}{E} - \frac{\nu}{E}(\sigma_y + \sigma_z) \qquad \gamma_{xy} = \frac{\tau_{xy}}{2G}$$

Where σ_x, σ_y, σ_z are the stresses in the x-,y- and z direction and ε_x, ε_y, ε_z and γ_{xy}, γ_{yz} and γ_{xz} are the resulting strains. ν is the Poisson's ratio, a measure of lateral expansion relative to a longitudinal contraction, while G is the shear modulus and is a measure of the rocks resistance against shear deformation. Note that here as well as in the rest of this thesis, due to most downhole stresses being compressive in nature, compressive stresses are defined as positive.

The theory of linear elasticity is often sufficient to describe the stress response in solid materials at relatively small stresses, but the region of validity for linear elasticity is often exceeded in practical situations and for instance nonlinear elastic behaviour may be observed. For a nonlinear elastic material, the stress-strain relationship may be written as:

$$\sigma = E_1\varepsilon + E_2\varepsilon^2 + E_3\varepsilon^3 + \ldots \quad (4.10)$$

Where E_1, E_2 and so on are functions of the strain (or alternatively stress).

Since both σ and ε generally are tensors, nonlinear elasticity can be become very complicated mathematically and for simplicity it will therefore not be given much attention in this thesis. Fig. 4.1 shows some typical examples of stress-strain relations seen in elastic materials. Fig. 4.1a illustrates a linear elastic material. Fig. 4.1b shows a nonlinear perfectly elastic material. Meaning that although there is a nonlinear relationship between stress and strain, the relation is identical during the loading and unloading process. Fig. 4.1C illustrates a relation commonly seen in rocks called hysteresis, where the unloading path is different from the loading path. The explanation behind the latter is that the work done during loading is not entirely released during unloading, i.e. a part of the strain energy dissipates in the material (36).

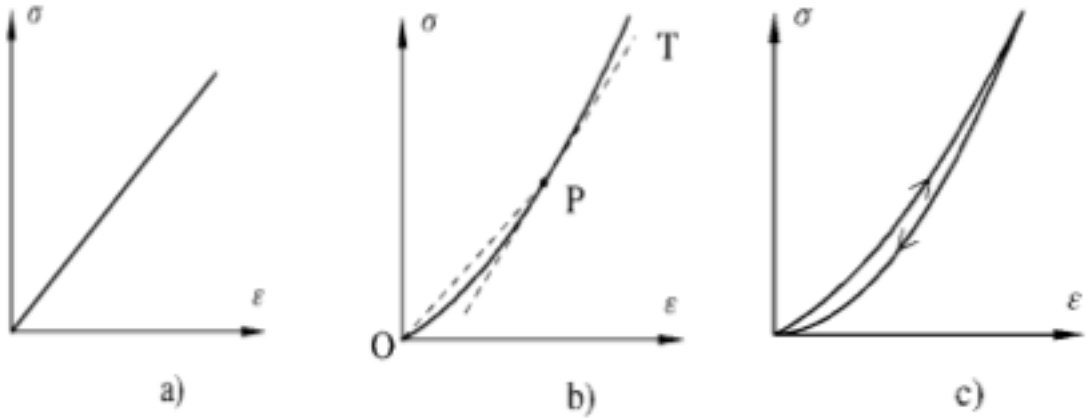

Figure 4.1 Stress- strain relations for elastic behaviour: a) linear elastic material. b) Perfectly elastic material. c) Elastic material with hysteresis. Free after (36).

4.1.1.2 Elastoplastic behaviour

As discussed in the previous section, an elastic material is a material where the induced strain due to an external force vanishes when the stress state returns to its origin. For sufficiently large stresses, many rocks enter a phase where permanent deformation occurs, yet the material is still able to resist further loading (i.e. the slope of the stress strain curve is still positive). The phase is called the plastic (or ductile) region and materials that responds to stresses in this way is said to have elastoplastic behaviour. To describe such materials a model called elastoplastic behaviour model is used.
The model assumes that for small stresses the elastic theory is valid. But after reaching a certain stress state, defined by a yield criterion, the stresses starts to induce permanent deformation in the material. Hence, according to the model the total strain can be seen as the sum of the elastic and plastic contributions, given as (12):

$$d\varepsilon_{tot} = d\varepsilon_{ij}^{el} + d\varepsilon_{ij}^{pl} \quad (4.11)$$

In the equation the elastic part, ε_{ij}^{el}, will vanish when the stress is released, while the plastic part, ε_{ij}^{pl}, is irreversible and will not be recovered.

On a microscopic scale the difference between elastic and plastic deformation is that the former only involves stretching of atomic bonds, while ductile deformations comprises breaking and rearrangements of inter-atomic bonds. The latter is obtained through slip, which is defined as sliding of planes of atoms over one another. This typically occurs along weakness planes, caused by irregularities in the atoms structure known as dislocations. Exactly how the plastic strain will develop for a given loading situation is given by flow rule, which typically is function involving the yield criterion and a constant dependent on the shape of the stress strain curve (42).

As mentioned, although irreversible deformations are accumulated when the material reaches the plastic region, this does not necessarily mean that the material completely looses its integrity. This is illustrated in figure 4.2, which shows typical behaviour of a rock during an unconfined uniaxial compression test.

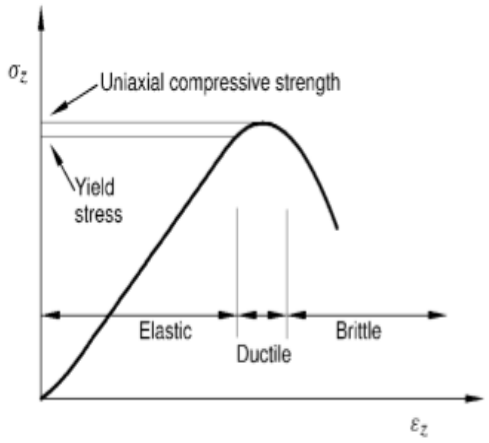

Figure 4.2 Stress vs. strain plot for uniaxial compression of rocks (36).

The highest point on the curve is the uniaxial compressive strength, which is the maximum load that the material can take under the given confining pressure. Material failure is often defined as either the yield point (point where yield criterion is fulfilled) or the peak stress point on the curve. However, since for ductile materials the material continues to support load even after this point a better definition may be where the material completely looses its integrity, seen as a rapid drop in the stress-strain curve due to e.g. developments of cracks. Using such definition, ductility can be seen as the extent to which a material can undergo plastic deformation before fracture.
Material failure and yield criterions will be discussed further in chapter 5.

Although more realistic, the elastoplastic model is as seen way more complicated than the elastic model. In addition to what is already mentioned, the behaviour is also typically a function of loading history due to strain hardening or strain softening properties of the material. The former is seen as an expansion of the yield surface when the material is taken to a higher stress levels than what it previously has been exposed to. This is illustrated in figure 4.3, and can be explained by the increasing number of dislocations created as plastic deformation proceeds impeding further deformation due to intersections of dislocations moving on different planes (42).
Strain softening on the other hand is defined as an unstable response, where stress is a monotonically decreasing function of strain. In contrast to strain hardening, strain softening is associated with a deformation mode, which is inhomogeneous on macro scale (e.g. formation of shear band), thus it cannot be interpreted strictly as a material response, but rather as a foretaste of failure (43).

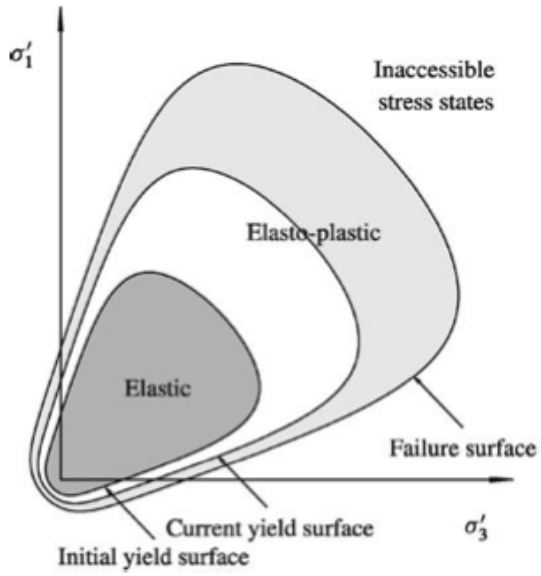

Figure 4.3 Sketch of strain hardening in stress space. Initial yield surface is the original yield surface, current yield surface is the yield surface after some plastic straining, while failure surface is defined as the surface separating accessible states from inaccessible states. After (36).

As mentioned, most materials will experience some sort of strain hardening or strain softening when exposed to stress states that fulfil the yield criterion. However, theoretically it is possible to define extreme cases where no such behaviour is observed, such materials are called perfectly brittle and perfectly plastic materials. The former represents materials that completely looses their integrity when stresses exceeds the yield criteria, while the latter will as a response to stresses above its yield, endure infinite plastic strain without ever losing its ability to carry load. The difference between a perfectly brittle and a perfectly ductile/plastic material is illustrated in figure 4.4. The effect of borehole formations brittle or ductile behaviour on their ability to create an annular seal will be discussed further in chapter 5.

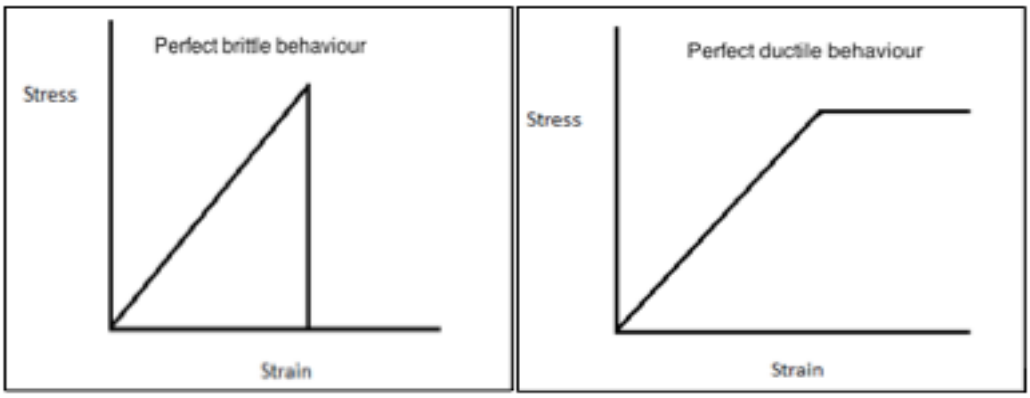

Figure 4.4 Perfectly brittle and perfectly ductile/plastic material. Free after (9).

4.1.1.3 Thermo elasticity

In addition to changes in the stress state due to external forces, the downhole rocks are often also subjected to temperature changes. Temperature changes may occur during production or injection in the wellbore or through for instance setting of cement.

Most materials expand when the temperature increases and contracts when it decreases. If the material is constrained in someway the desired behaviour, due to changes in temperature, may be prevented, hence leading to a change in stress state. As a consequence, thermal effects have to be taken into consideration when determining the stress state. The deformation caused by thermal effects is given by (12).

$$\varepsilon = \alpha_T T \quad (4.12)$$

Where T is the temperature change and α_T is the coefficient of linear expansion.
A elastic model including thermal effect can be written in cylindrical coordinates as (12):

$$\varepsilon_r - \alpha_T T = \frac{\sigma_r}{E} - \frac{\nu}{E}(\sigma_\theta + \sigma_z) \quad (4.13)$$

$$\varepsilon_\theta - \alpha_T T = \frac{\sigma_\theta}{E} - \frac{\nu}{E}(\sigma_r + \sigma_z) \quad (4.14)$$

$$\varepsilon_z - \alpha_T T = \frac{\sigma_z}{E} - \frac{\nu}{E}(\sigma_r + \sigma_\theta) \quad (4.15)$$

$$\gamma = \frac{\tau_{rz}}{2G} \quad (4.16)$$

Where subscripts θ and r represents changes in the tangential and radial direction respectively.
As changes in temperature occurs as a diffusion process, for calculation purposes with temperature as a function of time, the heat diffusion equation can be used (12):

$$\frac{\partial^2 T}{\partial r^2} = \frac{1}{r}\frac{\delta T}{\delta r} + \frac{\partial^2 T}{\partial z^2} = \frac{\rho C}{\lambda}\frac{\delta T}{\delta t} \quad (4.17)$$

Where λ are the thermal conductivity, ρ the density and C the specific heat.

4.1.1.4 Poroelasticity

So far, only general behaviour models for solid materials have been discussed. However, rocks are porous materials and their response to stresses, depend to a large extent on the non-solid part of the material. It can be shown that for porous materials the deformation is proportional to the effective stress, σ', defined as(36):

$$\sigma' = \sigma - \alpha p_p \quad (4.18)$$

rather than the total stress σ. In the equation p_p is the internal pore pressure and α is the Biot-coefficient. The latter is a parameter that varies between 0-1 and describes the efficiency of the pore pressure to counteract the total applied stress. Thus physically, eq. 4.18 states that the solid framework carries the part σ' of the total external stress, while the remaining part αp_p, is carried by the fluid. Since hydrostatic pressures don't contribute to shear stress, only the normal effective stress is dependent on pore pressure (36).
The Biot α is given as:

$$\alpha = 1 - \frac{K_{fr}}{K_s} \quad (4.19)$$

Where K_{fr} and K_s is the bulk modulus of the rock frame and solid part of the rock respectively. From eq. 4.19 it can be seen that the Biot-coefficient is approximately 1 for unconsolidated or weak rocks (K_{fr}=>0), while stronger rocks will yield lower positive values.

4.1.1.5 Time-dependent behaviour

So far, the behaviour models discussed has assumed that a change in applied stress is followed by an instantaneous deformation. However, quite often the deformation continuous for a long time after the change stress is applied. The time-dependent effects can be divided into two groups: consolidation and creep. The former is due to pore pressure gradients induced by a change in stress state, and the fact that it takes time to re-establish pore pressure equilibrium. While, the latter is related to visco-elastic behaviour of the solid framework (36). A more detailed description of the two effects will be given in chapter 5.

Time-dependent behaviour is not an alternative model to the previously mentioned models, but rather an extension. In models that include time-dependent behaviour, deformation caused by it can for instance be added to the instantaneous deformation (12):

$$\varepsilon = \varepsilon_{el} + \varepsilon(t) \quad (4.20)$$

Where ε is the total deformation, ε_{el} is the elastic part and ε(t) is the time-dependent deformation caused by either consolidation or creep. As with instantaneous deformation, time-dependent deformation can be either permanent or reversible. In general high changes in stress will often also lead to permanent time-dependent deformations (36).

4.1.2 Shale as a soil

So far in the discussion about shale behaviour, shales has been assumed similar to solid materials. Another approach frequently used on weakly cemented sedimentary rocks, such as shales/clays, is to use the concept of soil mechanics. Soils mechanics has been developed for systems with little or no cement between the individual grains, and although it theoretically shares many of its origins with rock mechanics it has a distinct different approach to solving problems related to deformation and failure.

One of the main differences is that rock mechanics tends to emphasize the current stress state when predicting the behaviour of the rock, while soil mechanics is more focused on the stress history and the rocks ability to drain (39).

As with rock mechanics, isotropic compression and a series of triaxial test at different confining pressures are typically conducted to determine the mechanical properties of materials also in soil mechanics. However, in contradiction to rock mechanics, which usually represent these tests in a stress-strain plot, the soil mechanics test are typically plotted in a q vs. p', ν vs. p' or in three dimensions in a q,p',ν plot. Where q is the generalized shear stress, p' is the effective mean stress and ν is the specific volume. A

more detailed description of these parameters and how they are defined can be found in appendix D.

On of the most important concepts within soil mechanics is the Critical State theory (CS-theory), which aim to explain the mechanical behaviour seen in soils when exposed to hydrostatic and triaxial loadings. As mentioned earlier, the behaviour of soils is very dependent on the stress states it has previously been exposed to. This is illustrated in figure 4.5, which schematically shows the principles of CS-theory for hydrostatic loading of clay under drained conditions. Starting with a virgin sample (i.e. sample that has never been exposed to any stress before), loading of the sample will lead to a reduction in the specific volume along the line AB. If the sample is unloaded at point B, it will follow the line BD. The change in slope can be seen as increased stiffness of the sample due to the sample previously being taken to higher stress levels. Furthermore, if the sample is reloaded at point D, the deformation will follow path DB, until it reaches the point B, thereafter it follows the line BC again with reduced stiffness. The example shows several important concepts within soil mechanics:

- A sample that is at the highest stress level it has ever experienced is defined as normally consolidated (represented by the line ABC).
- A sample that has been exposed to higher stress levels before is defined as overconsolidated (represented by line BD).

As seen overconsolidated samples are stiffer than normally consolidated samples. In general the more overconsolidated they get the stiffer they become. The stiffness can be quantified through the overconsolidation ratio defined as the highest stress state it has experienced, divided by the current stress state. The highest stress state is frequently also referred to as the preconsolidation stress (36). Moreover, according the CS-theory, states to the right of the normal consolidation line are forbidden states. Thus, all intact materials are therefore always either in a normal or over-consolidated state (39).

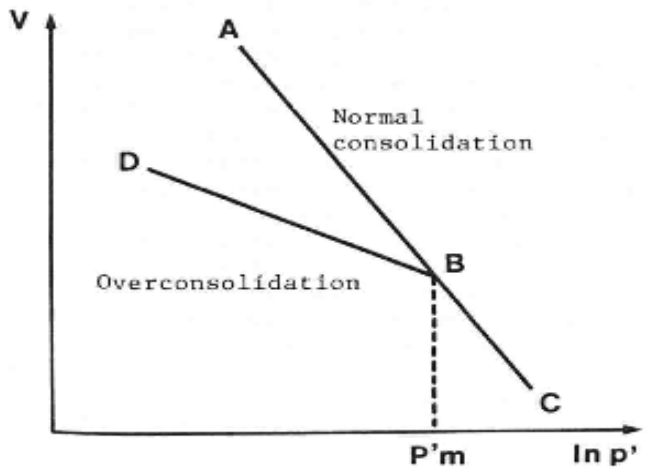

Figure 4.5 Schematic illustration of isotropic compression of clay. After (39).

Another important concepts within soil mechanics and the CS-theory is the existence of the critical state line (CSL), Roscoe-and Hvorslev surfaces for each material. The Roscoe-

and Hvorslev surfaces are surfaces in the v-p'-q space, that describes how the materials will behave under a triaxial tests depending on whether they are normally or overconsolidated respectively. The critical state line represents boundary between the surfaces and can be seen as the ultimate stage where large shear strain may occur at no change in shear stress. The CSL and the surfaces are illustrated in figure 4.6. By extrapolating the surface down in the q-p' plane it can be seen that for a normally consolidated clay (follows the Roscoe surface) the loading path curves to the left, i.e. the pore pressure increases. While, for a strongly overconsolidated clay (follows the Hvorslev surface) the same projection shows that loading path curves to the right, i.e. pore pressure decreases.

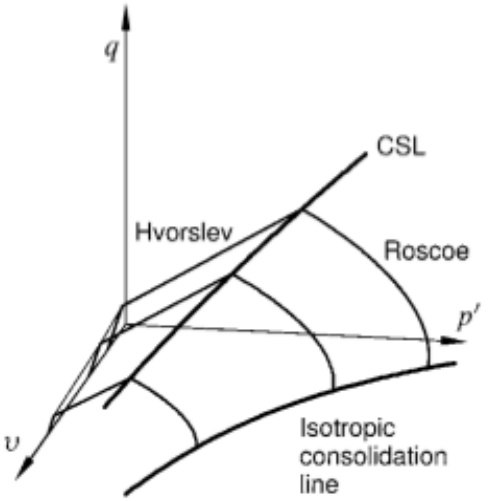

Figure 4.6 Hvorslev and Roscoe surfaces in v-p'-q space. After(36).

4.2 Initial stress state

Up to now, only behaviour models that can be used to describe the deformation due to a change in stress state have been discussed. To be able to use these models the change in stress state has to be calculated. Since the behaviour of the shales is dependent on the change in effective stress state, both the initial and the final effective stress state are of interest. Here the focus will be on the initial stress state, while the final stress state will be discussed in the next section.

4.2.1 Background

The initial stress situation within the earth in sedimentary rocks before a well is drilled is greatly dependent on the long and in many cases complicated process from the initial state as loose sediments until the present state as a solid rock (36). It consists of three mutually orthogonal principal stresses, plus the pore pressure. It is a common assumption that the vertical stress is a principal stress, and since for most cases at large depths the assumption is valid, it will also be used in this thesis. As a consequence the two other directions are in the horizontal plane, typically referred to as the maximum and minimum horizontal stress, denoted σ_H and σ_h respectively.

Knowledge about the initial stress state is essential when planning a well, due to its impact on the required mud weight to avoid wellbore instability problems and casing setting depths.
Information about it is usually based on experience from directly measured values during drilling in adjacent wells. However, for wildcats and exploration wells, when no such knowledge is present, the well planners have to rely on indirect or empirical models for estimations (44). For illustrative purposes, and to be able to make some simplified calculations on the deformation behaviour of different shales later on, some of these estimation methods will be presented in the subsequent sections.

4.2.2 Initial vertical stresses

The vertical stress, frequently referred to as the overburden, at a particular depth in the earth is equal to the combined weight of the overlaying formation divided by the area that supports the weight. For a homogenous column of height z, the vertical stress is given by:

$$\sigma_v = \rho_{ovb} g z \quad (4.21)$$

Where ρ_{ovb} is the average density in the overburden and g is the acceleration of gravity. Normally the density varies with depth, and in such cases the vertical stress at depth D can be given as

$$\sigma_v = g \int_0^D \rho_{ovb}(z) dz \quad (4.22)$$

Where ρ_{ovb} (z) is the local or in-situ density of the fluid saturated formation at depth z. It can be found through for instance sonic logs during drilling or through some equations correlating it to measured seismic data, such as velocity and interval transit time (44) . Although the density increases with depth due to reduced porosity, the average density of sediments in the overburden is usually between 1800-2200kg/m3, thus as a rough estimate the vertical stress increases downwards with approximately 20 MPa/km (36).

4.2.3 Initial pore pressure

Knowledge about the initial pore pressure is important during drilling to avoid problems such as stuck pipe, kicks and in the worst case blowouts. Since the effective stress has to be used to determine the behaviour of downhole rocks, it also has a huge impact on wellbore stability and thus also the behaviour of the downhole rocks.
The pore pressure within the downhole formations can be either defined as normal or abnormal.
Normal pore pressure means that the pore pressure is equal to the hydrostatic pressure exerted by the pore fluid column above the depth of interest. Thus, in a similar way to eq. 4.22 the normal pore pressure, p_{fn}, can be given as:

$$p_{fn} = g \int_0^D \rho_f(z) dz \quad (4.23)$$

Where p_f is the pore fluid density, which typically is in the range of 1030-1070kg/m3 (36). Thus for normally pressured regions, the pore pressure increases with about 10MPa/km.
The term abnormal pore pressure is used for zones where the pressure is above the normal pressure. It could occur as the result of numerous mechanism, such as rapid sedimentary loading, tectonics, or changes in the pore fluid (45). A further description of these mechanisms can be found in appendix D.

To estimate the downhole pore pressure several techniques such as the Hottman & Johnson, Equivalent depth, Eaton and Bowers methods exist (46). They are all based on the assumption that the pore pressure influences rock properties such as porosity, density, sonic velocity and resistivity, i.e. compaction dependent properties. They can furthermore be divided into either direct or effective stress methods.
The direct methods involve directly relating the amount a pore pressure indicator diverges from its normal trend line to the pore pressure gradient at the depth of investigation, while the effective stress methods uses the principle of effective stress to relate measured values to pore pressure (46). For further information about these methods and examples on how to apply them the reader is referred to the book " Pressure control during Oil Well drilling" (47) and the master thesis "2D Vertical Effective stress modelling of the Tor Area" (46).

4.2.4 Initial horizontal stress

The horizontal stress is induced by the vertical (overburden) stress and tectonic activity. Assuming no tectonic activity, elastic behaviour and that the formation under consideration is laterally constrained, i.e. no horizontal strain. Eq. 4.4-4.9 yields:

$$\sigma'_h = \frac{\nu_{fr}}{1-\nu_{fr}}\sigma'_v = K_{eff}\sigma_v' \quad (4.24)$$

Where K_{eff}, is a coefficient describing the relationship between the vertical and minimum horizontal effective stress. For a fluid where Poisson's ratio is equal to 0.5, K_{eff} is equal to 1. Thus, the horizontal stress is equal to the vertical stress as is the case with pressure in a fluid, referred to as a hydrostatic stress state. For rocks however, due to their ability to resist shear stress the Poisson's ratio are in general different to 0.5, consequently the effective vertical and horizontal stress will diverse. At shallow depths (0-150m) K_{eff} may be in the region of 1-10 or higher, while values from 0.2-1.5 may be found at greater depths (36).
It has been suggested that with time K_{eff} approaches 1 due to creep, thus indicating the stress state moves towards hydrostatic where the principal stresses are equal (for rocks alternatively also called lithostatic stress state). The theory is called Heim's rule. Because the transition towards lithostacy is normally very slow, together with general uncertainties and complexities, such as stress history, chemical compaction and behaviour models, it is almost impossible to find a general rule for predicting horizontal stresses at depth (36).

Although difficult several relatively simple methods have been developed with the purpose of estimating the minimum horizontal stress, such as the Hubbert & Willis, Matthews & Kelly, Eaton's, Daine's method (46). These are all based on ways of estimating the effective stress ratio, K_{eff}, but due their simplicity they hardly resemble the subsurface conditions. Thus, the by far best way obtaining the minimum horizontal stress is to measure it directly through for instance an LOT or an XLOT.
However, a simple and quick estimate of the minimum horizontal stress, in cases where the pore pressure is known, can be found using the Breckels & van Eckelen equations (48):

$$\sigma_h = 0.0264D - 31.7 + 0.46(p_p - p_{fn}) \quad (D > 3500m) \quad (4.25)$$

$$\sigma_h = 0.0053D^{1.145} + 0.46(p_p - p_{fn}) \quad (D < 3500m) \quad (4.26)$$

Where D is the depth (TVD), p_p and p_{fn} is the pore pressure and normal pore pressure respectively. In the equation the stress and pore pressure are in MPa and depth in meters. The equations are derived based on fracturing field data in the gulf of Mexico at zero or shallow water depths, but due to the lack of tectonic activity they can also be used with a fair degree of confidence in the North Sea (36).
Although so far assumed, the principal stresses are generally not equal, the main reason being tectonic activity. While, there are no straightforward methods available for measuring the maximum horizontal stress, the horizontal stress directions can be determined with borehole imaging or borehole shape measurements (e.g. 4-arm caliper) in areas where the wellbore has failed either through shear or tensile failure. Shear failure will be induced in the direction parallel with the smallest horizontal stress, while tensile failure will occur in the direction parallel to the largest horizontal stress (36).

4.3 Stress state around the borehole

As described in the previous section prior to drilling a well, there are compressive stresses present in the formation. When the well is drilled, the rock stresses in the vicinity of the wellbore are redistributed as the hydraulic pressure of the mud column replaces the support originally offered by the solid rocks. The exact redistribution of these stresses is however subjects of complex matter affected by for instance: hole deviation, inhomogeneity, anisotropy, and plasticity as well as instantaneous and time-dependent physical and chemical processes. As a consequence, general analytical equations cannot be derived. However, for illustrative purposes this section gives a description of how these stresses can be found or estimated assuming several simplifying assumptions. For more accurate results numerical simulators have to be used.

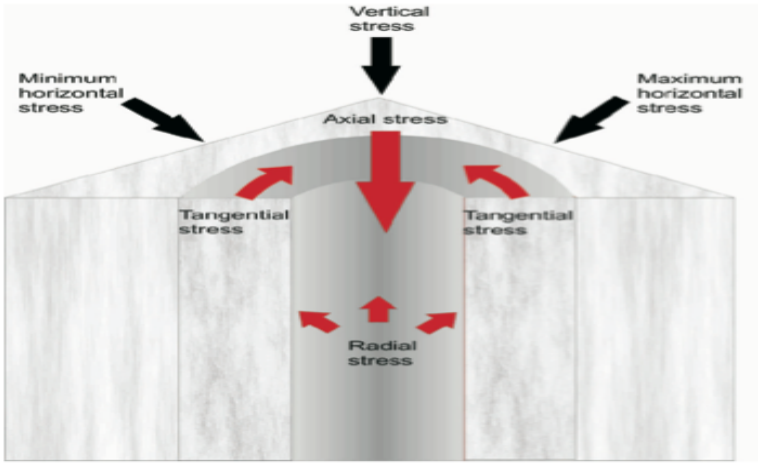

Figure 4.7 Wellbore Stresses. After (49).

4.3.1 Mechanical stress state contributions

As a simplification of what's happening during drilling in shale sections one could assume that only mechanical effects play a role when it comes to hole stability and the stress situation. By transforming stress and strain from cartesian to cylindrical coordinates, expressing Hook's law (eq. 4.4-4.9) in cylindrical coordinates, using equilibrium and standard boundary conditions and furthermore assuming a vertical and impermeable borehole with radius R_w and isotropic horizontal stresses, it can be shown that the principle stresses vs. distance, r, from the centre of a cylindrical borehole can be given as(9) :

$$\sigma_\theta = \sigma_h + (\sigma_h - p_w)\frac{R_w^2}{r^2} \quad (4.27)$$

$$\sigma_r = \sigma_h - (\sigma_h - p_w)\frac{R_w^2}{r^2} \quad (4.28)$$

$$\sigma_z = \sigma_v \quad (4.29)$$

Where p_w is the well pressure and $\sigma_\theta, \sigma_r, \sigma_z$ and is the tangential (hoop), radial and axial stress respectively. The different directions are illustrated in Fig 4.7. In a case where $\sigma_\theta > \sigma_z > \sigma_r$ at the borehole wall the stresses vs. distance from the centre of a cylindrical borehole is illustrated in figure 4.8. As illustrated the wellbore stresses diminish rapidly with distance from the wellbore wall and eventually converting to the far field stresses. This is because away from the wellbore the rock is in an undisturbed state.

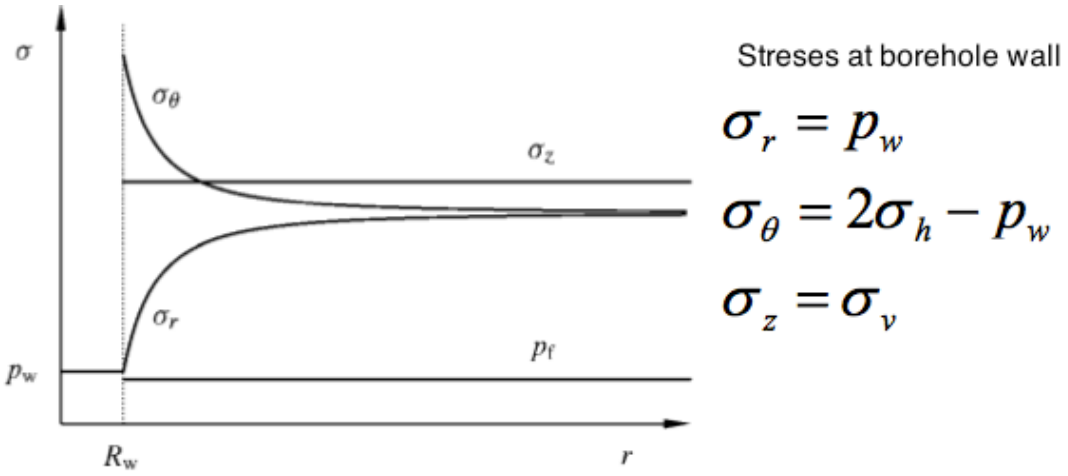

Figure 4.8 Stress around a borehole in a linear elastic formation. Free after(36).

The equations above assumed isotropic stresses, a more general version including horizontal anisotropy is given as:

$$\sigma_\theta = \sigma_H + \sigma_h - 2(\sigma_H - \sigma_h)\cos 2\theta - p_w \quad (4.30)$$

$$\sigma_z = \sigma_v - 2\nu_{fr}(\sigma_H - \sigma_h)\cos 2\theta \quad (4.31)$$

$$\sigma_r = p_w \quad (4.32)$$

Where θ is the angle measured relative to the direction of the major horizontal stress. So far only equations for vertical boreholes have been presented; however by interchanging the far-field stresses, expressions for a horizontal borehole along a principle stress direction can be easily derived. For deviated boreholes the equations includes shear stress and becomes much more complex. As the purpose of this chapter is mainly to illustrate qualitatively what is happening downhole these equations is not included here. However, the interested reader is referred to the book " Petroleum Related Rock Mechanics" for a more detailed description(36).

4.3.2 Temporary stress state contributions

Although, as a simplification, one could assume that only the mechanical effects play a role when it comes to the stress situation at the wellbore wall, the assumption is clearly somewhat wrong. Typically, effects such as pressure equilibrating, thermal and chemical differences between the wellbore and surrounding rock play a role. As these effects are temporary, they will only contribute during a transition period, and when the differences has equilibrated they will vanish. Here equations describing the stress contribution of these time dependent effects will be presented. Since the governing equations (elasticity, thermoelasticity etc.) that the stress equations below are derived from are linear, the final expression can be seen as a sum of them according to the principle of superposition (36).

4.3.2.1 Stress state contribution of pore and well pressure equilibrating

Immediately after a well is drilled in a low permeable formation, such as a shale zone, the pressure in the wellbore will normally be higher than the pressure in the pores. Though a diffusion process the pore pressure close to the borehole wall will gradually approach the well pressure. The increase in pore pressure will result in the material trying to expand, eventually leading to an increase in stress in the tangential and axial direction given as (36):

$$\Delta\sigma_{perm} = \alpha \frac{1-2\nu_{fr}}{1-\nu_{fr}}(p_w - p_{fn}) \quad (4.33)$$

Where P_w and P_{fo} are the well and initial pore pressure respectively.

The time,τ_D, it takes for the pressures to equilibrate over a distance l_D, hence the effect to be maximized (as seen in eq. 4.33), is governed by both fluid and rock properties and can be given as (36):

$$\tau_D = \frac{l_D^2}{C_D} \quad (4.34)$$

Where C_D is the consolidation coefficient:

$$C_D \approx \frac{kK_f}{\mu\phi}\left[1 + \frac{K_f}{\phi(K_{fr} + \frac{4}{3}G_{fr})}\right]^{-1} \quad for \quad K_{fr} \,\&\, G_{fr} << K_s \quad (4.35)$$

For normal shale sections with permeability of about 1 nanoDarcy, pressure equilibration in the near wellbore region (10cm) typically takes about 5-10 days (36). After this the stress state will stabilize according to eq. 4.33.

As seen by eq. 4.35 the consolidation coefficient depends not only on fluid parameters, but also on the elastic properties of the rock. This is because pressure equalization is not only a pure flow process, but also (especially in low permeable and soft formations) highly dependent on the rocks ability to transmit external stress towards the pore pressure, as described by Biot-Hooks's law. This will be further discussed in chapter 7.

4.3.2.2 Thermal stress contribution

When a well is drilled the drilling fluid is usually colder than the formation to be drilled. As a consequence, the drilling fluid will alter the temperature of the surrounding formation. According to the theory of thermoelasticity (section 4.1.1.3) when the temperatures changes, the formation expands or shrinks, which again affect the stress state. By applying thermoelastic equations it can be shown that the thermal contribution to tangential and axial stress at the borehole wall is given as (9):

$$\Delta\sigma_T = \alpha_T \frac{E_{fr}}{1-\nu_{fr}}(T_w - T_o) \quad (4.36)$$

Where T_w is the temperature in the well, T_o is the reservoir temperature and α_T is the thermal expansion coefficient (in the region of 10^-5°C^-1). Hence, according to the equation in cases where the drilling fluid is colder than the formation the thermal contribution will be a reduction in tangential and axial stress.
Moreover, cooling of a low permeability rock like shale will reduce the pore pressure, due to a larger thermal expansion coefficient for the fluid than for the solid parts of the rock. Hence, resulting in a further reduction of the effective stresses in the tangential and axial direction. Furthermore, rock properties such as strength and stiffness may be altered as a result for temperature changes. This will be further discussed in chapter 6. As with pressure equilibrating the effect of temperature is only temporary, unless means of keeping the mud temperature different from the formation is actuated, the mud will heat up and the effect will vanish.

4.3.2.3 Chemical stress contributions

Another time-dependent effect that contributes to the stress situation in shales sections is chemical interactions between the drilling fluid and the formation through a process known as osmosis. Osmosis is based on the fact that when a semipermeable membrane separates two areas with different water activity, water will diffuse from the low activity to the high activity area until they are equalized. In petroleum wells the semipermeable membrane permitting and preventing water and ion exchange respectively, can be thought of in two different ways (36):

1. Oil based mud may act as semipermeable membrane. Ions associated with salts are prevented to move between the water phase of the mud and the formation.
2. The shale itself may act as permeable membrane when in contact with water based mud. In this case the membrane properties are caused by surface charges of the clay mineral hampering ion movement.

The differences in water activity across the membrane sets up a osmotic potential given as

$$\Delta\Pi = \sigma\left(\frac{RT}{V_w}\right)\ln\frac{a_{w,df}}{a_{w,sh}} \quad (4.37)$$

Where R is the molar gas constant (8.31 J mol^-1 K^-1), V_w is the molar volume of water (0.018 l/mol), T is the temperature in kelvin, $a_{w,df}$ and $a_{w,sh}$ is the chemical activity of water in the drilling fluid and shale pore water respectively, and σ is the membrane efficiency. The activity denotes the effective concentrations of water in a solution, thus for freshwater a_w=1 and for salt water a_w<1. Membrane efficiency is a added coefficient, with typical values in the region of 0.05-0.30, to take into account the fact that ions move through shales and interact through e.g. ionic exchange (50).

As described above the osmotic potential give rise to water flow either out of or into the formation, hence either reducing or increasing the pore pressure respectively. As with the process of pressure equilibrating this " depletion/injection" of pore fluids will result in the material trying to shrink/expand, thus leading to changes in the tangential and axial direction given as (9):

$$\Delta\sigma_{osm} = a\frac{1-2\nu_{fr}}{1-\nu_{fr}}\Delta\Pi \quad (4.38)$$

The process of osmosis is illustrated in figure 4.9.

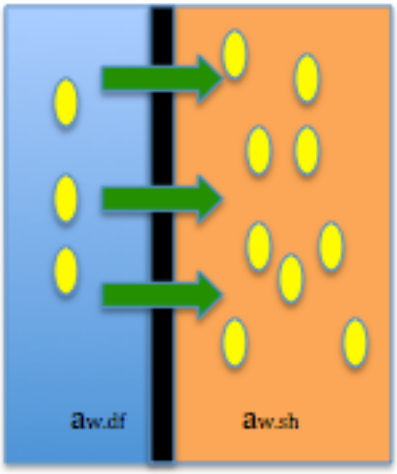

Figure 4.9 Osmosis process with aw,df> aw,sh. Water goes from area with lowest salinity level (wellbore) to the one with highest salinity level. Ion particles (yellow) cannot go through semipermeable membrane (black) formed by charged clay particles.

4.3.3 Time dependent stress state contributions

So far only mechanical and temporary effects, set up by physical or chemical differences, occurring when the wellbore is drilled due to the formation initially in place being replaced by drilling fluid with different properties has been discussed. Another reason for change the stress state, as a function of time after the well is drilled, is due to heavy particles, such as for instance Barite, settling out of the mud, hence making mud density a function of time and depth.

In a static situation, as when at rest in the annulus after the cement operation, the mud will develop a gel structure with a certain mechanical strength, τ_g. Equilibrium between the gravitational forces acting on the volume element of a particle and the gel strength which act on the surface of the sphere can be written as (51):

$$4\pi r_p^2\tau_g = (\rho_p - \rho_{fluid})g\frac{4}{3\pi r_p^3} \quad (4.39)$$

According to eq. 4.39, the gel strength necessary to suspend a spherical barite particle with a diameter of 60 µm, density 4200kg/m3 in a 1500kg/m3 mud is 0.26 Pa (51). This is much lower than typical standard values for gel strength in drilling muds. As a consequence, at static conditions barite settling will according to eq. 4.39 seldom occur. However, with time there is significant evidence that suspended solid particles, substantially denser than the suspending fluid, settle out vertically due to gravitational

effects (41). Typically the particle concentration continuously increases from top to bottom until equilibrium is reached when all heavy particles is at the bottom underlying a column of free water, as illustrated in figure 4.10.

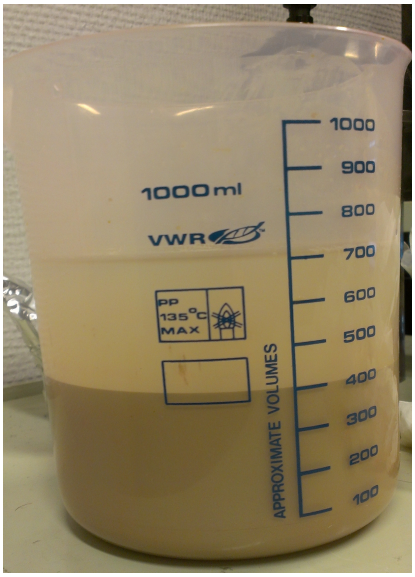

Figure 4.10 Settling of heavy particles. Micro-barite at the bottom, underlaying a column of water.

As mentioned the behaviour seen in fig. 4.10 is not possible according to eq. 4.39. The explanation for what is seen is related to a deterioration of the mud strength severe enough for the mud no longer to be able to suspend the solid particles. This will occur naturally in all muds containing organic substances due to degradation. As most additives are of this type, particle settling out due to gravity with time will occur in most wells (52).

Although much research has been conducted on settling of solid particles in drilling fluids, the exact behaviour and time-dependency of the settling is a complex and not fully understood process. It is dependent on parameters such as plastic viscosity, particle concentration, flow regime, particle interactions, particle shape and size distribution, degree of clustering, gel strength, inclination angle, effect of sliding and mud density (51) and (53). Hence, accurately predicting settling becomes very difficult. However, several simplifying equations are described in the literature. For instance, the settling velocity of single spherical particle, $v_{s,l}$, in a fluid due to gravity can be expressed as (51):

$$v_{s,l} = d_p^2(\rho_p - \rho_{fluid})\frac{g}{18\mu} \quad (4.40)$$

The equation is known as Stoke's law where d_p is the diameter of the particle, ρ_p is the density of the particle, ρ_{fluid} is the density of the fluid, g is gravity and μ is viscosity. As stoke's law assumes no interactions between particles a more realistic equations expressing the slip velocity at higher concentrations, $v_{s,c}$, can be given as (51):

$$v_{s,c} = \frac{v_{s,l}}{(1+1.5c^{1/3})} \quad (4.41)$$

Where c is the solid particle concentration.

Combining eq. 4.40 and 4.41 with a barite particle concentration of 10 vol%, particle density and diameter of 4200kg/m3 and 20µm respectively, in a 1500kg/m3 fluid with viscosity of 40cP,yields a settling rate of 31.27mm/h or 273.92 m/year. Thus in cases where the gel strength deterioration with time is severe, making the mud unable to suspend the solid particles, it is likely that for many wells at the time of PP&A the situation will be settled particles above the casing cement under laying a large column of free water. This is illustrated in figure 4.11.

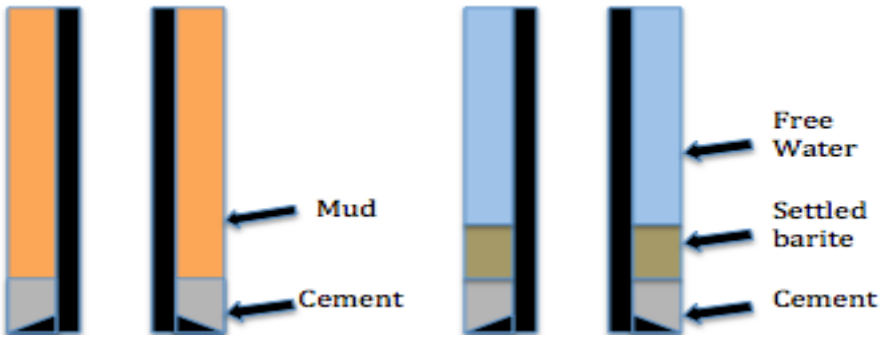

Figure 4.11 Effect of solid particles settling out. Left hand illustration shows initial situation with mud column above the casing cement, while the right hand illustration shows equilibrium situation where heavy particles is accumulated above the casing cement under laying a column of free water.

The equations above rely on several simplifying assumption, for instance it has been shown that settling of particles is more rapid in inclined wellbores than in vertical ones due to a phenomena called Boycott settling (53). For more advanced equations, including effects of e.g. inclination angle, the reader is referred to the paper "Mechanisms, Measurements and mitigation of barite sag"(53).

5. Displacement mechanisms

As mentioned in previous chapters both during and after drilling through some formations, such as certain shale sections, the rock moves radially inward and begins to close off the well. The behaviour occurs as a response to the change in the downhole stress state around the wellbore during and after drilling, and the exact behaviour is furthermore dependent on chemical processes as well as the material properties of the rock. In the previous chapter ways for determining the initial and change in stress state after the hole is drilled was presented. In this chapter common values for shale properties as well as the different mechanisms thought to be responsible for the observed shale movements and their significance for the wellbore closing off will be discussed. In spite of its obvious shortcomings only linear elastic theory will be used. Compared to the more sophisticated elasto-plastic models requiring numerical simulators, linear elastic theory is usually more conservative. Thus, the values presented in this chapter, for the different displacement mechanisms contributions, can be considered lower limits, and slightly higher values could be expected.

5.1 Premise for formations creating an annular barrier

In the rest of this chapter different displacement mechanisms and their possible contribution to the hole sealing off will be presented. Although, rock failure and different failure modes will be discussed in chapter 5.3, that discussion is based on stress states and thus only directly relevant for instantaneous mechanical displacement mechanisms. For the rest of the displacement mechanisms, such as chemical, thermal and creep, whether the material will fail or not when strained due to the mentioned mechanisms is merely dependent on the materials flexibility, i.e. ability to remain intact when strained.

The flexibility is a function of mineral content, stress state, degree of cementation, preconsolidation ratio as well as temperature (54) and (55). Moreover, it is likely to be effected by strain rate and anisotropy. Thus, due to its complexity, estimating flexibility values is very difficult, and the only reliable source of data is laboratory tests executed under the same conditions with the same displacement mechanism as the one being assessed. However, reliable laboratory tests on shales are a scarcity (36). This is mainly caused by 2 reasons. First of all few core samples are taken since shales is not a reservoir rock. Secondly and maybe even more problematic is that laboratory test on shales are very time consuming due to shales low permeability. For instance, a creep test on a shale could take several years, thus since it also require advanced equipment (e.g. triaxial cell) it will be very costly and as a consequence they are seldom conducted.

Because of the difficulty in predicting flexibility, this chapter will mainly assess the different mechanism possible contribution to the formation radially sealing off the annular space. In all cases where it is not obvious, for instance through shear failure being induced due to the stress state, it will be assumed, as premise, that the formations are flexible enough to seal of the annulus. In cases where this assumption is not valid,

the formation will independent of displacement mechanisms not be able to close of the annular space, hence with respect to the creation of annular barrier be uninteresting.

For the formation to be able to seal of the annular space, as mentioned it must be able to take a certain strain. The exact required strain is dependent on the casing and borehole diameter D_{CSG} and D_{OH} respectively, and can be found by applying eq. 4.2 in the tangential direction, which gives:

$$\varepsilon_\theta = -\frac{\Delta L_\theta}{L_\theta} = \frac{2\pi(\frac{D_{OH}}{2} - \frac{D_{csg}}{2})}{2\pi\frac{D_{OH}}{2}} == \frac{D_{OH} - D_{csg}}{D_{OH}} \quad (5.1)$$

A list of different required strains for some standard borehole and casing sizes can be found in table 5.1.

Table 5.1 Required strain to fill annular gap for some standard hole and casing sizes.

Hole size	Casing size	Gap size (in)	Required strain
26"	20"	3	0.23
17 ½"	13 3/8"	2.0625	0.24
12 ¼"	9 5/8"	1.3125	0,21
12 ¼"	10 ¾"	0,75	0,12
8 ½"	7"	0,75	0,18

5.2 Elastic deformation

According to theory of elasticity all solid materials (e.g. rock formations) will instantaneously respond to changes in stress by deforming. Assuming no failure, linear elasticity and a vertical and impermeable borehole with isotropic horizontal stresses, it can be shown that the radial displacement at the borehole wall due to drillout is given as (39):

$$u = \frac{\sigma_h - p_w}{2G_{fr}} R_w \quad (5.2)$$

Where G_{fr} is the shear modulus of the formation, R_w is the borehole radius and p_w is the well pressure.

To illustrate the effect of the elastic deformations, assume the following situation:
A 9 5/8" (0.2445m) casing is placed in a 12 ¼"(0.3111m) wellbore with the casing shoe at 2800m. The casing cement together with settled mud additives make up a column 300m from the casing shoe to 2500m. Above this depth there is a 300m shale section (from 2200-2500m) with sufficient strength and minimum horizontal stress to provide a barrier element if this formation close around the casing. The situation is illustrated in figure 5.1.

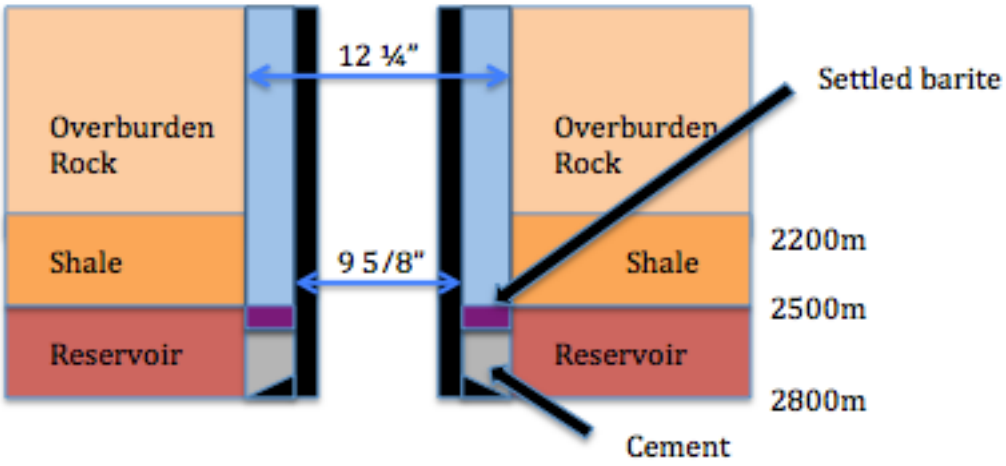

Figure 5.1 Schematic illustration of elastic deformation in 12 ¼" borehole with 9 5/8" casing.

According to Breckels van Eckelen's empirical relations (eq.4.26), assuming normally pressured pores, the horizontal stress at 2500m is

$$\sigma_h = 0.0053 \cdot 2500^{1.145} = 41.2 MPa$$

In the most extreme case, all mud additives have settled out. Hence, leaving a column of water (ρ=1030kg/m3) from 2500m and up, the well pressure at 2500m is then:

$$p_{w,2500} = 1030 \cdot 9.81 \cdot 2500 = 25.3 MPa$$

To close of the whole wellbore the radial displacement has to be:

$$u = \frac{12^{1/4"} - 9^{5/8"}}{2} = \frac{0.3111m - 0.2445m}{2} = 0.0333m$$

By solving eq. 5.2 for G_{fr} and inserting the above calculated values the required shear modulus for the formation to close off the whole wellbore purely due to elastic deformation is:

$$G_{fr} = \frac{\sigma_h - p_w}{2u} R_w = \frac{(41.2 \cdot 10^6 - 25.75 \cdot 10^6)}{2 \cdot 0.0333} \cdot 0.3111 = 0.072 GPa$$

Some typical values for shale and clay shear moduli, as well as calculations showing the percentage of the required deformation that the different shales/clays will undergo using the same assumptions as above, can be found in table 5.2.

Table 5.2 Effect of elastic deformation in different shales/clays. Shear moduli values found in (36)and (39).

Shale	Shear Modulus (GPa)	Percentage of annular gap closed off in 12 ¼" hole with 9 5/8" casing.	Note
Shale (El Paso)	11.8	0.63%	
Weak Shale (North Sea)	0.38-0.5	14.86%-19.55%	
Stiff shale	35	0.21%	
London Clay	0.02	371.42%	• Retrieved close to surface. • Content: Quartz :10-40%, smectite: Ca. 20%,

Weald Clay	3-4	2.48%-1.86%	• Retrieved close to surface. • Content: Quartz rich, Clay fraction dominated by illite and kaolinite, no smectite.
Mo clay	0.1-0.2	74.28%-37.14%	• Retrieved close to surface. • Content: High content Opaline silica Smectite: Ca. 20%
Smectite Clay	Ca. 0.02	371.42%	• Retrieved close to surface. • Content: Nearly pure Smectite
Pierre Shale	Ca. 0.33	22,51%	• Retrieved close to surface

As seen from table 5.2, typical deeply buried shales are several orders of magnitude too stiff in order for elastic deformation to play a significant part. However, for weak shales, for instance weak North Sea shale, it could play a quite important role in the closure of the annular gap.

The stiffness of shales (shear moduli) is a function of the current stress state, preconsolidation stress, mineral content and degree of cementation (36)and (39). The stiffness due to the degree of cementation typically increases with depth and increasing temperatures because it is a function of diagenesis. Hence, the deeper the shales are buried the less likely is elastic deformation to be important. Moreover, from table 5.2 it appears that the shear moduli is somewhat related to the smectite content of the shale. Because a gradual mineral transformation process from smectite to illite occurs at temperatures in the region of 70-90°C (with typical geothermal gradients), increased stiffness due to reducing amounts of smectite will typically occur at depths between 2-3km (36). Hence, further reducing the importance of elastic deformation at deep depths. The gradual mineral transformation is illustrated in table 5.3, which shows typical mineralogy composition for sediments at different depths.

Table 5.3 Mineralogy composition (%) and CEC of typical sediments at different depths. Top of the reservoir starts at 2400 meters depth. After (38).

Depth (m)	2000	2200	2400	2600	2800
Quartz	10	15	55	40	75
Feldspar	12	15	8	10	6
Calcite	11	-	2	10	5
Pyrite	5	-	2	10	4
Smectite	22	25	8	5	-
Chlorite	10	5	6	-	-
Kaolinite	8	15	10	15	5
CEC	28	22	14	8	3

5.3 Rock failure

In the previous section the elastic deformation was calculated assuming no failure.

However, when exposed to sufficiently severe stress states all solids materials will somehow fail. This implies that the rock changes its shape permanently and possibly also looses its ability to carry load and thus fall apart (36).
As seen in section 4.3.1 the well pressure gives a contribution to the stress concentration present in the near wellbore vicinity. Thus, if the well pressure becomes high or low enough the wellbore will sooner or later fail. This has for instance been observed at Statfjord where initially tight holes after some time have developed into oversized boreholes due to collapse at the borehole wall (39).
In general there are two main mechanisms leading to failure; Shear and tensile failure, but also pore collapse can occur especially in highly porous materials (36).
Although several predictive models exist for assessing whether or not failure will occur, for simplicity here only two of the most widely used are presented.

5.3.1 Shear failure

Shear failure is caused by excessive shear stress and is the main failure mode when the material is exposed to compression. The material fails along weakness planes, and when failed the two sides of the plane will move relative to each other in a frictional process as illustrated in Fig. 5.2.

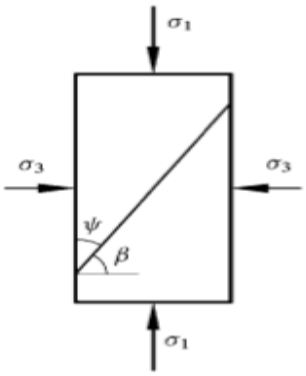

Figure 5.2 Shear failure. β is the failure angle and σ_1 and σ_3 is the maximum and minimum horizontal stress respectively. After (36).

A very simple and widely used model for evaluating borehole shear failure is the Mohr-Coulomb criterion. The criterion states that in order to initiate failure the shear stress has to overcome the inherent shear strength (cohesion) and the frictional force created by the compressive stress. In its most simple way the criterion can be expressed as(36):

$$\sigma_1' = C_o + \sigma_3' \tan^2 \beta \quad (5.3)$$

Where β is the failure angle, which is a material property independent of stress state. Co is the unconfined compressional strength, related to the cohesion, S_o, through:

$$C_0 = 2S_o \tan \beta \quad (5.4)$$

The model neglects the intermediate principal stress, but takes effect of directional strength of the material into consideration. Thus, failure is dependent on stress states rather than a specific stress. As a consequence instead of a certain stress limit for failure, there exists a failure surface, defined as surface in the principal stress space consisting

of all possible stress paths leading to failure (36). The dependency of failure on confining stress is illustrated in fig 5.3, which shows typical stress vs. strain curves for triaxial test done at different confining pressures.

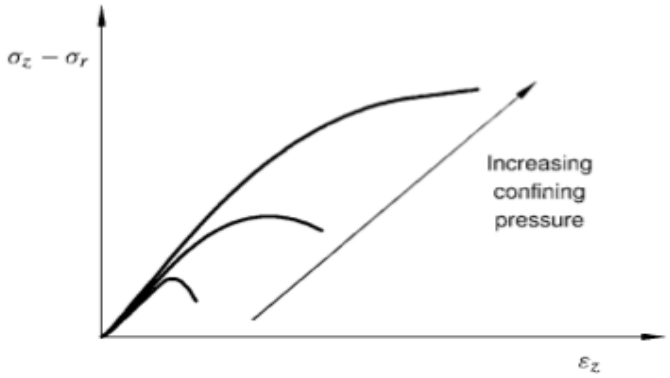

Figure 5.3 Influence of confining pressure on rock strength. After (36).

There are several other criteria's that try to predict shear failure, such as Tresca, Drucker-Prager, Von-Mises, Modified lade and the Griffith criterion (49), (36) and(46). However, some of these are very complex and since the description here is mainly for illustrative purposes, these criterions have been omitted.

5.3.2 Tensile failure

Tensile failure occurs when the material is exposed for tensile stress that exceeds the critical limit called tensile strength, T_o. The tensile strength is a characteristic property of the rock, but since tensile fractures initiates along flaws, joints or pre-existing cracks for most sedimentary rocks the tensile strength will be very low and for practical applications using zero tensile strength is often a good approximation (49).
Typically tensile fractures are oriented more or less normal to the direction of tensile stress, as illustrated in figure 5.4.
For isotropic rocks where the conditions for tensile failure always will be fulfilled first for the lowest principal stress, the tensile failure criterion can be given as:

$$\sigma_3' = -T_o \quad (5.5)$$

The equation states that failure initiates as soon as the minimum effective principal stress falls below the tensile strength, T_o, of the material. One of the primary reasons for tensile stresses downhole is a situation where the pore pressure is larger than the confining pressure, hence resulting in negative effective stresses. This is for instance the reason for fractures created during hydraulic fracturing.

Figure 5.4 Tensile failure. After(36).

5.3.3 Ductile and brittle failure behaviour and their effect on formations creating an annular seal

As seen in section 4.3.1 the stress concentration around the wellbore is dependent on the well pressure, p_w. By applying the failure criterions for shear and tensile failure (eq. 5.3 and 5.5) together with equations for the stress state around the borehole (i.e. 4.30-4.33, 4.36 and 4.38) it can be shown that for a case where $\sigma_\theta > \sigma_z > \sigma_r$ in a vertical and permeable borehole, the upper and lower mud weight limit for the formation to avoid failure is given by:

$$p_{w,\min} = \frac{3\sigma_H - \sigma_h - C_o - \alpha \frac{1-2\nu_{fr}}{1-\nu_{fr}} p_{fr} + \Delta\sigma_T + \Delta\sigma_{osm}}{2 - \alpha \frac{1-2\nu_{fr}}{1-\nu_{fr}}} \quad (5.6)$$

$$p_{w,\min} = 3\sigma_h - \sigma_H - p_{fo} + T_o + \Delta\sigma_T + \Delta\sigma_{osm} \quad (5.7)$$

The failure criterions predict that the material will fail when it reaches the maximum stress that the formation can take (peak stress). However, as seen in fig. 4.2 for ductile materials this does not necessarily mean that the material completely looses its integrity and falls apart. Thus, exactly what exceeding the limits set by eq. 5.6 and 5.7 leads to is very dependent on the properties of the formation itself and the stress state. In general for perfectly brittle materials they can be used to predict failure, but for ductile materials they can be seen as yield criterions predicting the transition from the elastic towards the plastic region.

With respect to the formation creating an annular seal after the casing is set, brittle failure is in general detrimental, while plastic deformation is beneficial. The former is mainly related to the fact that spalling, erosion and breakouts created by brittle failures leads to larger boreholes (increased annular gap), instead of smaller ones. Moreover, the

breakouts that fall into the boreholes typically create permeable rubble zones that are unlikely to become seals. For plastic formations the situation is a bit different. When exposed to large stresses the formation will to a much higher degree be able to deform radially inward and thus close of the well. Both situations are illustrated in figure 5.5.

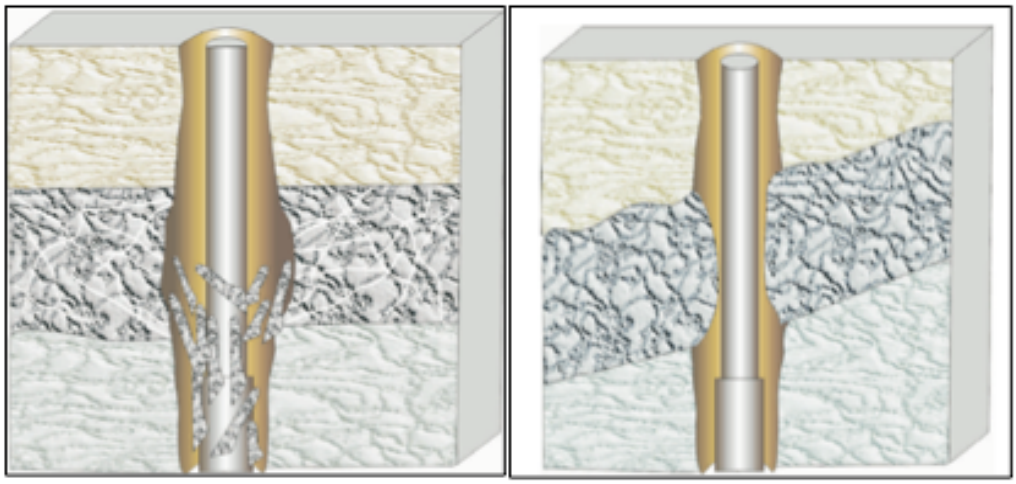

Figure 5.5 Brittle and ductile deformation in wellbores. The first illustration to the left shows Brittle Tensile failure resulting in characteristic splintery caving's, while the illustration to the right shows plastic deformation leading to wellbore closing off. Free after (49).

As seen the behaviour of the formation is very important for its ability to create a seal. Several parameters that could serve as indicators of shales brittleness (i.e. tendency for brittle failure behaviour) have been suggested (54). These are typically related to how plasticity evolves (or does not evolve) prior to rock failure or descriptions of how the post failure behaviour of the rock occurs. Although most brittleness indicators requires core sample tests, also indicators based on log data exist. These are however highly influenced by the stress states in the rocks and should therefore at best be considered to be indirect indicators of brittleness (54).

As mentioned, since few core samples are taken it is hard to predict rocks failure behaviour. However, some practical guidelines exist. In general for low confining stresses most materials are brittle, while a gradual transition towards a more plastic material with decreasing stiffness, but still with an increased ability to carry load as the strain increases, as illustrated in figure 5.3, is often seen(54). Moreover, shales ductility is likely to be a function of smectite content, in general the higher the smectite content, the more ductile will the post-peak strength behaviour of the rock be(39).
As a consequence, for maximum ductility deeply buried smectite rich shales seem to be ideal. Due to the mineral transformation process from smectite to illite occurring at 70-90°C, the most ductile shales are likely to be found in the region of 2000-3000m, while shales found below or above this region will tend to be more brittle. Hence, with respect to finding shales that have the ability to seal around the complete circumference of the casing without loosing their integrity, depths from 2000-3000 m are most likely optimal.

5.4 Liquefaction

Another deformation mechanism, driven by static shear stress, which could lead to very large deformations, is liquefaction. As mentioned earlier, in addition to shear and tensile failure another failure mode known as pore collapse could occur in highly porous rocks when exposed to high compressive stresses. During pore collapse grains are typically loosened or broken and then pushed or twisted into the open pore space, hence reducing both the total and pore space volume. If this occurs during undrained conditions, i.e. no pressure equalization, the pore space reduction will lead to an increased pore pressure, subsequently reducing the effective stress and corresponding confinement. In poorly consolidated or previously damaged rocks, this can moreover lead to a highly unstable condition, known as liquefaction (36). Liquefaction behaviour is sometimes observed in connection with earthquakes, but as bond logs done to verify formation as annular seals, generally indicates solid material, the mechanism is not likely to be a key mechanism when it comes to the annulus closing off (15).

5.5 Thermal Expansion

In the previous chapter, the stress contribution due to thermal effects was presented. During drilling the formation is cooled down and the effect is increased stability with respect to shear failure and shrinkage of the formation. The latter obviously counteracts the desired radial inward movement required for the formation to close off the wellbore. However, during production the production fluids produced from hot and deep laying reservoir may heat up shallower laying shale zones, which moreover lead to a thermal expansion of these zones into the wellbore. For instance the stress contribution from heating up a shale zone initially at 60°C to 80°C, with a thermal expansion coefficient of 10^-5K and a Young's modulus of 10GPa is:

$$\Delta\sigma_T = 10^{-5} \cdot \frac{10 \cdot 10^9}{1 - 0.25} \cdot (80 - 60) = 2.67\,MPa$$

Furthermore, assuming that the well fluid used is a perfect hydrostatic match with the formation, i.e. $\sigma_h = p_w$ everywhere, only the thermal effects will participate in the deformation of the wellbore. Inserting the stress increase calculated above, for 12 ¼" borehole, with a shear modulus of 4 GPa, into eq. 5.2 gives a deformation of

$$u = \frac{\Delta\sigma_T}{2G_{fr}} R_w = \frac{2.67 \cdot 10^6}{2 \cdot 4 \cdot 10^9} \cdot 0.311 = 0.1mm$$

This is about 0.3% of the required distance to close the annular gap if a 9 5/8" casing is used. Thus, even in HPHT reservoirs, with temperature as high as for instance 170°C (Kristin field), the effect of thermal expansion is negligible as long as the shale is not extremely soft. As both the temperature difference between the production fluid and formation, and the shale softness generally decreases with depth, thermal expansion could however be of some importance at shallow depths.

The effect of thermal expansion is illustrated in figure 5.6, which displays the thermal effects on the required radial displacement as a function of temperature for a stiff (El

Paso), soft (north sea weak shale) and very soft (smectite clay) shale using rough engineering assumptions with respect to material properties.

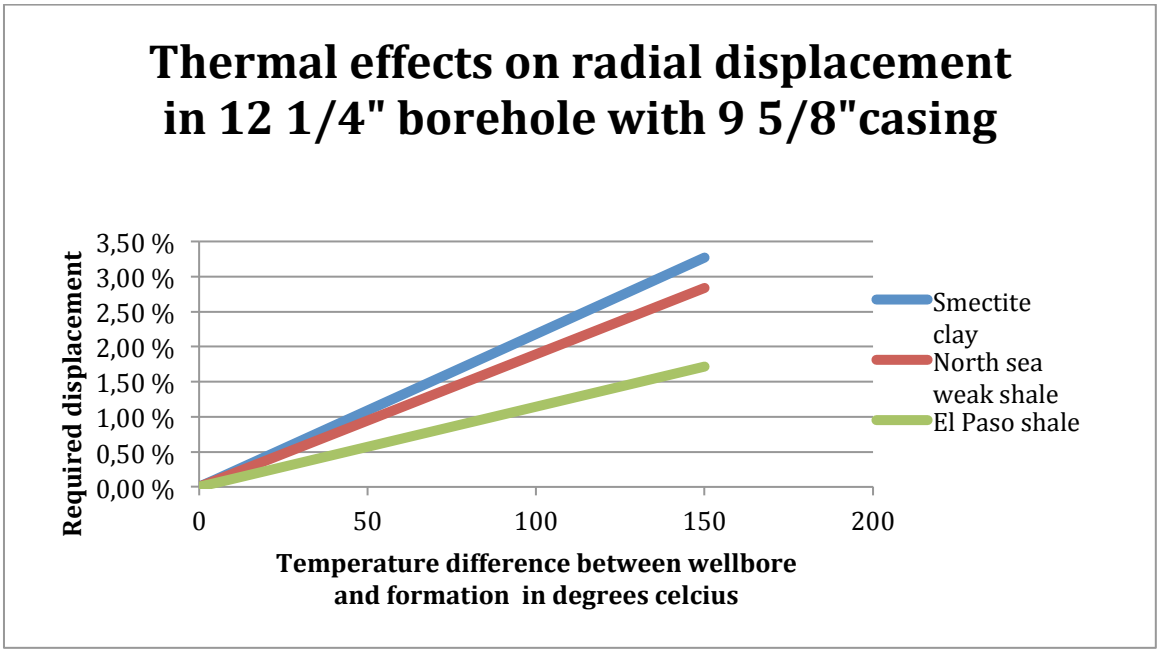

Figure 5.6 Thermal effects on required radial displacement in 12 ¼" borehole with 9 5/8" casing for smectite clay, North Sea weak shale and El Paso shale. Calculations based on material properties found in (36) assuming a poisons ratio of 0.4 for smectite clay and 0.35 for weak north sea clay.

As seen, for a 12 ¼" borehole with a 9 5/8" casing, even with a very high temperature differences the thermal effects only have the potential to contribute to about 3% of the required displacement. Thus, although they do not do not have the potential to be the main displacement mechanism, in some areas their contribution should not be completely neglected.

5.6 Shale swelling

As with thermal effects, chemical effects was also discussed in the previous chapter and their contributions to the stress state has been taken into consideration. In that discussion, the theory of osmosis was briefly described, and from the theory it appeared that by exposing shales to high activity water (e.g. freshwater), many of them would swell, thus consequently leading to borehole shrinkage. Moreover, as the volume increase due to swelling in shales containing high contents of smectite in laboratory studies have been reported as high as 80% (50), exposing shales to freshwater, after the casing is set, may seem like a good option for creating an annular seal. This can for instance be obtained either by using a freshwater spacer or perforating the casing and subsequently circulating with freshwater. However, the theory is to some extent contradicted by the log responses from areas where the formation has been displaced onto the casing, which shows that the observed bonding occurs regardless of drilling mud used (15).

A possible explanation for this was given in Santarelli and Carminati paper from 1995 "Do shales swell? A critical review of available evidence", where it was concluded that

the observed behaviour often seen in the laboratory is caused by capillary forces, set up by coring effects of bringing the sample from in situ to surface conditions (see appendix E), instead of swelling (50). Moreover, because in situ shales are fully water saturated "swelling" was found unlikely to be an issue at downhole conditions.
Practical evidence of downhole swelling, such as the superiority of OBM over WBM in shale sections, was explained by the fact that due to capillary effects for an OBM to enter the shale an overpressure equal to the threshold pressure (see section 3.2.5) would be required, while no such overpressure would be needed in the case of WBM. As previously seen, in section 4.3.2.1, pore pressure equalization with the well pressure has a destabilizing effect on the wellbore and could therefore very well explain the differences in success ratios of the two types of mud.
Others have also obtained similar results or conclusions. For instance in a study on brines effect on shales, a shale was exposed to a 16wt% $CaCl_2$ brine. According to the theory of osmosis this should have resulted in reduced pore pressure and associated shrinkage, however no such results where observed (55).

Although the theory of capillary pressure in many ways seems rational, most researchers still seem to believe that osmosis have something to do with hydration of shales (36). Nevertheless, the evidence presented by Santarelli and Carminati gives reason to believe that capillary effects at least have some impact on the observed behaviour seen in the laboratory. Thus downhole-swelling effects are likely to be far less important than previously thought.

5.7 Creep

The last mechanism that is commonly believed to have some effect on the radial displacement of the formation towards the casing is creep. Creep is a time-dependent plastic deformation that occurs in solid materials that are exposed to constant stress below their yield strength. It originates from visco-elastic effects in the solid framework and the rate of deformation is dependent on material properties, exposure time, temperature and the applied stress (42). Unlike brittle fractures, creep deformation does not occur suddenly and upon the application of stress, but is rather seen as a slow movement where strain accumulates as a result of long-term stress.
Whether the material fails is dependent on if the cumulative strain, accumulated over time, exceeds the critical strain limit for the material or not.

5.7.1 Mechanisms of creep

Earlier, in section 4.2.3, it was stated that according to Heim's rule the downhole stress state moves towards lithostacy due to creep. Moreover, as creep occur only in materials exposed to deviatoric stress states, it can be briefly explained as deformations that occur in the solid material due to the material trying to avoid shear stress (12). However, on microscopic scale creep is quite complex, and several interatomic movement mechanisms, such as viscous flow, dislocation movement and diffusional creep, are involved(42).

The first creeping mechanism, viscous flow, occurs due to grain boundary sliding being viscous in nature, as the counteracting friction forces are dependent on the velocity of the movement. Thus, when the material is exposed to a constant external stress, there will be a time-dependent effect on the deformation known as creep. This mechanism is usually predominant in amorphous materials and mathematically often described with a spring and a dashpot coupled in series in a model known as the Maxwell model (36) and (42).
At high deviatoric stress levels (relative to the shear modulus) and low temperatures, creep is mainly due to the second mechanism of creep, movement of dislocations. Dislocations are irregularities within the crystal structure of the material, and can for instance be visualized as being caused by the termination of a plane of atoms in the middle of a crystal, as illustrated in figure 5.7. In the illustration the dislocation is at the bottom edge the extra half plane. When exposed to large enough stress, the dislocation can move if the atoms from one of the surrounding planes break their bonds and rebond with the atoms at the terminating edge. Since breaking all ionic bonds along the plane at once would require extreme levels of energy, the movement takes place step by step and is therefore time-dependent.

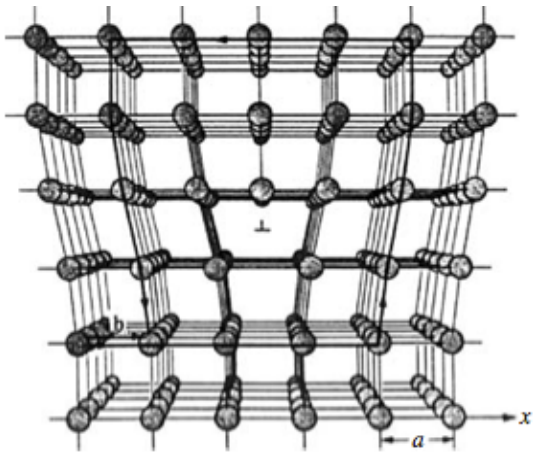

Figure 5.7 Edge dislocations in crystal structure. After(42).

The last mechanism of creep, diffusional-controlled creep, is based on diffusion of atoms within the structure of the material. Since diffusion processes are highly dependent on temperatures, the mechanism typically becomes more and more important the higher the temperature gets. The maybe best way to illustrate diffusional controlled creep is through an example. Imagine a rock sample, consisting of multiple grains, being exposed to tensile stresses in the vertical direction, as illustrated in figure 5.8. The tensile stresses will increase the separation of atoms on grain boundaries that are normal to the stress axis, and because of Poisson contraction, decrease the separation of atoms on grain boundaries that are parallel to the stress axis. The differences in atom separations at different areas will lead to a diffusional transport of atoms from grain boundaries parallel to the tensile stress to boundaries normal to the tensile stress. Depending on

whether the diffusion occurs through the lattice or along the grain boundaries the process is called either Nabarro-Herring creep or Coble creep respectively (42).

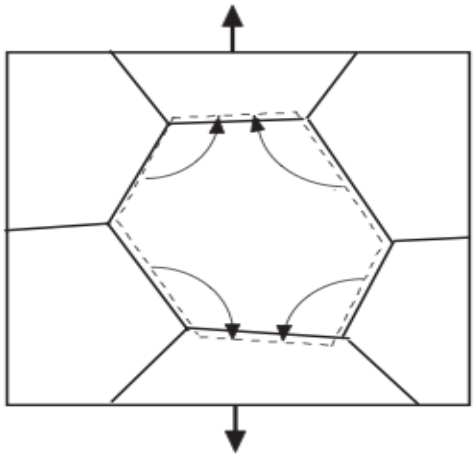

Figure 5.8 Nabarro –Herring creep. Creep occurs due to diffusion between grain boundaries. Atoms diffuse from lateral boundaries to boundaries normal to the tensile stress. The grain elongates vertically, and contracts laterally. After(42).

Regardless of mechanism, as a consequence of the systematic changes in intermolecular alignments, creep will effectively reduce the shear and Young's moduli of the material, while the Poisson ratio will be increased (36).

5.7.2 Creep behaviour

As mentioned the creep rate of deformation is dependent on material properties, temperature and the applied stress. Moreover, the creep rate is also typically a function of time since typical creep behaviour, as a response to changes in stress state, occurs in 3 distinct distinguished stages as illustrated in fig. 5.9.

First, as soon as the load is applied, as always there will be an instantaneous elastic response. This is followed by a period of transient creep, where the creep rate decreases with time because of material strain hardening. If the load is high enough this will eventually lead to steady-state creep, where the creep rate is a constant non-zero positive function of time. However, due to the necking phenomena, defined as creep induced reduction of cross-sectional area, there will be a gradual increase in the stress on the material. Thus, as a consequence of this the creep rate will eventually start rapidly increasing until the material fails in a stage known as accelerating or stage 3 creep (42).

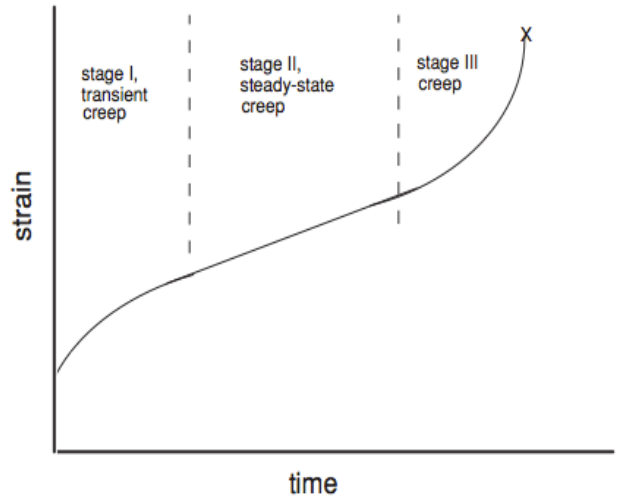

Figure 5.9 Typical creep behaviour. After (42).

The exact creep behaviour, the time-dependency and whether or not the material will run through all the stages is highly dependent on material properties, temperature and the applied stress. In general the higher the temperature and the applied stress the faster will the creep rate be (42). The effect of the applied stress on the creep rate is illustrated in figure 5.10. From the figure it can be seen that for low stresses the material will only reach the transient stage and virtually stabilize after some time, while for high stresses the material will quickly run through all stages of creep and finally fail.

Another important concepts illustrated in the figure, is the fact that as long as the material reaches steady state creep, the material will eventually fail. Thus, even when exposed moderate stresses in region of 50-70% of the ultimate strength, if the stresses are maintained over time the material will continue to creep till failure or until the creep movement becomes somewhat constrained, by for instance running into the casing (36).

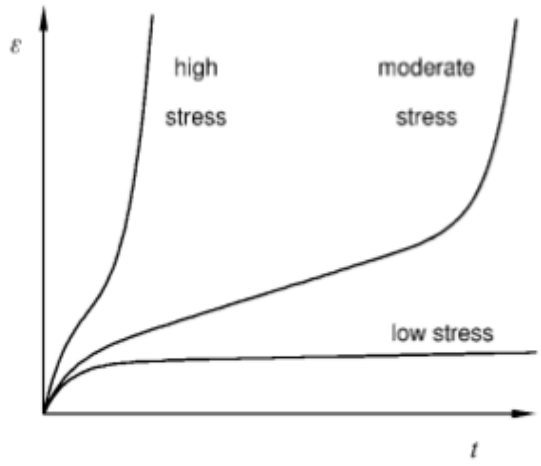

Figure 5.10 Development of creep as a function of the applied stress. After (36).

5.7.3 Significance of creep with respect to formation creating an annular seal

So far, only mechanisms of creep and general creep behaviour have been discussed. As seen, as long steady state creep is reached the material will eventually creep to failure or alternatively if the material is flexible enough creep until constrained by for instance the casing. Thus, as with all other displacement mechanisms a premise for the formation creating an annular barrier is that it is flexible enough to stay intact when displaced over the entire annular gap. However, due to creep's time-dependency, with respect to creep being the mechanism behind the creation of shale annular seals for PP&A, two additional questions arise:

1. Is the stress state around the borehole sufficient to reach at least steady state creep?
2. If steady state creep is reached. Could creep create annular seals within the time frame for PP&A?

5.7.3.1 Steady state creep in the borehole

During drilling the minimum well pressure to avoid shear failure is given by equation 5.6. However, as seen in section 4.3.3 with time the mud degrades resulting in settling of particles at the bottom underlying a column of water. As consequence, with time the mud weight will be equal to that of water. Assuming a stress state where, $\sigma_\theta > \sigma_z > \sigma_r$, from equation 4.30 and 4.32 it can be seen that, as the mud degrades and the mud weight subsequently decreases ,the deviatoric stresses on the borehole wall becomes larger. Hence, with respect to shear failure the situation becomes more and more severe.
In the end at the time of complete mud degradation to avoid shear failure in a situation with normally pressurized pores, isotropic horizontal stresses and negligible thermal and osmotic effects, equation 5.6 yields the following criteria for C_o:

$$C_o > 2\sigma_h - 2p_w \quad (5.7)$$

Where p_w is the hydrostatic well pressure caused by the water column. If the Co is lower than this value, the formation will somewhere between the mud weight being at its initial value until fully degraded fail due shear or creep, or in cases with sufficiently flexible formations where the creep rate is higher than the degradation time for mud, seal off the annular gap.

As mentioned in section 5.7.2 if the material is exposed to a stress state where the deviatoric stresses are up to 50-70% of the materials ultimate strength, steady state creep will occur. Thus, if choosing 70% to be conservative, the material will fail or obtain steady state creep somewhere between drilling time and time for fully degraded mud if:

$$C_o < \frac{2\sigma_h - 2p_w}{0.7} \quad (5.8)$$

Where p_w is once again the well pressure caused by the water column.

The upper C_o limit for steady creep to occur (eq.5.8) and the limit for shear failure to occur (eq.5.7) as a function of depth is plotted in figure 5.11. Formations with C_o values above the upper limit represents formations where large creep strains is unlikely to occur. Formations that are in between the upper and lower limits represents formations where steady state creep occur without shear failure interfering, while formations below the lower C_o limit for shear failure represents formations where shear failure will be induced as the mud is degraded into water. For formations within the last region, for creep to be the mechanism displacing the formation around the casing, the creep time required to displace the annular gap has be to lower than the mud degradation time to initiate failure.

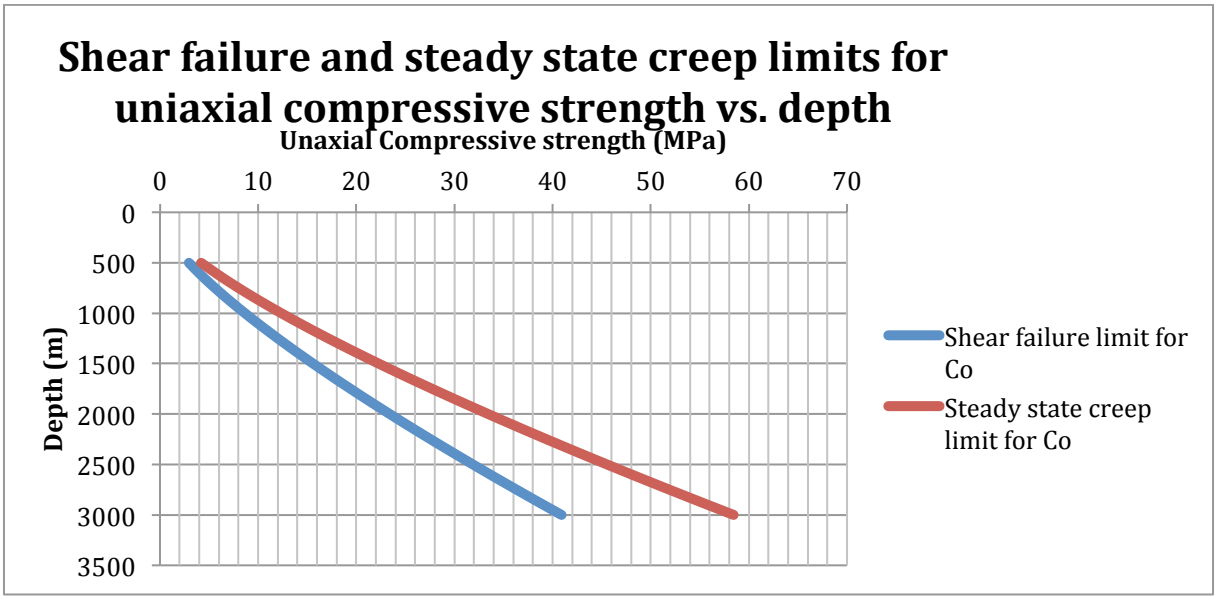

Figure 5.11 Shear failure and steady state creep limits for uniaxial compressive strength vs. depth. Applying the Mohr Coulomb criterion on a vertical and permeable borehole. Assuming linear elasticity, normally pressurized pores, isotropic horizontal stresses and negligible thermal and osmotic effects. Minimum horizontal stresses estimated with Breckels van Eckelen eq. 4.26.

As seen from fig.5.11, for a formations located at approximately 2500m, steady state creep is likely to occur as long as the uniaxial compressive strength is below 50MPa. Typical shale values for the uniaxial compressive strength is in the region of 2-250MPa (36). However, as the strength generally is reduced with increasing clay content, many shales with high clay contents are likely to fall into the required area. Moreover, the simple linear elastic model used, tends to overestimate the minimum mud weight to avoid failure (56). Thus, when using more correct elastoplastic models the C_o limit values are likely to be higher than the rough estimates presented in figure 5.11.

5.7.3.2 Time scale of creep

So far, only mechanisms of creep and general creep behaviour have been discussed. As seen, as long steady state creep is reached the material will eventually creep to failure or in a cased hole, if the material is flexible enough creep until the annular gap is closed. The main question for flexible formations where the steady state creep will be reached

is therefore whether or not creep has the potential to be a mechanism creating an annular seal within the time scale required for PP&A.

As seen, creep rates are a function of time, dependent on material properties, exposure time, temperature and the applied stress state. The total creep may be represented by (57):

$$\varepsilon_{cr} = \varepsilon_{el} + \varepsilon_1(t) + \varepsilon_2(t) + \varepsilon_3(t) \quad (5.10)$$

Where ε_{el} is the instantaneous elastic strain, $\varepsilon_1(t)$ is the transient creep, $\varepsilon_2(t)$ is the steady state creep and $\varepsilon_3(t)$ is the accelerating creep.

Because of the time-dependency to estimate creep strain accurately advanced models, such as the power-law has to be used. The power-law model is given as (58)

$$\varepsilon_{cr} = k\sigma_d^p t^n \quad (5.11)$$

Where σ_d is the deviatoric stress, t is the time and k,p and n are fitting parameters obtained by comparing numerical experiments to experimental data from creep tests (58).

As mentioned in section 5.1, for various reasons there are few reliable creep tests conducted on shales. Moreover, creep tests are even more seldom performed at enough different deviatoric stresses to calibrate the power law for a certain shale rock. Even if this is done, differences in confining pressures and temperatures as well as general uncertainties due to shale anisotropy from the test to the actual field situation, will give rise to uncertainties. Thus, as a consequence it is very hard to predict creep behaviour accurately.
However as a simplification, a simple way of obtaining rough "engineering" estimates of the creep rate can be obtained by assuming that creep rate is constant and equal to the steady-state creep rate measured in creep tests. A list of measured creep rates for some shales can be found in table 5.4. Although these creep test are generally conducted at different deviatoric stress, confining pressures and temperatures and therefore not directly comparable, they do however indicate the order of magnitude for the creep in the different shales. They can therefore be used as an indication for the potential of creep creating a barrier within the time frame for PP&A for the given rocks.

Table 5.4 Measured creep rates for various shales.

Material	Total clay content (%)	Swelling clay content (smectite+mixed layer) (%)	Porosity (%)	Depth found (m)	Critical strain	Creep rate (strain/day)	Source
Tertiary (miocene)	53	15-20	55	N/A	0.01	10^{-3}	(59)
Tertiary (Oligocene)	65	15-20	35	N/A	0.016	$1.4 \bullet 10^{-3}$	(57)

Marcellus	40	N/A	Unknown	1800	N/A	10^{-4}	(58)
Barnett	25	N/A	Unknown	1675	N/A	10^{-5}	(58)
Bure argillite	40	Ca.0	N/A	491,7	N/A	$3.9 \cdot 10^{-6}$	(60)
Oxfordian argillite	40-45	Ca.15	15.5	N/A	N/A	$1.9 \cdot 10^{-5}$	(61)
Tournemire Argillite	55	8.3	8.9	N/A	N/A	10^{-6}	(61)

Figure 5.12 illustrates the effect of steady state creep vs. time in a 17 ½" borehole for some of the shales in table 5.4.

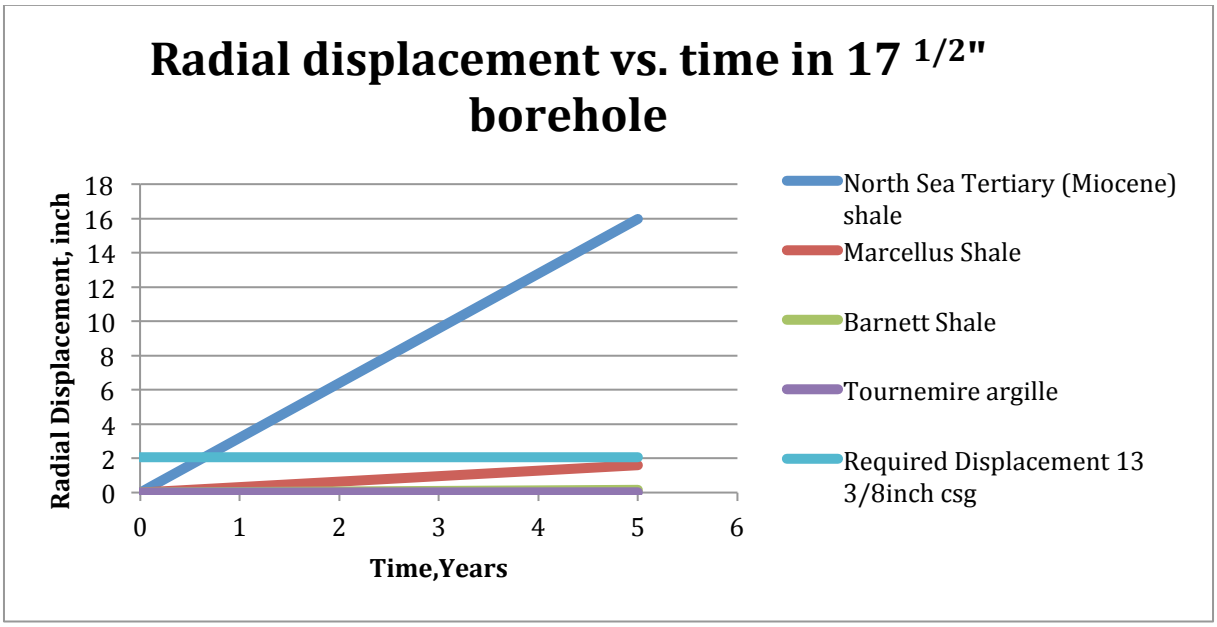

Figure 5.12 Radial displacement vs. time in a 17 ½" borehole assuming steady state creep rates from table 5.4. Included is also the required radial displacement to close of the hole if a 13 3/8" casing is used.

As seen from the figure only the North Sea Tertiary (Miocene) shale will fill the gap between the borehole and a 13 3/8" casing within a time frame of 5 years. However, as this shale has been found to collapse at strain values of 0.01, while 0.24 is required to seal the gap, the integrity of this shales seal may be questionable(59).

A more comprehensive list of the required time to fill the annular gap for some standard hole and casing sizes for the shales illustrated in figure 5.11 can be found in table 5.5.

Table 5.5 Required time to fill the annular gap, for different shales, in different boreholes with standard casing sizes. Assuming creep rates to be constant and equal to the steady state creep rate for the shales.

Shale	Borehole size	Casing size	Required time (years)
North Sea Tertiary (Miocene) Shale	17 ½"	13 3/8"	0.64
North Sea Tertiary (Miocene) Shale	12 1/4"	9 5/8"	0.59
North Sea Tertiary (Miocene) Shale	8 ½"	7"	0.48
Marcellus	17 ½"	13 3/8"	6.46
Marcellus	12 1/4"	9 5/8"	5.87
Marcellus	8 ½"	7"	4.83
Barnett	17 ½"	13 3/8"	64.57
Barnett	12 1/4"	9 5/8"	58.71
Barnett	8 ½"	7"	48.35
Tournemire argille	17 ½"	13 3/8"	645.79
Tournemire argille	12 1/4"	9 5/8"	587.08
Tournemire argille	8 ½"	7"	483.48

A natural question that arises is how good these estimates are. In a so far unpublished work performed at SINTEF Petroleum Research in Trondheim, it has been confirmed using finite element numerical simulations that rough estimates similar those performed above, could be used and still give reasonable results (59).
Thus, from the data presented above it could be concluded that the creep rates found in some shales definitely have the potential to seal the annular gap within the time frame for PP&A (e.g. 20-30 years). However, in some cases the required strain may jeopardize the integrity of the seal making it less valuable.

Although, the shales discussed here don't have the potential to seal within the time frame from 2 days to 2 weeks after the casing is set, as sometimes observed on the NCS, it does not mean that shales with properties that enable that kind of behaviour does not exist (62). Moreover, based on the displacements contributions from the mechanisms discussed earlier in this chapter, it seems likely that creep is one of the major contributors to the wellbore closing around the casing.
In general it has been found that the stiffer the shale is the lower is the contribution from creep. Moreover, shales with higher amounts of clay and organic material creep more than shales with high quartz content and less clay (58). Thus, useful indicators of the creep potential for a specific shale could be the Young's modulus and clay content. However, to be completely sure of a shales creep potential careful laboratory experiments, evaluating the creep rate under the prevailing in situ conditions, is required. Hence, to be able to better predict shales creep potentials there is a need for more creep tests.

6. Methods to increase chance for shales closing the annular gap

In the previous chapter the mechanisms thought to be responsible for the radial inward movement of certain shale sections was thoroughly discussed. It became clear that not all shales naturally have the ability to close of the whole gap between the wellbore and casing. For many, and especially the stiff and brittle shales, closing the gap simply requires too much deformation. Instead of closing the annulus they will typically, as a response to decreased well pressure or other deformation mechanisms, mechanically fail with the result being the creation of highly permeable "rubble zone" made up by borehole breakouts. For the shale sections to close off the annular gap without this undesirable failure behaviour, the key property was found to be flexibility. Moreover, a highly plastic behaviour was found advantageous, as ductile materials do not lose their integrity immediately after reaching their peak load, but rather deforms with a continued ability to carry load. The possibility of increasing the flexibility and plasticity of shale sections as well as other means to optimizes or otherwise increase the chance of shale zones becoming barrier elements will be the topic of this chapter.

6.1 Methods to maximise shale flexibility

As seen in the previous chapter, shales failure behaviour is a function of confining stress and likely also the clay and smectite content. The latter two parameters are in general hard to influence downhole, while reducing the well pressure could increase the confining stress. In addition to reducing the well pressure there are also some other ways of increasing the flexibility and ductility of the downhole shales. Some of these will be discussed here.

6.1.1 Cation exchange

As discussed in chapter 3.2 shales consist of large amounts of clay minerals. These are furthermore composed of hundreds of negatively charged basic unit layers, bond together either through hydrogen or Van Der Waal's forces. Between the unit layers there is bound and free water. The difference being that bound water is related to absorbed cations to neutralize the surface charges, while free water is driven in between the layers due to osmotic potential differences between the pores and surrounding fluids. The absorbed cations can be exchanged according to the theory of cation exchange (see section 3.2.2) and will replace each other (when present in equal concentrations) in the following order (38):

$Al^{3+} > Mg^{2+} > Ca^{2+} > H^{+} > K^{+} > Na^{+}$

Most shales naturally contains mainly sodium ions. Thus, by exposing them to fluids containing cations with higher affinity to the exchangeable positions than sodium, the sodium ions will be replaced. This is important because type of cations in the exchange positions of the clay has significant impact on its ability to attract and store water in

between its unit's layers, which furthermore have large impact on its physical properties.

The mechanical effects of exposing smectite rich shales naturally containing sodium ions to brines containing different concentrations of KCL and $CaCl_2$ is illustrated in figure 6.1.

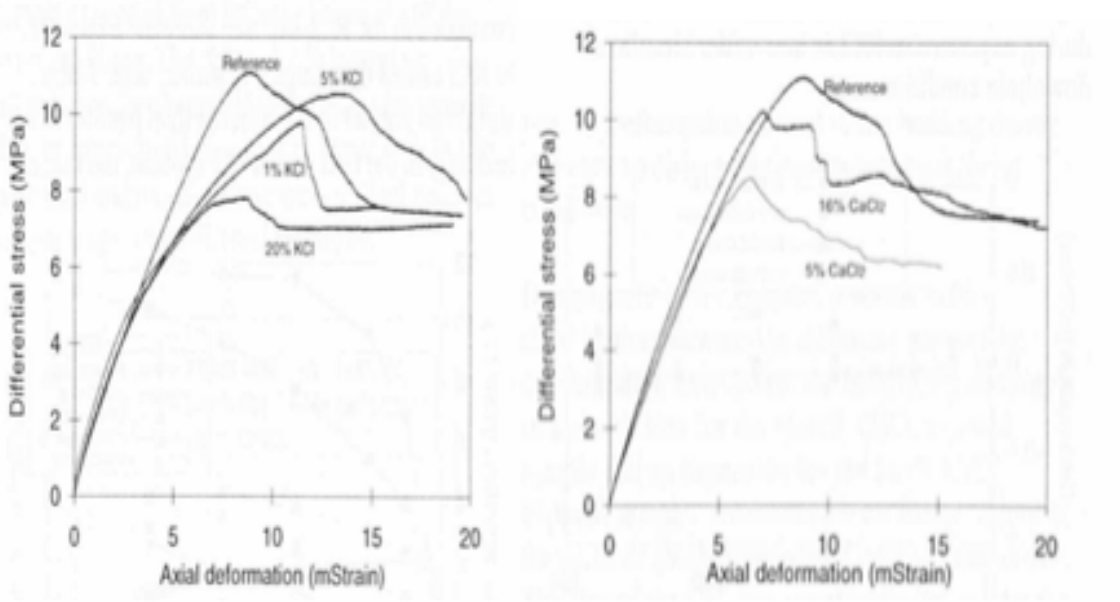

Figure 6.1Effect of cation exchange on mechanical properties of shales. Figure shows differential stress vs. axial strain for samples previously exposed to KCL and $CaCl_2$ brines at different concentrations compared to a unexposed reference test. After (55) and (56).

As seen from the figure, initially the effect of exposure of KCl brine is negligible, however beyond approximately 50% of the peak stress value, the exposed samples exhibit a much larger plastic deformation than the reference sample. Moreover, especially at high concentration of KCL there appears to be a reduction in the peak strength of about 30%. In contrary the exposure of $CaCl_2$ brine does not seem to affect the stiffness and behaviour much. Although there appears to be a reduction in strength also for $CaCl_2$ exposure, due to possible inhomogeneity between the samples, the strength measurements in the figure are not conclusive (55).

The reason for the change in mechanical properties is thought caused by differences in the radius of the hydrated ions. A list over hydrated radiuses for some common cations can be found in table 6.1. As seen from table hydrated potassium ions are smaller than hydrated sodium ions, while hydrated calcium ions are larger than both. Hence, for instance the replacement of hydrated sodium ions with hydrated potassium ions will lead to a reduction in bound water within the matrix structure. This will furthermore induce compaction leading to breaking of cementation bonds. The result is a weakened and more plastic material (56).
Another theory is that the structurally bound water has an ordered crystal like structure, set up by unit layer surface charges, that is contributing to the total stiffness of the rock (63). Therefore, by exchanging cations, this structure will be influenced, hence leading to changes in the mechanical properties of the rock.

Table 6.1 Hydrated radiuses for some common cations. Free after (64).

Ion	Hydrated Radius (nm)
Li^+	0.73-1.00
Na^+	0.56-0.79
K^+	0.38-0.53
NH^+	0.54
Rb^+	0.36-0.51
Cs^+	0.36-0.50
Mg^{2+}	1.08
Ca^{2+}	0.96
Sr^{2+}	0.96
Ba^{2+}	0.88

Since plastic behaviour, as seen in the previous chapter, is very beneficial with respect to the formation closing the annular gap, so far from the discussion it may appear that exposing the formation to high concentrations of low radius hydrated ions, such as potassium, caesium or rhodium may be ideal. However, the exchange to smaller ions, also have some detrimental effects on the formations ability to close in. First of all, the reduction in bound water leads to shrinkage, which is negative in itself, due radial inward expansion being the ideal movement. Moreover, similar to thermal cooling, this chemical shrinkage leads to reduction in the compressive stress in the tangential direction of the wellbore given as (56):

$$\Delta\sigma_{\theta,ch} = \frac{E}{1-\nu}\varepsilon_{shr} \quad (6.1)$$

where ε_{shr} corresponds to the shrinkage induced by the ion exchange (shrinkage defined as negative), and $\Delta\sigma_{\theta,ch}$ is the associated change in hoop stress. The change in hoop stress could be quite large (10-15MPa), hence possibly inducing tensile fractures on a micro or macro scale, with the result being increased permeability or borehole instability. Regardless of fractures, KCl-exposure to shales have been found to increase the permeability of a shale up to 2.6 times the initial value due to shrinkage opening new flow channels and enlarging the existing channels (56).
As a consequence of the beneficial and detrimental effects of potassium, it appears to be an optimum KCL concentration that should be used in each case. This will be further discussed in chapter 8.

6.1.2 Thermal effects on mechanical behaviour of shales

Another parameter that affects the deformation behaviour of shales is temperature. Since shales are solids, it is easy to assume that they will behave in a similar manner to metals, which typically become more ductile, forgeable and easier to form at elevated temperatures. However, since shales are porous materials composed of solid grains (including absorbed water) and free water filling the voids, their response to heating is more complex.

In general the thermal influence on shales mechanical behaviour is very dependent on the rate of heating (65). This is mainly related to the fact that the pore fluids have larger thermal expansion coefficients than the solid part of the shale, thus for instance heating increases the pore pressure. Moreover, since shales typically have very low permeabilities, it may take a long a time for this excess pore pressure to dissipate. Thus, since as mentioned earlier, rocks are affected by the effective stress rather than he total stress, whether the thermally induced pore pressure rate exceeds the dissipation rate or not becomes important for its behaviour. The effect of slow and fast heating rates on the mechanical behaviour of rocks, when exposed to deviatoric stress are illustrated in figure 6.2.

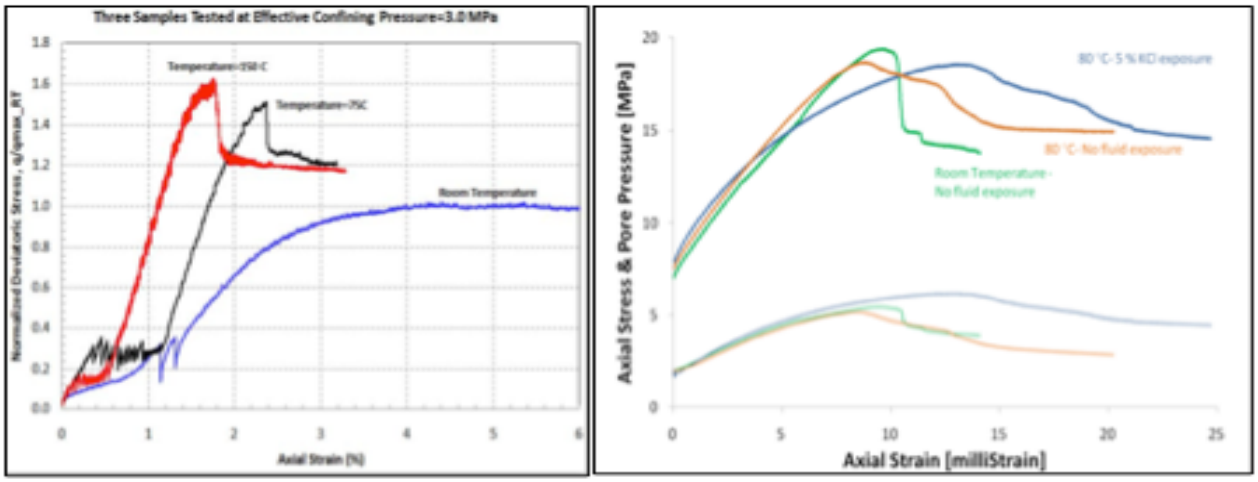

Figure 6.2 Shale deformation behaviour at different temperatures for drained (slow heating) and undrained (fast heating) samples respectively. After (65)and (54).

As seen from the figures slow heating results in increased stiffness, shear strength and brittleness of the shale, while fast heating leads to a more advantageous ductile behaviour. The former is caused by the fact that during slow heating the thermally induced pore pressure has enough time to dissipate and since the grains expands, the result is a more compacted microstructure leading to the observed changes in behaviour (65).In contrary for fast heating the large thermally induced excess pore pressure does not have time to dissipate, and since the pore fluids expand more than the solid grains, the microstructure becomes less compacted resulting in a more ductile behaviour. It must be stated that contrary to the cation exchange, which affects the bound water, the difference between fast and slow heating is related to the amount of free water inside

the shale structure, therefore the effect of compaction of the structure becomes different.

From the above discussion, and the wanted ductile behaviour, it appears that high heating rates are ideal. However, when the pore pressure is increased the stress state is brought closer towards failure since the effective confinement (eq.5.4) approaches zero, as illustrated with the Mohr circle in figure 6.3. Because of the reduction in confinement pressure, unwanted thermal cracking and material weakening possibly resulting in lost material integrity, becomes more and more likely to occur. As a consequence, the rate of heating should not be too high. The optimum rate of heating is function of permeability and thermal conductivity of the shale as well as the difference in thermal expansion coefficients between the pore fluid and the solid grains. Since correct values of the former, due to the impact of coring effects and the extremely low permeabilities of shales could be hard to obtain, in practice it may be difficult to know exactly what heating rates that ideally should be applied. However, cycles of thermal heating should be avoided since more water is expelled during heating than adsorbed by cooling. Hence, the result of heating cycle is a reduction in free water content and thus also ductility (66).

.

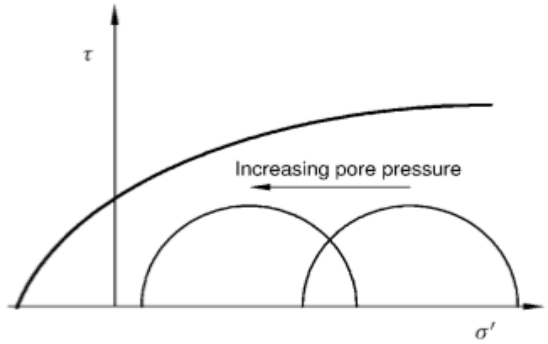

Figure 6.3 Mohr Circle and failure lines: the effect of increasing pore pressure. After(36).

6.2 Increase creep rates

As seen in the previous chapter the main contributor to the wellbore closing in is likely to be creep. Creep rates generally increases with higher stresses and temperatures. Moreover, also the overall strains before failure typically increase with increasing stress and temperature, as illustrated in figure 6.4. As a consequence, to maximise the creep effects both with respect to strain and time, the temperature and deviatoric stresses should be as high as possible without the shale mechanically failing. However, although the stresses and temperatures are increased the creep rates are still likely to be in same order of magnitude. For instance a increase in temperature from 50°F (23.9 °C) to 250°F (123.9 °C) increased the creep rate 5 times, while a increase in stress ratio from 0.3 to 0.75 increased it 4 times (67). Therefore, based on the required creep times presented in the previous chapter, only for shales with creep rates larger than 10^{-6} strain/day could the increase in temperature and stress state have an impact on the shale creating an annular barrier or not within the time frame for PP&A.

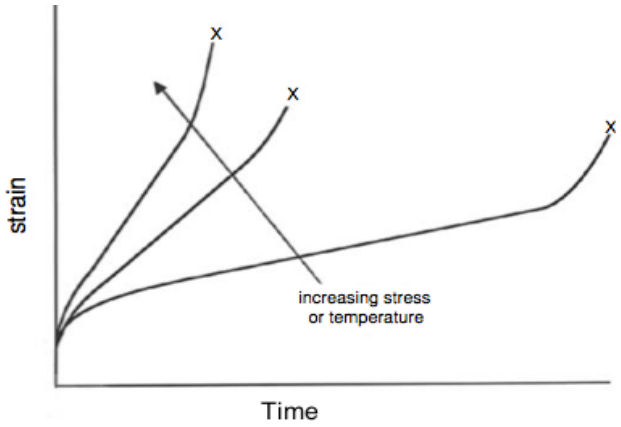

Figure 6.4 Effect of increasing temperature and stress on creep rates and failure strain. After (42).

6.3 Optimize annular gap

In the previous chapter creep was found to be the most likely mechanism for the annular displacement observed in many wells. However, as seen in many cases the creep rate is too low to provide an annular barrier within the time frame of PP&A. One possible solution to increase the chance of creep being able to provide a barrier element within the given time frame is reducing the annular gap. This could be obtained either through using expandable casing strings or initially using larger casing strings than what is conventionally used. Table 6.2 shows the required time to fill the annular gap for a 12 $^{1/4}$" borehole with different casing sizes for different types of shales. From the table it appears that especially for shales with creep rates in the range of 10^{-4} strain/day (Marcellus) to 10^{-5} strain/day (Barnett), increasing the casing size could be the difference between the shale providing a barrier or not within a time frame of 10-30 years.

Table 6.2 Required time in years to fill annular gap for a 12 ¼ " borehole with different casing sizes for different types of shales. Assuming steady state creep values given in table 5.4.

Type/casing size	10 ¾"	10 ½"	10 ¼"	10"	9 5/8"
North sea Tertiary (miocene) Shale	0.33	0.39	0.44	0.50	0.58
North Sea Tertiary (Oligocene) shale	0.24	0.28	0,32	0,36	0,42
Marcellus	3.35	3.91	4.47	5.03	5.87
Barnett	33.55	39.13	44.73	50.32	58,71
Bure Argillite	86.01	100.35	114.69	129,03	150,53
Oxfordian Argille	17,65	20,59	23,54	26,48	30,90
Tournemire Argille	335,47	291,39	447.30	503.21	587.08

6.4 Shales in combination with other sealing materials

Even though efforts are made to increase the flexibility of shales, many of them will still be too brittle to close off the whole annular gap without loosing their integrity. Although, closing the whole gap, in many formations may be too much, most shales have the ability do deform to some extent without failing. Thus, if combined with another sealing material they could contribute to the creation of a good annular barrier element.

The sealing material, which is likely to benefit most from the presence of inward moving formations, is Sandaband. As discussed in section 2.7.3, Sandaband is a deformable Bingham plastic behaving sealing material. The main problems with the material are cost and lack experience, and therefore also concerns about the materials long term sealing ability. However, as will be illustrated, combined with inward moving shales both these problems could be reduced.
As mentioned in section 2.7.3 the high costs are related to the high volume price as well as the large quantities of the material required to seal of the wellbore compared to other sealing materials. The later is especially true in highly deviated wells, drilled into high-pressure reservoirs, and is related to the fact that the main contributor to its pressure seal capability is the weight of the Sandaband column itself ($\rho_{Sandaband}$=2150kg/m3). The three contributors to Sandabands pressure seal capability and the effect of well deviation on its pressure seal ability, assuming that the effect of yield stress is negligible, is illustrated in figure 6.5.

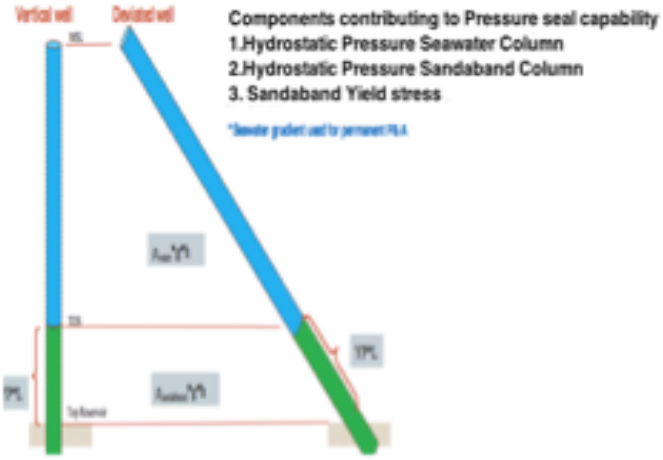

Deviation from vertical	Distance required for Sandaband Column to seal the same pressure (m)
0 °(vertical well)	1000
20°	1064
45°	1408
60°	2000
80°	5882
85°	11111

Figure 6.5 Pressure seal capability of Sandaband plugs and list of required distances for deviation wells to seal the same pressure with Sandaband as in a 1000meter vertical column, assuming yield stress effects are negligible. Free after (13).

From the figure it can be seen that, if assuming that the effect of yield stress is negligible, for a Sandaband column to seal the same pressure in wells deviated at 60° from the vertical a twice as large column of Sandaband would be required compared to a vertical one. As a consequence in wells with long and highly deviated wells using Sandaband becomes very expensive. However, if the annular gap with time is reduced due to the

formation closing in towards casing the required volume and thus also cost could be significantly reduced. The reduction in gap will induce stresses in the Sandaband column and due to it's liquid like behaviour it will be displaced upwards in a similar manner as toothpaste when squeezed, hence resulting in increased height of the column as illustrated in figure 6.6.

If a short solid plug composed of e.g. cement or Thermaset is used at the bottom of the well to provide a pressure seal initially (as illustrated fig. 6.6), the expected increase in height, due to the formations inward movement, could be used to save considerably amounts of Sandaband volume without compromising with the required long term pressure seal. If no such short solid plug is set, and the Sandaband volume used is the amount required assuming no reduction in annular gap, the result of the increase in height would be a longer sealing material plug. Hence, increased safety in the case of unexpected events, such as for instance earthquakes, leading to losses and reduction in sealing material height. Moreover, the compression due to the inward movement of the formation, could possibly reduce the permeability of the Sandaband, hence increasing its sealing ability even further (68).

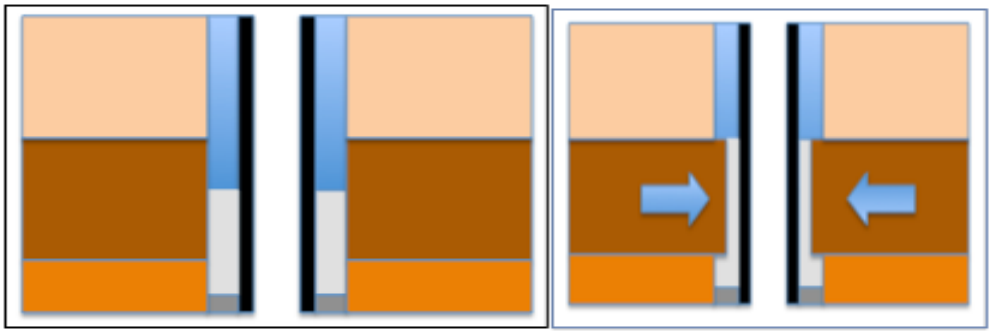

Figure 6.6 Increase in height of Sandaband column in the presence of radially inward moving formation. Sandaband (light grey), Solid plug composed of e.g. cement or Thermaset (dark grey).

7. Weight materials in combination with inward moving formations as barrier element

In the previous chapter Sandaband in combination with inward moving formations was discussed as a possible solution in areas where closing the whole annular gap would require too much deformation from the formation. Another possible solution that could provide a barrier in combination with inward moving formations is settled weight materials, such as barite. Initially, just through gravitational settling, barite plugs are likely to be too porous and permeable, but if the formation deform slightly inward, the settled weight material will get compressed and thus perhaps create an everlasting impermeable seal. The possibility of such seals will be the topic of this chapter. First a theoretical approach to the problem, assuming that the theory of rock mechanics can be used to describe the behaviour of compressed settled weight materials, will be thoroughly discussed. This is followed by a set of lab experiments where settled barite is mechanically compressed up to 100 bars before its sealing ability is tested. In addition to standard barite, also a newly developed product consisting of finer particles called micro-barite has been tested.

7.1 Theory Background

7.1.1 Introduction

Barite ($BaSO_4$) is a finely ground mineral mainly consisting of particles between 75µm and 6µm (69). It is used as a weighting agent in drilling fluids due to its high density, which is in the excess of 4200kg/m^3. The barite particles, originally suspended in the mud, will when the mud stays static over longs periods of time in relatively vertical wells, due to gravity settle out and form a layer above the casing cement. Originally only due to gravity, settled barite plugs are not likely to form an impermeable layer, because the porosity is too high. This has been confirmed in a previous Master Thesis conducted at NTNU, where settled barite failed to seal a water pressure of 5 bars (70). However, assuming only gravitational settling is not very realistic. In a downhole situation, as seen earlier in this thesis, the adjacent formation will move radially inward and mechanically compress the column with a force equal to the formation stress (typical values 30-70MPa). This will reduce the porosity, and if the particles are compressed enough together, due too the low particle sizes, the column may end up being practically impermeable. Moreover, the radial compression is likely to induce high enough shear forces against the casing and formation walls for the column to stay in position, even when exposed to large differential pressure. The described process is illustrated in figure 7.1.

.

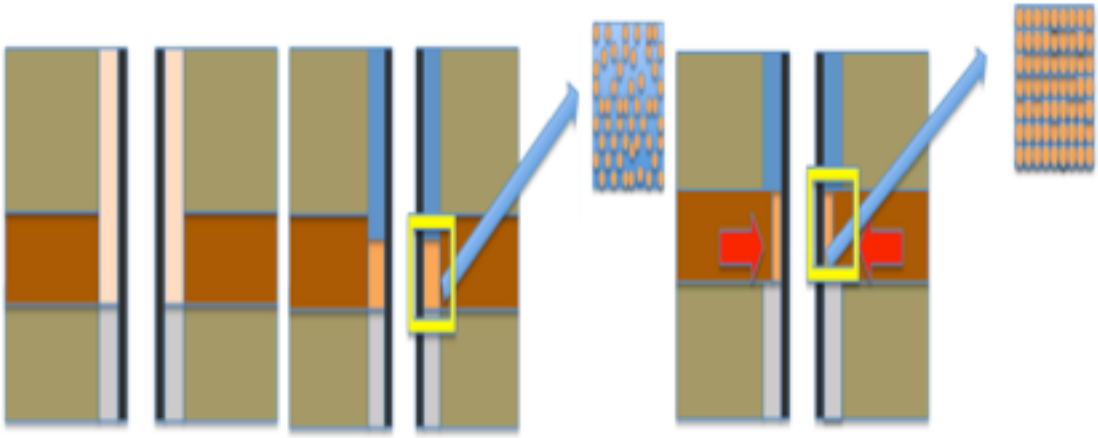

Figure 7.1 Concept of compressed settled weight materials as barrier element. First illustration to the left shows the borehole with casing right after drilling and cementing. The illustration in the middle shows the situation when barite has settled out at bottom on top of the casing underlaying a column of water. The right hand illustration shows the situation when the formation is displaced inward and compressing the barite column, making it less permeable.

The impermeability of barite plugs have been claimed by several authors (71) and (3). In fact ConocoPhillips have qualified it for use as a permanent well barrier and it has been used for PP&A in wells on the West Ekofisk and Edda Platforms (3). On these wells, the settled barite column was discovered, due to unexpected resistance when trying to cut and pull the casing string during PP&A in sections with no cement. The sealing ability of the column was furthermore verified by setting a bridge plug inside the casing, cutting the casing above the plug, and pressure test pressure test the exposed column to 70 bar above the fracture gradient of the formation (3). However, to the author's knowledge no attempts were made to verify that the sealing column was in fact barite. Thus, the observed seal could for instance be caused by displaced formations. As a consequence it is still of interest to check barites sealing ability. If compressed settled barite is proven to seal, its usefulness will still be limited to relatively vertical wells. Hence for deviated wells, alternative solutions have to be used.

The other test material was micro-barite. Micro-barite is a relatively recently developed material. It consist of particles with sizes smaller than the lower limit for conventional barite and has a typical average size between 1µm and 3µm (72). The product is mainly used in ERD wells and is designed to improve hydraulic pressure management while mitigating sag. However, field experience has also shown that the product reduce the surge and swab pressures, improves MWD transmission rates and quality as well as lowering the ECD and thus allowing for higher flow rates with the result being better hole cleaning (72). As a consequence, the product is growing in popularity. As opposed to barite, which settles above the casing cement due to gravity, because of the small particle size this will not happen for micro-barite. As a consequence, alternative means of getting the material "in position", adjacent to a deforming shale zone, has to be initiated. One possible solution would be to put high amounts of the material in viscous plug pumped in front of the cement during the cement job (52).

7.1.2 Initial Porosity

The initial porosity (non-solid fraction) of the settled material before any compaction has taken place is affected by 4 parameters (73):

1. Particle size
2. Particle shape
3. Particle packing arrangement
4. Distribution of particle sizes

In general, all other factors equal, a given weight of course particles will be stabilized at a lower porosity than the same weight for finer particles. This is because the equilibrium porosity is dependent upon the stability given to the material by frictional and cohesive forces. These forces are proportional to the exposed surface area of the particles, which again are inversely proportional to particle size (73). Moreover, the more angularly shaped the particles are the higher will the porosity be. Thus, for instance all non-spherical particles will yield a higher porosity than spheres. Both the effect of particle size and shape on porosity is illustrated in figure 7.2.

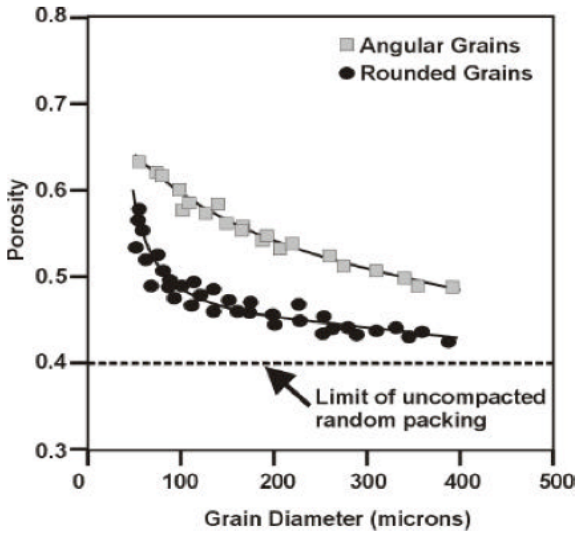

Figure 7.2 Relation between porosity, grain size and grain shape. After (73)

As seen from the figure the increase in porosity is quite rapid when the particle size falls below 100µm. Moreover, as the particle size increases past 100µm the frictional forces decrease, making better packing (reduction in porosity) possible, until a lower limit for one sized particles is reached. This lower limit is furthermore dependent on the particle packing arrangement. A list over some common ones can be found in figure 7.3

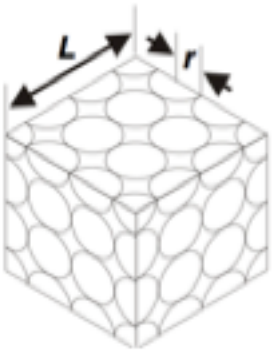

Packing arrangement	Maximum Porosity (fractional)
Close random packing	0.359
Loose random packing	≥0.399
Cubic	0.476
Hexagonal	0.395
Orthorhombic	0.395
Rhombohedral	0.260
Tetragonal	0.302
Triclinic	0.260

Figure 7.3 Cubic packing of identical spheres and maximum porosity for different packing arrangements. Free after (73).

Note that in the figure the porosity values are labelled maximum porosity. This simply means that they are the maximum porosity that a structure can have and still be threated as a "rock". If the porosity exceeds these values the grains/particles will no longer be in contact with each other, as a consequence the frame moduli will vanish, and the rock mechanics approach will no longer be valid. Moreover, it is important to be aware of that although the term "maximum" porosity is frequently used, the values also represent the minimum values for porosity for uniform sized particles unless the particles undergo compaction.

As seen from figure 7.3, for uniformed sized particles the minimum porosity, without compaction is quite high. However, combining different particle sizes yields a lower porosity than 100% of each size. In general the porosity is lowest when there is a wide difference between the particle sizes. By using particles with different size at specific volumetric ratios is it possible to have a solid to bulk volume ratio of 0.95, compared to 0.64 if sphere shaped particles with the same size is randomly packed (12).

Although, both barite and micro-barite consists of particles with wide-range of sizes due to the fact settling occurs fastest in the largest particles initially the distribution in the settled layer is likely to be quite uniform. Thus, due to their small particles size the initial porosity is likely to be quite high.

7.1.3 Flow through concentrated particle layer

The permeability of a concentrated particle layer is highly dependent on the particle size and porosity of the layer. In a similar manner to the famous Darcy equation describing the flow velocity though a homogenous porous mass, given as

$$v = \frac{k}{\mu}\frac{\Delta P}{\Delta L} \quad (7.1)$$

The flow through a packed sand bed (comparable to a layer of concentrated particles) can be estimated by the semi-empirical Blake-Kozeny equation (74):

$$v = \frac{d_p^2}{150\mu} \frac{\varepsilon^2}{(1-\varepsilon)^2} \frac{\Delta P}{\Delta L} \quad (7.2)$$

Where d_p is the sand (barite/micro-barite) particle diameter, ε is the beds non-solid fraction, $\Delta P/\Delta L$ is the pressure drop per unit length and μ and k is the viscosity and permeability respectively. The factor 150 is an empirically adjusted factor that includes the geometrical terms arising from treating flow around spheres.
By looking at the two equations, it is obvious that the Blake-Kozeny equation is equal to the Darcy equation if the permeability k is given as:

$$k = \frac{d_p^2}{150} \frac{\varepsilon^2}{(1-\varepsilon)^2} \quad (7.3)$$

Typical barite requirements for petroleum purposes is that 97% of the material by weight has to pass through a 200-mesh (75μm) screen, and no more than 30%, by weight, can be less than 6μm in diameter (69). Micro-barite consists of particles smaller than this.
For conventional barite the larger particles alone would give a fairly permeable matrix, but the fact that the pore volume is filled with smaller particles, and the new pore volume with even smaller particles means that particles of a few microns could define d_p. Moreover, since the particle distribution includes both particles smaller and larger than d_p, the permeability is likely to be even lower than stated by the equation since it is derived for particles with equal size. This is illustrated in figure 7.4

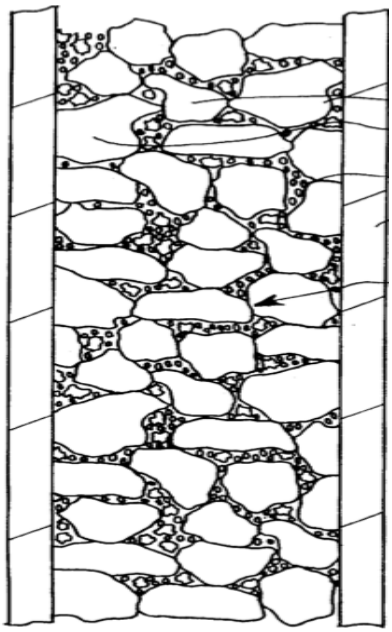

Figure 7.4 Schematic illustration of annulus filled with particles of different size. After(75).

As seen from equation 7.2 one of the components that determines the velocity through the particle layer is the length of the layer. By assuming that drilling fluid consist only of water (ρ_w=1030kg/m3) and barite (ρ_b=4200kg/m3) and by furthermore knowing the density of the drilling mud and the height of the well, it is possible to determine the

length of the settled plug. This is illustrated in figure 7.5 for wells with lengths of 1000, 2000 and 3000 meters respectively.

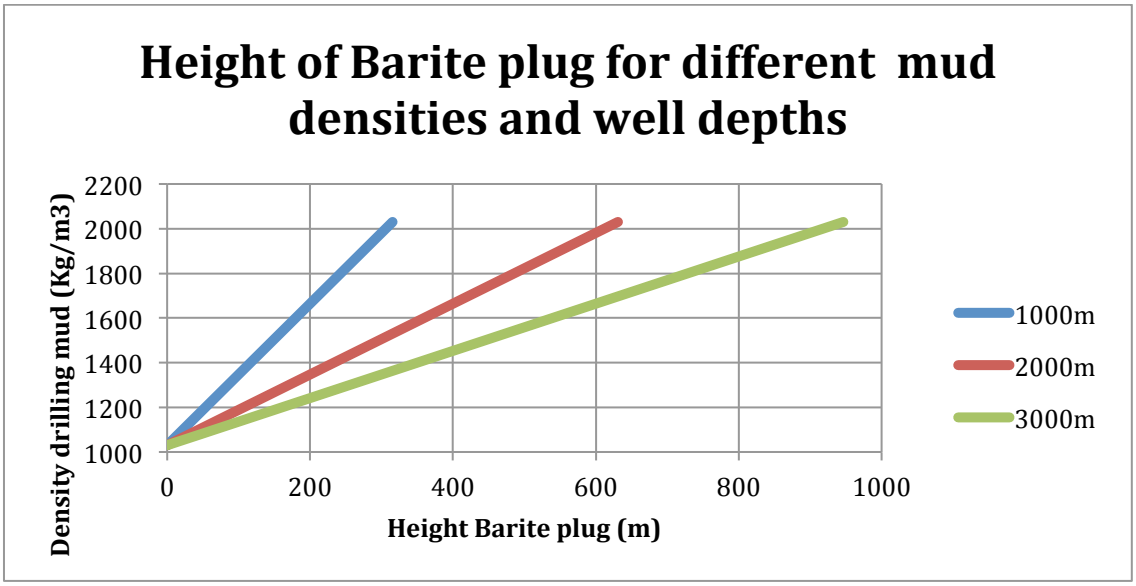

Figure 7.5 Height of barite plug for different mud densities and well depths. Assuming drilling mud consists of a mixture of water and barite.

Assuming a 400 meter particle column in a 12 ¼" borehole with a 9 5/8" casing. A list over volume leakages, flow rates and permeabilities for different particle sizes, void ratios and differential pressures for water (μ=1cp) can be found in table 7.1.

Table 7.1 Theoretical sealing parameters for a 400 meter particle column in a 12 ¼" borehole with 9 5/8" casing exposed to water (μ=1cp).

Particle size (μm)	Void ratio	Permeability (mD)	Differential pressure plug (bar)	Velocity (m/year)	Volume leakage (m^3/year)
50	0.4	$7.41*10^3$	100	$5.84*10^3$	32.6
20	0.45	$1.79*10^3$	100	$1.41*10^3$	8.83
20	0.35	$7.73*10^2$	100	$6.10*10^2$	2.98
20	0.20	$1.67*10^2$	100	$1.31*10^2$	0.37
20	0.20	$1.67*10^2$	300	$3.94*10^2$	1.1
20	0.10	32.9	100	26	$3.62*10^{-2}$
5	0,35	48.3	100	38.1	0.19
5	0.35	48.3	300	$1.14*10^2$	0.56
5	0.20	10.4	100	8.21	$2.29*10^{-2}$
5	0.20	10.4	300	24.6	$6.87*10^{-2}$
1	0.8	$1.07*10^2$	100	84.1	0.94
1	0.6	15	100	11.8	$9.89*10^{-2}$
1	0.45	4.46	100	3.52	$2.21*10^{-2}$
1	0.35	1.93	100	1.52	$7.44*10^{-3}$
1	0,20	0.42	300	0.99	$2.75*10^{-3}$
0.1	0.35	$1.93*10^{-2}$	100	$1.52*10^{-2}$	$7.44*10^{-5}$
0.1	0.20	$4.17*10^{-3}$	300	$9.86*10^{-3}$	$2.75*10^{-5}$

Assuming that particles in the 20 µm range defines the maximum permeability for barite and furthermore that the column has a void ratio of 0.45, it will take water with a differential pressure of 100bar 0.28 years to go through the plug. Moreover, the leakage will be 8.83m^3 per year, which is quite substantial. However, if the defining particle size is reduced to 1µm for the same situation it will take water 114 years to go through the plug. Moreover, the leakage is only 22.1 litres per year, which means that the column is practically impermeable. Thus, from a purely theoretical viewpoint it appears that conventional barite may have too large particles to make up a good seal, unless either the defining particle size is much lower than the average (ca. 20µm) or the void ratio is significantly reduced from its initial. For instance, a void ratio of 0.1 gives a leakage rate of 36.2 litres/year, and although the leakage appears only after 15.4 years, it is still practically impermeable. On the other hand micro barite seems to create a good seal more or less independent of void ratio, unless it gets really high like for instance 0.8.

7.1.4 Theory behind porosity reduction due to compaction

From the previous section it became evident that for the barite to seal its porosity must be reduced from the initial through compaction. Moreover, micro-barite was proved to theoretically seal even at quite high porosities. However, as smaller particles gives higher viscosity, it may be difficult to pump high concentrations of micro barite (72). Thus, the material is still likely to require some compression to reach low enough void ratios to be impermeable. Furthermore, without compression the shear forces against the annular walls are likely to be too small for the material to stay in position when exposed to large differential pressures.

Compaction can be caused by compression and will occur in the concentrated particle layer during radial inward movement of the formation. It occurs because when the material is compressed, particles may loosen or break and then pushed or twisted into the open pore space, resulting in a closer packing of the material as schematically illustrated in figure 7.6. In addition to compression, another factor that could contribute to better compaction is vibration. However, as this was not used in the laboratory tests it will not be discussed further in detail here.

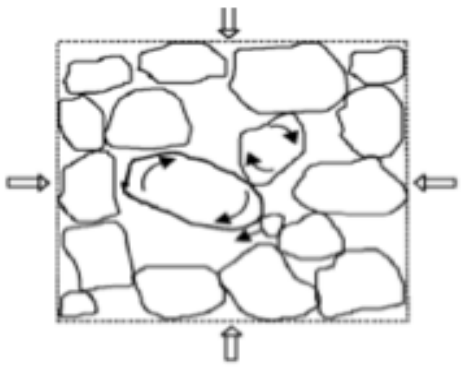

Figure 7.6 Compaction induced reorientation of particles resulting in closer packing. After (36).

To determine the change in porosity due to the radial movement the 3 main questions to be answered is:

1) What is the magnitude of the external stress, σ, applied onto the settled material from the moving formation?
2) How is the pore pressure in the settled material, p_f, affected by the applied external stress?
3) How will the porosity, φ, of the settled material change as a result of changes in the confining pressure, σ, and/or the pore pressure, p_f?

So far in thesis the description of the poroelastic theory has been limited to brief explanation of the concept of effective stress, as this was sufficient to explain the stress situation at the borehole. However, to determine what will happen to a poorly consolidated material (e.g. settled barite) when compressed by a deforming adjacent formation, a more comprehensive description referred to as the Biot-Poroelastic theory, is needed. The theory as well as a material model needed to determine some of the required parameters in the presented poroelastic equations will be addressed here.

7.1.4.1 Biot-Poroelastic Theory

In general, as previously seen, for an isotropic, porous and permeable medium, consisting of two components: a solid and a fluid part, the stress "felt" by the solid part when exposed to an external stress, σ, is given by the principle of effective stress.

$$\sigma_{ij}' = \sigma_{ij} - \alpha p_f \delta_{ij} = K_{fr}\varepsilon_{vol} \quad (7.4)$$

Where σ_{ij}' is the effective stress, α is the Biot coefficient defined as

$$\alpha = 1 - \frac{K_{fr}}{K_s} \quad (7.5)$$

p_f the pore pressure, δ is the Kronecker symbol, ε_{vol} is the volumetric deformation, K_{fr}, K_s and is the frame and solid bulk modulus respectively. Although equation 7.4 in many ways is sufficient when looking at failure criteria's and borehole stability analysis it does not say anything about how the external stress and pore pressure is related. For such analysis a set of two equations often referred to as Biot-Hook's law can be used (36).

$$\Delta\bar{\sigma} = K\varepsilon_{vol} - C\xi \quad (7.6)$$

$$\Delta P_f = C\varepsilon_{vol} - M\varsigma \quad (7.7)$$

Where $\Delta\sigma_{avg}$ is the mean stress. Defined as

$$\Delta\bar{\sigma} = \frac{\sigma_x + \sigma_y + \sigma_z}{3} \quad (7.8)$$

K is the undrained bulk modulus, defined as the bulk modulus in a situation where the pore fluid is trapped and cannot escape when the material is exposed to external stress. It is given by an equation often referred to as the Biot-Gassmann equation:

$$K = K_{fr} + \frac{K_f}{\varphi}\frac{(1-\frac{K_{fr}}{K_s})^2}{1+\frac{K_f}{\varphi K_s}(1-\varphi-\frac{K_{fr}}{K_s})} \quad (7.9)$$

Where φ is the porosity and K_f is the bulk modulus of the pore fluid.
ξ is a strain parameter that describes the volumetric deformation of the fluid relative to the solid. It is positive when the amount of fluid in the volume element is increasing and negative when the amount of fluid is decreasing and can therefore be seen as a parameter describing increment in fluid content.
There are two possible reasons for change in mass of fluid in a volume element attached to a solid. The first one is due to change in pore volume as a response to changes in external and/or internal (pore pressure) stresses. The other explanation is related to compression/decompression of the fluid as the pore pressure changes. ξ can therefore be written as:

$$\xi = \frac{\Delta V_p - \Delta V_f}{V} = -\varphi(\frac{\Delta V_p}{V_p} - \frac{\Delta p_f}{K_f}) \quad (7.10)$$

Where V_p and V_f is the pore and fluid volume respectively.

C and M are elastic moduli required to describe the two-phase medium, and are given by

$$C = (1-\frac{K_{fr}}{K_s})M = \frac{K_f}{\varphi}\frac{1-\frac{K_{fr}}{K_s}}{1+\frac{K_f}{\varphi K_s}(1-\varphi-\frac{K_{fr}}{K_s})} \quad (7.11)$$

$$M = \frac{K_f}{\varphi}\frac{1}{1+\frac{K_f}{\varphi K_s}(1-\varphi-\frac{K_{fr}}{K_s})} \quad (7.12)$$

By eliminating ε_{vol} from eq. 7.6 and 7.7, inserting the resulting expression for ξ in eq. 7.10, and furthermore inserting K, C and M from eq. 7.9,7.11 and 7.12 it can be shown after some algebra that (36).

$$\frac{\Delta V_p}{V_p} = -\frac{1}{\varphi}(\frac{1}{K_{fr}} - \frac{1}{K_s})\Delta\sigma + -\frac{1}{\varphi}(\frac{1}{K_{fr}} - \frac{1+\varphi}{K_s})\Delta p_f \quad (7.13)$$

By furthermore combining equation 7.4 and 7.13 and expression for the change in porosity as a function of changes in σ and p_f is given as

$$\Delta\varphi = -(\frac{1-\varphi}{K_{fr}} - \frac{1}{K_s})(\Delta\sigma - \Delta p_f) \quad (7.14)$$

For a more detailed derivation of the equations above the reader is referred to the book Petroleum Related Rock Mechanics (36).

7.1.4.2 Material model

In the previous section equations relating the external stress, pore pressure and porosity to each other through common elastic parameters where presented. Some of these where related to the fluid or solid constituents of the material of interest and are more or less constant. A list over some of them can be found in table 7.2.

Table 7.2 Physical parameters of fluid and solid constituents in weight material sealing layers. After (36)

Material	Density(kg/m3)	Bulk Modulus (GPa)	Shear Modulus GPa)
Barite	4500	53	22
Crude oil (room temp.)	700-1100	1.2-2.8	0
Water (fresh)	1000	2.25	0

Although some are more or less constant, others such as the frame bulk and shear moduli are variables depending on the relative amount-, the elastic properties- and the geometrical distribution of each component (36). A common approach, when estimating the frame moduli, is to look for the most probable microstructure of the material and try and estimate the moduli for such a structure. For instance, as mentioned earlier, for different packing structures there exists a maximum porosity, above which the grains will no longer be in contact with each other and the frame moduli will vanish. For a simple cubic packing of equally sized spheres, this critical porosity,φ_c was shown in section 7.1.2 to be 0.476, while other values where given for other structures. Based on this argument, combined with the fact that the moduli should be equal to the moduli of the solid material if the porosity is zero, estimates for the frame bulk and shear moduli can be given as

$$K_{fr} = K_s(1 - \frac{\varphi}{\varphi_c}) \quad (7.15)$$

$$G_{fr} = G_s(1 - \frac{\varphi}{\varphi_c}) \quad (7.16)$$

Where φ_c is the maximum critical porosity for the structure.

Other ways to estimate the moduli frequently used in rock mechanics include using the geometrical averages of extreme upper and lower values of the moduli called Reuss and Voigt bounds or the narrower Hashin-Shtrikman bounds (36). However, since these are slightly more laborious and doesn't necessary give better estimates for they will not be presented here.

7.1.5 Porosity reduction due to radial compression in three extreme situations

So far only the basic theory necessary to analyse the situation downhole when the formation is deforming radially inward and thus compressing the settled material has been presented. Here a practical approach to illustrate how the equations can be applied to estimate the well pressure that gives the desired porosity reduction will be looked into. For simplicity 3 scenarios representing 3 extreme limit phases during the compression will be addressed. It is important to be aware of that the real situation

occurring downhole is likely to be somewhere in between these extremes. Moreover, in addition to the studied cases being mainly of theoretical interest, due to the complexity of the problem the analytical solutions presented below is based on several simplifying assumptions and are presented mainly for illustrative purposes. For more realistic solutions advanced numerical simulations has to be performed.

7.1.5.1 Initial situation in settled material

Initially, as mentioned previously, the material is suspended in the mud and after a while it gradually starts to settle out. The first particles to reach the top of the casing cement will be the ones closest to this top when the mud became static and the last ones will be the ones closest to surface. The first particles will therefore settle out without much reduction in well pressure, and for these particles it can be assumed that the wellbore wall is non-moving, and that the situation is similar to what in the literature is typically described as an "unjacketed test". In an unjacketed test the material is embedded in a fluid in such a way that the hydrostatic pressure (from the above laying fluid column) on the sample is balanced by the pressure in the pores, i.e. $p_f=\sigma_p$ (36). An illustration of the situation can be found in figure 7.7.

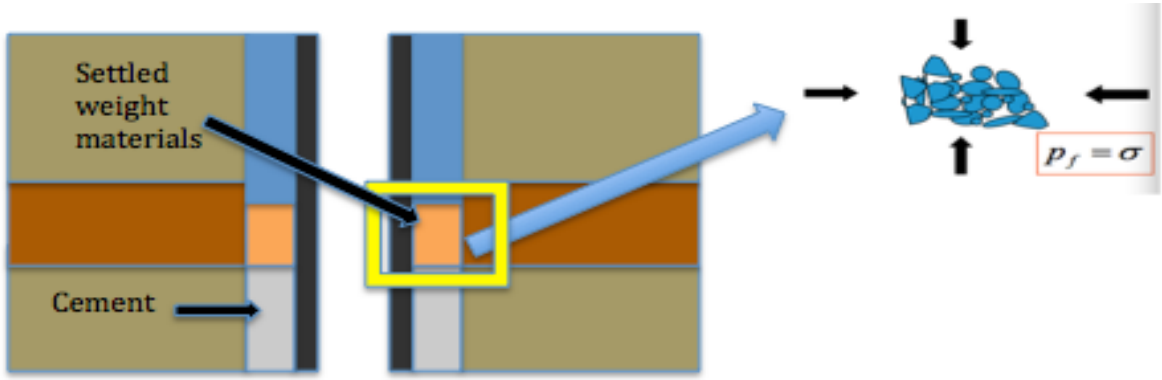

Figure 7.7 Initial situation in settled material similar to "unjacketed test". Free after (9).

According to eq. 7.14, $p_f=\sigma_p$, means that the porosity remains unchanged. Moreover, since the pore pressure equals the external stress there is a uniform stress within the sample, which means that the rock framework deforms uniformly according to (36).

$$-\varepsilon_{vol} = -\frac{\Delta p_f}{K_s} \quad (7.17)$$

For barite the solid grain bulk modulus is in the region of 53GPa, thus in addition to no porosity change, during this phase there will be very little deformation of the settled material.

7.1.5.2 Drained phase situation

After a while, when enough particles have settled out, the well pressure will be reduced and the stress on the settled material will increase until it reaches the horizontal formation stress. This stress increase will compress the settled material and thus affect the pore pressure, porosity and permeability. However, initially while the porosity and permeability is still quite high, the situation may be approximated by a situation, which

in the literature is often referred to as drained conditions. Drained conditions refers to a situation where the pore fluid is allowed to escape during loading, hence the pore pressure is kept constant and the external stress is carried entirely by the solid framework (36). Thus, the change in porosity can be found by combining equation 7.14 and 7.15 with the change in pore pressure equal to zero.

7.1.5.3 Undrained phase situation

Later on, when the settled particles has been compressed enough, the porosity and permeability will in an ideal case eventually become so low that the material becomes practically impermeable. Thus, there is no fluid movement in the material, ξ=0, and the material is referred to as undrained. During undrained conditions equation 7.6 and 7.7 becomes

$$\Delta p_f = C\varepsilon_{vol} \quad (7.18)$$

$$\Delta \bar{\sigma} = K\varepsilon_{vol} \quad (7.19)$$

Combining the two equations yields an equation that describes pore pressure increase as a function of increase in external stress

$$\Delta p_f = \frac{C}{K}\Delta \bar{\sigma} \quad (7.20)$$

The ratio C/K is often referred to as the Skempton B-coefficient and describes how the pore pressure responds to a change in mean stress under undrained conditions. By combining eq. 7.11 and 7.12 and neglecting K_f relative to K_s, it can be shown that the Skempton B-coefficient is given as (36).

$$B = \frac{K_f}{K_f + \frac{\phi}{\alpha}K_{fr}} \quad (7.21)$$

From the equation it can be seen that B decreases with increasing porosity and decreasing fluid bulk modulus.

In a similar way to drained conditions, the change in porosity due to the exposure of an external stress,σ, can be found by combining eq. 7.21, 7.20 and 7.15 and inserting the obtained values into eq. 7.14.

7.2 Laboratory experiments

Laboratory experiments with settled barite and micro-barite have been conduced. Here the Experimental set-up, procedure, results and discussion for the two conduced test will be presented.

7.2.1 Experimental set-up

In order to check the sealing ability of the barite and micro-barite an Oedometer have been applied. An Oedometer is an apparatus using the lever principle to apply high mechanical loads on a sample. It is conventionally used for measuring the rate and amount of consolidation of soil specimens under uniaxial strain compression. In

addition to the standard components, the Oedometer used has the possibility to measure both horizontal and vertical P-waves in combination with vertical S-waves. However, as no acoustic velocities has been measured in the conducted experiments for this thesis, exactly how that works will not be discussed in further detail.

In general the used set-up of the applied apparatus can be divided into an internal and external part.

The internal part is composed of 4 main components

1. Load frame
2. Load cell
3. Piston
4. Main chamber

The load frame is based on the lever principle and is used to apply force on the rest of the system through a thick steel rod and a load cell mounted on the top of the piston, which moreover exert the load onto the sample located in the main chamber as illustrated in figure 7.8. The function of the load cell is to be measure the exact load exerted by the lever, as this will change slightly with degree of compaction for a certain amount of weight, due to angular differences. However, at the time for the conducted experiments the load cell was not working appropriately. Therefore the exact load vs. time remained unknown, but due to the vast experience with the apparatus, good estimates were still obtained.

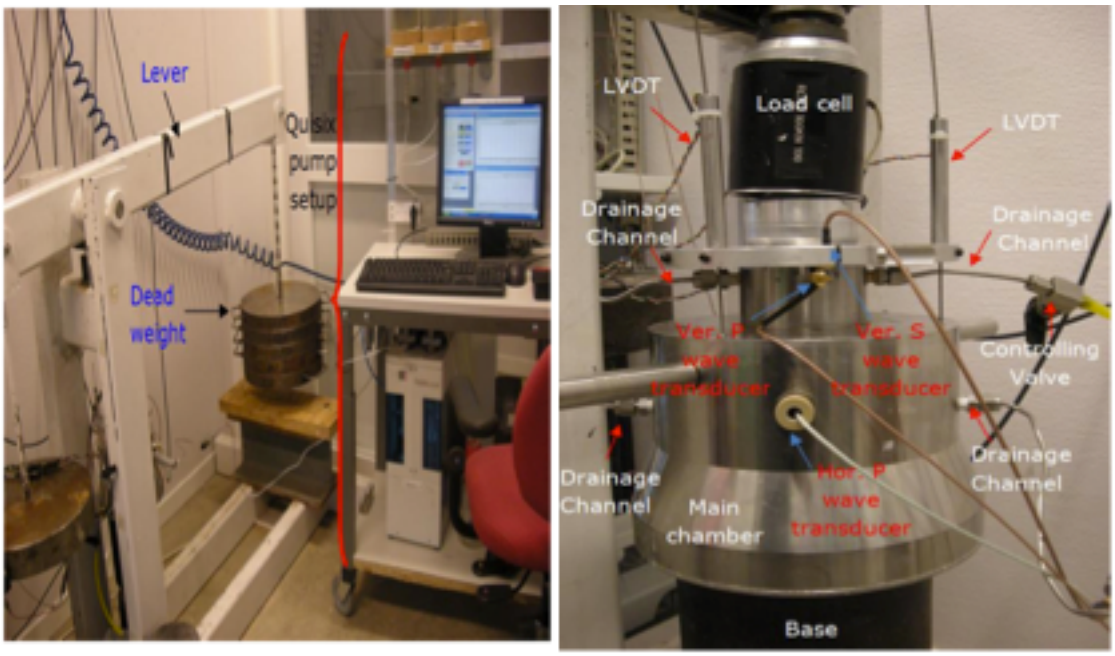

Figure 7.8 Load frame and Quizix pump with operating computer to the left. Basic set-up of the load cell, piston and main chamber part of the Oedometer to the right. After (70).

The main chamber and piston are made of stainless steel. The most important part of the former is the sample holder. It has a diameter of 69.90 mm, a height of 40 mm and is

located in the middle part of the main chamber. The thickness of the outer ring measured from the wall of the sample holder to the outskirt of the main chamber is 50 mm. Thus, negligible lateral strain can be expected during the tests. A schematic illustration of the main chamber is illustrated in figure 7.9

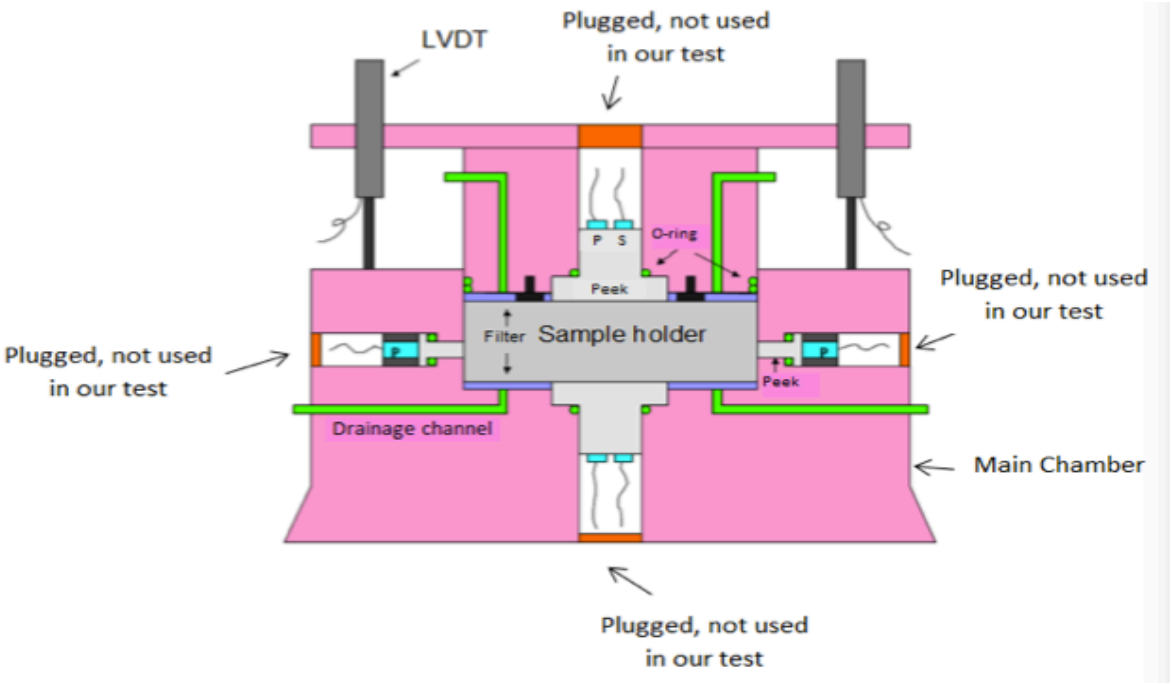

Figure 7.9 Schematic illustration of the main chamber. After (70).

As seen from the figure there are two flow channels connected to the base of the sample holder and additional two connected to the piston part. During the compression part of the experiment ideally all of these are open to make sure that the sample is drained as fast as possible. In order to prevent the sample material from escaping through the drainage channels (flow channels), a 3 mm thick filter made of stainless steel, with a specific filtering capacity of 0.5 µm is placed above the lower drainage channels and similarly below the upper drainage channels. To assure complete sealing at the base, a second paper filter with identical properties is placed beneath the steel filter and the areas outside the steel filter filled with silica gel.

The external part of the setup consist of

1. Quizix pump with accompanying software
2. Device to measure compaction and accompanying software

The Quizix pump is used to apply the desired test pressure onto the sample. The pump is automatically software controlled and consists of two completely independent, positive displacement piston pumps, which can be used as a pair to provide pulseless continuous fluid flow for a single fluid. Moreover, it can be programmed for accurate pressure control and both received and delivered pressures and volume can be measured (76).

The axial displacement is monitored using three linear variable displacement transducers (LVDT's), as illustrated in fig 7.8 and 7.9. The acquired data is sent to a computer where it can be monitored.

7.2.2 Experimental procedure

The following steps where conducted in advance for each of the two tests:

1. Mix water and test material (barite/micro-barite) in a blender.
2. Pour mixed blend into a container and wait for the weight material to settle out at the bottom.
3. Remove above laying water column

After this the sample holder was filled with the settled weight material and the compression stage was conducted. This was done in the following manner:

1. Start compression with 7 bars pressure; leave the sample to consolidate until now further effect of the applied stress is observed.
2. Increase compression in steps of 7 bars or 14 bars depending on whether the effect of the added compressive stress is large or not. Leave the sample to consolidate until now further effect of the applied stress is observed.
3. Repeat stage 2 until no observed effect of adding more weight is seen or the lever levels with the ground.
4. To give the final sample as much height as possible, the sample holder was refilled with fresh sample. The number of refills conducted was dependent on the amount of the observed compression.
5. After each refill steps 1-3 was conducted each time. For the final filling the sample was compressed to up to a maximum stress in the excess of 100 bars.

After this the Quizix pump was attached to one of the upper flow channels, while the other upper flow channel was closed to prevent the water from escaping through it, rather than through the test material. Then the seal part of the test was then conducted in the following manner:

1. Pump freshwater into the sample holder and increase the pressure, over the course of 10 minutes, from 0 to 10 bars. Observe for leakage at the lower drainage channels.
2. Wait for 10 minutes, then increase the pump pressure from the previous point by 10 bars, over the course of 10 minutes, observe for leakage
3. Repeat stage 2 until a pressure equalling the compressive stress is reached or leakage is observed at the lower drainage channels.

7.2.3 Result and Discussion

7.2.3.1 Barite

The aim of this experiment was to investigate the sealing capability of compressed settled barite. A sample of 128.68 mL settled barite containing water was put into the sample holder. The sample had an initial porosity of 0.54 and amounted to a height of 33.55mm in the sample holder. The sample was put under compression for 45 hours. The compression force was increased stepwise (as described in section 7.1.2) until a final compressive force of 77 bars was reached. During this period the original sample had compacted an average of 7.21mm (over the 3 LVDT's) making up a volume of 27.67mL. Due to the high bulk modulus of barite (53GPa) this compaction is due to water being drained out of the sample. In the end of this first compression the sample had a final porosity of 0.41. The compression vs. time is illustrated in figure 7.10.

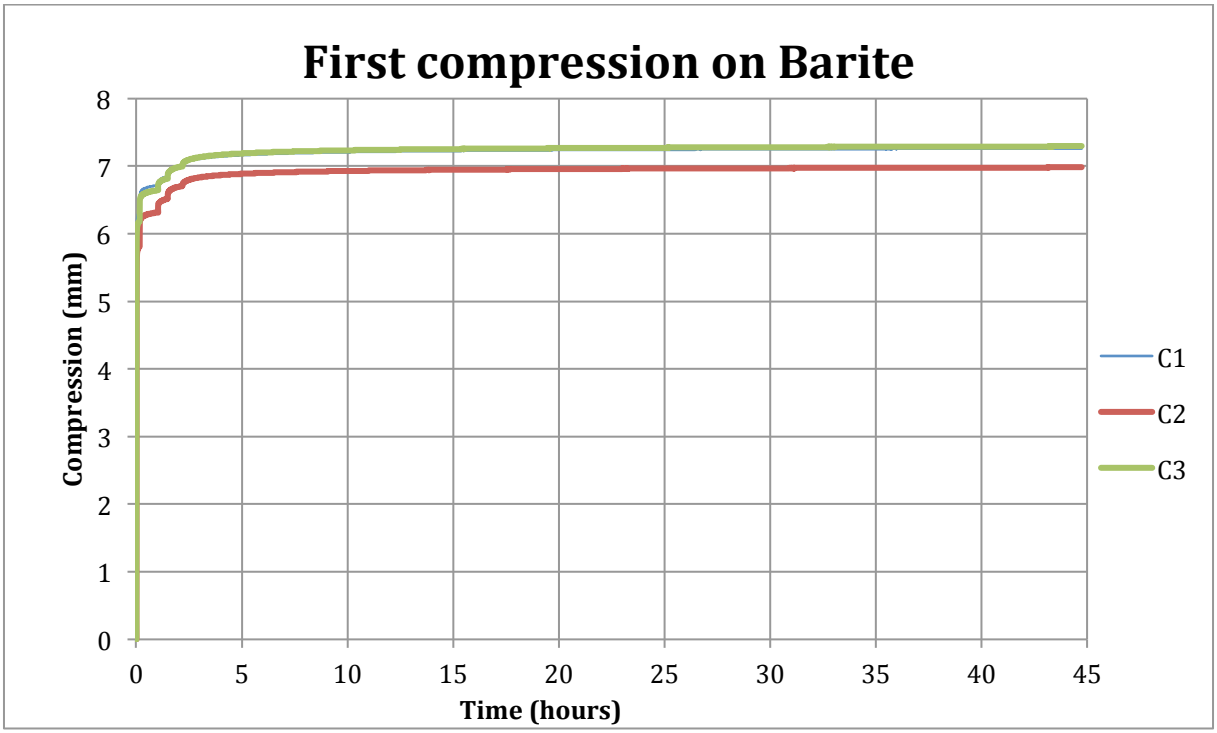

Figure 7.10 First compression part on barite in Oedometer cell. C1, C2 and C3 is the name of the 3 LVDT's respectively. The C1 line cannot be seen as it is hidden behind the C3 line. The difference between the lines is likely to be caused by calibration differences or possibly disturbance on the transducers.

As seen from the figure most of the compression occurs within the first few minutes. This could be because the grains are not really in contact with each other initially, but after some compression they get in contact and the plug starts building a frame moduli in accordance to eq. 7.15. As seen from eq. 7.14 the reduction in porosity due to increased stress is reduced significantly as K_{fr} is increased, this could explain the stiffer behaviour observed with time.

By taking a close look at the figure for every load increase (seen as minor steps), after the elastic response there is a time where the strain rate decreases as a function of time.

Initially, this could be caused by consolidation but after a while a more likely explanation is transient creep.

After the first compression, to gain height another 28.84 mL of sample was added, together with the original sample yielding a total height of 33.85mm. The second batch had compacted 2 more days than the first one, as well as been exposed to shaking and vibration during the collection of the first sample, and had an initial porosity of 0.42. The sample was then put under compression for 4 days, increasing the compressive force stepwise as described in section 7.2.1, until a final stress in the region of 115 bars was reached. During this final compression the sample had compacted an average of 1.99mm (over the 3 LVDT's) reducing the water content with 7.63mL and the porosity to a final of 0.38. The compression vs. time is illustrated in figure 7.11.

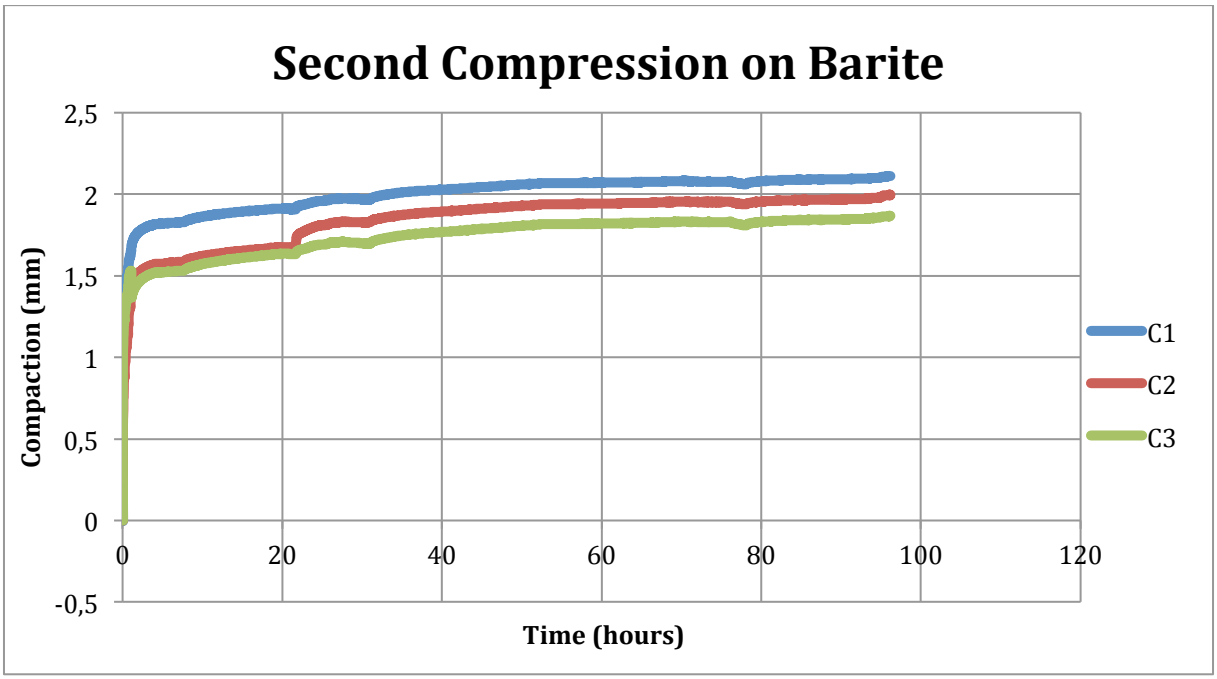

Figure 7.11 Second compression part on barite in Oedometer cell. C1, C2 and C3 is the name of the 3 LVDT's respectively. The difference between the lines is likely to be caused by calibration differences or possibly disturbance on the transducers.

As with the first compression, most of the compaction occurs initially. However, the sample is compacted approximately 3.5 times more in the first compression even though the compressive stress in the second goes almost 40 bars higher. This is because 77.8% of the sample in the second compression has been compacted to higher stresses before. Thus, the increased stiffness can be explained using a rock mechanics by saying that parts of the sample has developed a certain frame bulk modulus or similarly through soil mechanics that parts of the sample is overconsolidated

After the second compression the Oedometer was connected through one of the upper channels, to the Quizix pump. The pump was set to deliver freshwater and the pressure was gradually increased in accordance with the procedure in section 7.1.2. First the injected water goes through a steel filter located above the sample holder, hence making

sure that the water is evenly distributed across the whole top surface of the sample before it enters the sample.

The cumulative water volume injected into the sample holder vs. time is shown in figure 7.12.

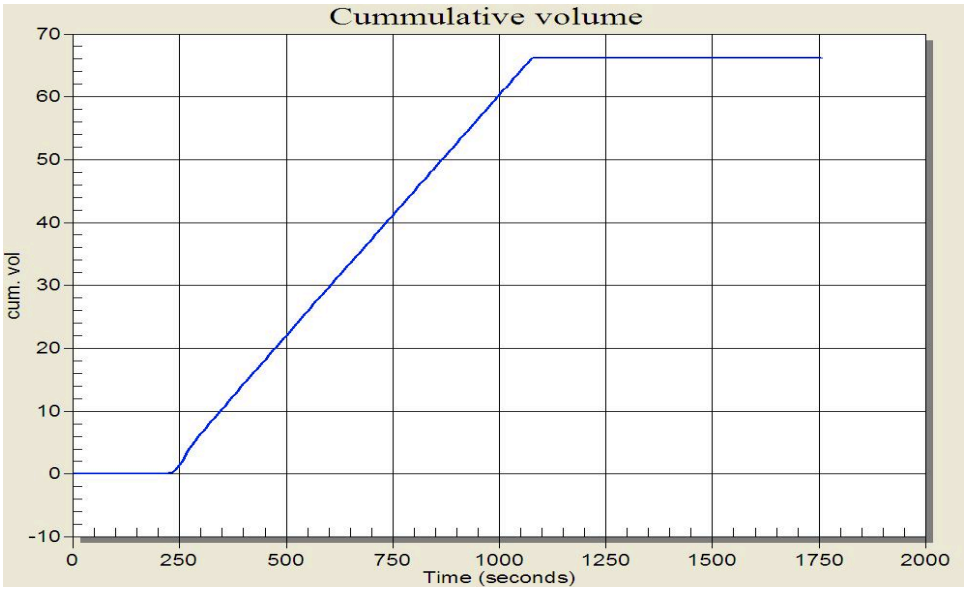

Figure 7.12 Cumulative water volume (mL) vs. time (seconds) for Barite seal test.

As seen, compared to the total volume of the sample, before exposing it to water 125,06mL, the injected water volume is very high. This illustrate the fact that right after the pump was connected, water was observed at the lower drainage channels, indicating that the compressed plug was not sealing at all. Instead it rather worked as a filter and the effect of exposing the sample to a pressure somewhere between 0-10 bars could be compared to that of pouring too much water into a potted plant, it simply goes straight through. A detrimental factor of the high permeability of the material is that both compression stages are likely to occur under drained conditions. Thus, no pore pressure build-up that could have somewhat resisted the water flow occurred.

To check that the observed leakage actually occurred through the sample, and not along the sample holder walls, a core of the sample was taken out. This is illustrated in figure 7.13. As seen from the illustration, the sides of the core is wet (shining) indicating that the injected water went through the sample rather than just along the sample holder walls.

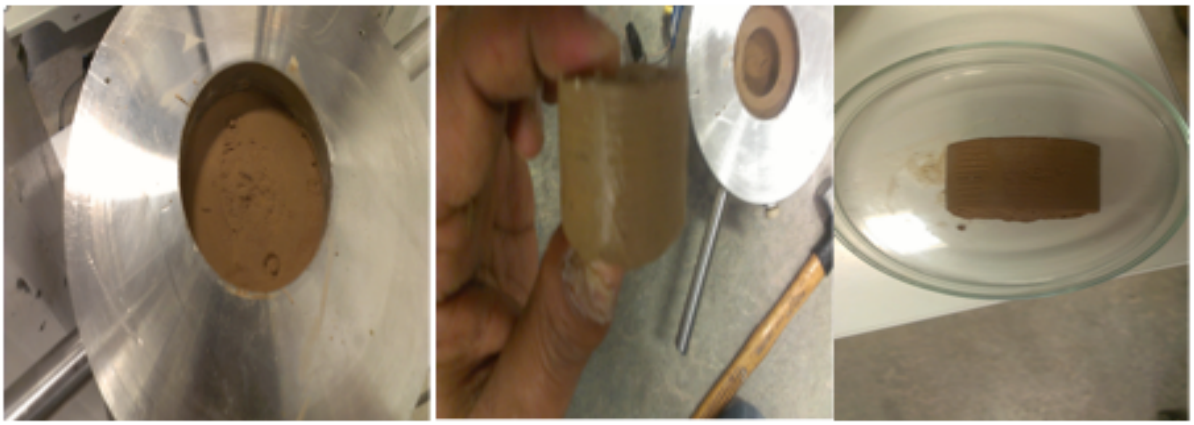

Figure 7.13 Barite sample at the end of the test. The left hand picture shows the sample inside the sample holder. In the middle picture a core of the whole sample has been taken out. As seen the side of the core is shining due to water, indicating that water went through the sample and not only along the sample holder walls. Right hand picture shows sample when dried.

From the conducted test it appears that compressed barite alone is not likely to become good a sealing material. Although, slightly higher compression (e.g. 3 to 7 times the applied stress in this test could be expected downhole) from the small changes in compaction seen at the end of this test it is unlikely that barite will be much more compacted, unless the stresses are high enough to compress the barite particles themselves. Barite has a bulk modulus of 53 GPa, i.e. to compress the particles with 20% a 10GPa stress is required. For the downhole situation this is highly unlikely. Thus, unless some kind of beneficial chemical or thermal reaction occurs downhole due to for instance the presence of bentonite or other drill fluid and adjacent formation constituents occurs, it is highly unlikely that standard barite can be able to provide a impermeable seal.

7.3.1.2 Micro-barite

In a similar fashion to the barite experiment, the aim of this experiment was to investigate the sealing capability of compressed settled micro-barite. Initially a sample of 127.96mL of settled micro-barite containing water was put into the sample holder. The sample had an initial porosity of 0.60 and amounted to a height of 33.38mm in the sample holder. Notice that compared to the initial porosity of settled barite (0.54) the initial porosity of micro-barite is slightly higher. This can be explained by the difference in grain size and is in accordance with figure 7.2.
After this the sample was put under a 7 bar compression pressure for 10 minutes before the compression stopped due to the lever levelling with the ground. During this period the original sample had compacted 5.32 mm. Thus, expelling a 20,43 mL of water and reducing the porosity with 7% down to 0.53. The compression vs. time is illustrated is figure 7.14. Notice that compared to the micro-barite test only one of the LVDT's was functioning during this compression. Moreover, despite countless efforts during all of the micro-barite compressions the two upper drainage channels had to be closed due to problems with leakage through the upper filter attached to the piston.

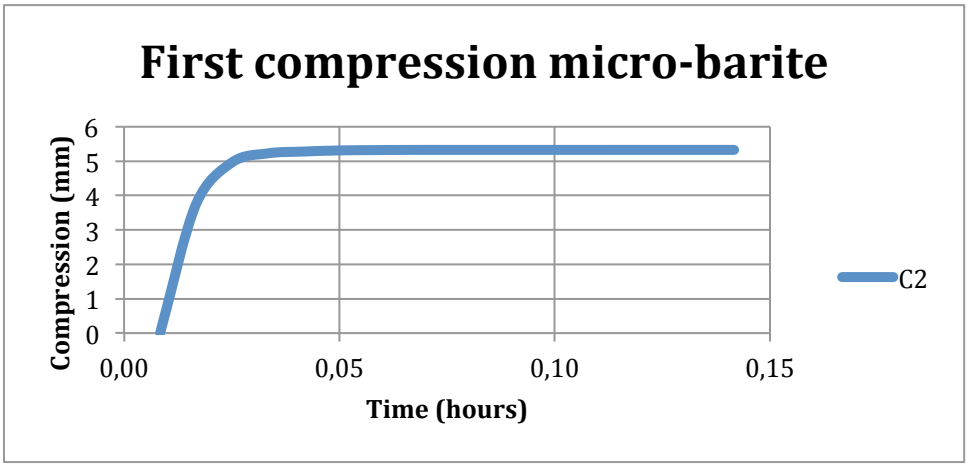

Figure 7.14 First compression of settled micro-barite. C2 represents the compression measured with one of the LVDT's.

After the first compression to gain height additional 3 sample fillings and subsequent compressions was conducted. The fillings were 21.90mL, 34.53mL, 27.17mL and maximum stresses of 21bars, 42bars and approximately 115 bars were reached respectively. In the end the sample had height of height of 30.09mm and a porosity of approximately 0.37. The different compressions vs. time can be found in figures 7.15 and 7.16. As with the compressed settled barite sample, most of the compression occurred in the beginning of each compression stage as the sample is getting stiffer and stiffer the more it is compressed. The explanations for this is the same as given for conventional barite.

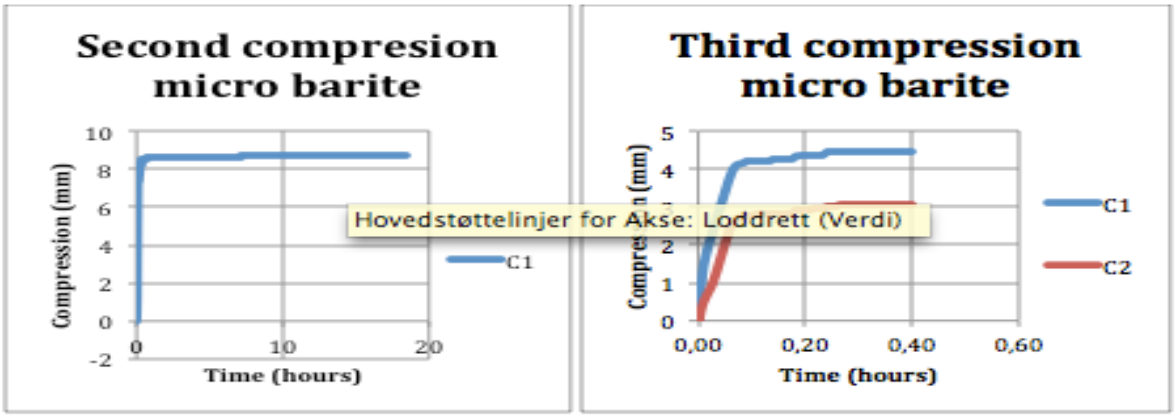

Figure 7.15 Second and third compression of settled micro-barite vs. time. C1 and C2 are the names of the LVDT's used to measure the compression. The difference in values is likely to be caused by distance to drainage channels, calibration differences and possibly also disturbance of the transducers.

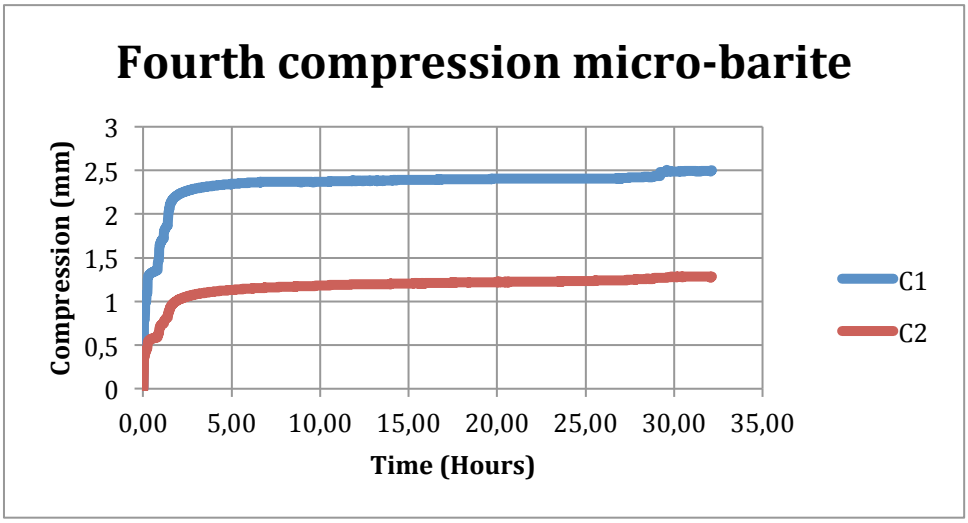

Figure 7.16 Fourth compression of settled micro-barite vs. time.

After the fourth compression the Oedometer was connected through one of the upper channels, to the Quizix pump. The pump was set to deliver freshwater and the pressure was gradually increased in accordance with the procedure in section 7.1.2 up to 50bars. After this the 10 min wait at each 10 bar step was omitted due to limited time. The cumulative water volume injected into the sample holder vs. time and the injection pressure vs. time is shown in figure 7.17.

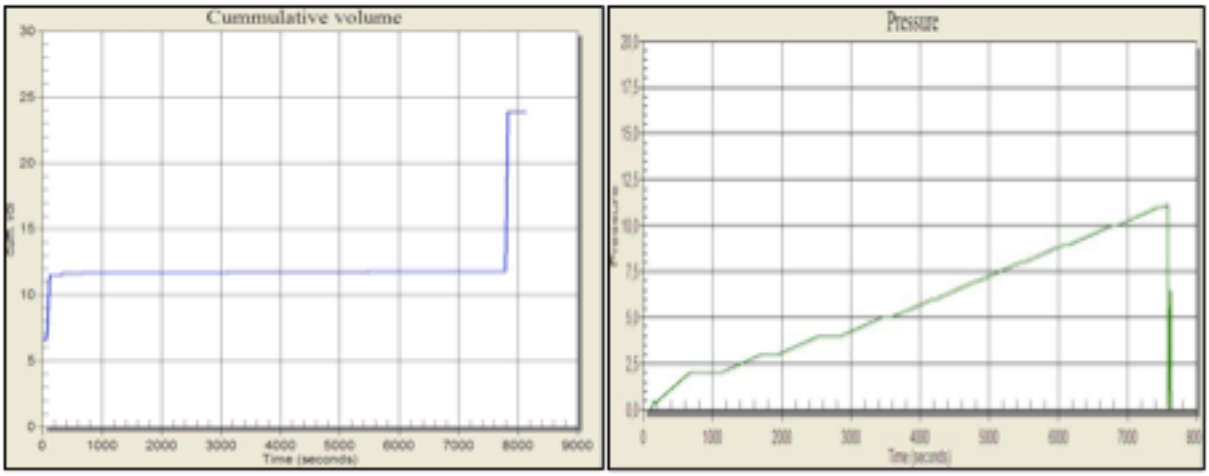

Figure 7.17 Cumulative volume vs. time and injection pressure vs. time for micro-barite test.

From the cumulative volume vs. time figure it can be seen that initially quite a lot (11.6mL) is injected into the sample. This was mainly caused by a small initial leakage in the setup, but part of the volume is also due to filling of the void space in the drainage channels. After this the injected volume is more or less constant, indicating that the material is sealing, until the pressure reaches 113 bars when a sudden large bump is observed indicating that the plug is no longer sealing. The latter could be explained by the fact that the vertical compressive stress is likely to be in the region of 113 bars. Moreover, since the sample is constrained the horizontal stresses according to eq. 4.24 are likely to be less than this and from eq. 7.4 it can be seen that the effective stress on the sample becomes very low and possibly also negative. As a consequence, hydraulic

fracturing (tensile failure) and debonding between sample and sample holder wall becomes more likely.

Due to the fact that the sample is constrained in all directions it is unlikely that the porosity is changed. Moreover, because the permeability is dependent on the grain size and porosity, the permeability of the whole plug will remain the same and the leak paths is likely to be either along fracture planes or along the sample holder walls. To investigate the leak paths a core of the sample was taken out and the sample holder walls was examined. This is illustrated in figure 7.18. As seen from the figure there is no signs of the water running neither straight through or along the sample holder walls. Since possible hydraulic fractures most likely would close after the water pressure is shut off, even though no such fractures were observed when examining the sample, it does not mean that they did not exist during the test. As a consequence, from this experiment it is not possible to make any conclusive statements about the leakage path for the injected freshwater. However, hydraulic fractures or debonding at the sample-to-sample holder wall seems to be the most likely leak paths.

Figure 7.18 Micro-barite sample at the end of the test. The upper left picture shows the sample inside the sample holder. The upper right picture shows the sample when a core of the whole sample is taken out. The middle left picture shows the core. The middle right picture shows a layer in the sample caused by a filling. The lower left picture shows the sample holder walls after the sample is carefully removed. The lower right picture shows the barite and micro-barite core sample.

From the conducted test is appears that compressed micro-barite, in accordance with the theory presented in section 7.1.3, is practically impermeable and sealing for liquids as long as the compressive stress is larger than the applied injection pressure. As this condition nevertheless has to be fulfilled for a shale formation to be part of a barrier element, it is likely that micro-barite in combination with inward moving sealing shales have the potential to constitute a good annular barrier. Although, slightly higher compressions, e.g. 3 to 7 times the applied stress in this test could be expected downhole, it is not likely that this will reduce the sealing capability of the material. It must be stated that the test is only conducted on a liquid. Thus, compressed micro-barites sealing capability for gas reservoirs remain unknown. To verify this more test with more advanced equipment is needed.

8. Discussion

So far in this thesis creep has been identified as the most likely reason for shales creating an annular barrier. However as shown, in many formations the creep rate may be either too slow or the shales too brittle for the shale section to provide a barrier within the time frame of PP&A. Several methods to increase the chance of shale zones becoming barrier elements has been identified, but the effect of them is too various degrees uncertain. Moreover, many of them are costly, hard to apply and have possible detrimental impact on other aspects of the drilling operation. As a consequence, whether they are likely to be applied or not is dependent on the possible upside of applying them. Here a cost evaluation comparing different ways of obtaining the required seal as well as a feasibility study of the different techniques that could be applied to increase the chance of shale sections providing an annular barrier will be discussed.

8.1 Cost evaluation of different ways to obtain required annular seal

In general there are 3 ways of improving the cost efficiency of obtaining the required annular seal for PP&A.

1. Improve the sealing material used
2. Improve the methods for repairing lack of annular seal
3. Increase the chance of a having a contingency plan in cases where the primary seal fails

These methods are not incompatible with each other and in an ideal world with unlimited resources of course all of them should be optimized. However, in the real world resources are scarce. Hence, from a strictly financial viewpoint for instance using a more durable, but more expensive sealing material may not be worthwhile if the costs for repairing the lack of annular seal are low or the chance for an almost “free” shale barrier is quite high. In other words, the choice of sealing material is dependent the on the cost of repairing a future lack of seal and the likelihood for the creation of a formation barrier. Similarly, the benefit from obtaining a formation barrier is dependent on the difference between the costs of a durable sealing material compared to the cost of a non-durable sealing material, in addition to the cost of repairing a possible lack of seal. Since the benefit from obtaining a formation seal is interrelated with the cost of different sealing material options, and the cost of repairing a possible seal failure, to decide how much effort that economically should be applied to obtain a formation seal, knowledge about the two former has to be obtained. Here, first a qualitative discussion on the cost of the different sealing materials is presented. This is followed by a discussion combining it with the cost of repairing a failed annular seal, to decide the most likely future sealing material, and thus also benefits with formation barriers.

8.1.1 Cost evaluation of improving sealing material used

So far in this thesis 3 different options to conventional cement has been discussed and their practical strengths and weaknesses has been identified. However, little focus has been given to the costs related to the materials. When assessing the cost related to each material there are in general three important aspects that has to be taken into consideration (13):

1. Direct cost of the material
2. Rig time used to deploy the material
3. Likelihood for remedial jobs

All of these parameters vary from well to well due to differences in downhole conditions. Thus, for simplicity only a qualitative discussion using conventional cement as a benchmark when assessing the other materials will be presented here.

The direct material cost of using standard class G Portland cement without expensive additives is quite low. However, as cement typically takes long time to deploy (WOC time around 12-24 hours) considerable rig time has to be expected. Moreover, as seen earlier in this thesis, for various reasons conventional cement is prone to failure. Hence, quite a few remedial jobs have to be expected.

To reduce amounts of remedial jobs, as seen several special and more complex cement systems with increased flexibility and durability have been developed. However, due to the increased complexity, these systems also have higher direct costs and since they are still cements, and the setting therefore is still hydration based, the WOC will still be quite high. Moreover, although their properties could by far exceed those obtained with standard cement, all cement systems are to some degree brittle, and their flexibility is limited compared to other perfectly ductile alternatives.

One of these perfectly ductile materials is Sandaband. Since the material is furthermore non-degradable the likelihood for remedial jobs is quite low. However, compared with most cements systems the direct volumetric costs are very high. In addition using the material also requires some extra wellsite equipment and possibly also some extra personnel, making the total cost even higher. These high costs are to some degree counteracted by the fast deployment, since the material does not require any setting time.

The last material discussed, Thermaset, has mechanical properties that by far exceeds those possible with cement systems. Therefore if used, the material will most likely significantly reduce the need for remedial jobs. Moreover, since the transition from liquid to solid state is temperature based it will be faster to deploy than cement, which typically requires a large safety margin to reduce the chance of early set. The main problem with the material is volumetric costs, which similar to Sandaband, are likely to be far higher than those for cement systems.

A summary of the cost evaluation for the different materials can be found in table 8.1.

Table 8.1 Summary of cost evaluation of different sealing materials

Sealing material	Cost of material	Rig time	Likelihood of remedial jobs
Conventional cement	Low	High	High
New Cement systems	Medium	High	Low/ medium
Sandaband	High	Low	Low
Thermaset	High	Low	Low

8.1.2 Future use of sealing materials and benefit from formation barriers

As seen in the previous section, one of the deciding factors when it comes to cost is the likelihood for remedial jobs. The cost of a remedial job is furthermore dependent on the technology used as well as the complexity of the operation. As seen in chapter 2 recently several new technologies has been developed with the purpose of improving remedial jobs. In a feasibility report made by Statoil, for a PP&A campaign on Statfjord, they estimated the cost saving potential of applying PWC or improved section milling techniques in cases with lack of annular seal to 8 days or 8.8 MNOK for each plug where the technology is applicable (77). Thus, in wells where there is a lack of annular seal at the setting depth of both barrier plugs, the total savings could be 16 days (17.6MNOK) or 40% of the total PP&A cost of the well (77).

As a consequence of the improved remedial techniques the benefit of using more durable sealing materials, such as for instance new cement systems, Sandaband and Thermaset diminish. However, the costs of a remedial job will never reach zero and it will always be advantageous that the primary job fulfil its purpose. Of the discussed new sealing materials, the wide variety of new cement systems appears to be the most likely material of choice in the near future. This has several reasons. The main one being that the petroleum industry as a whole is a very conservative business sector where well proven, although slightly changed, technology will almost always be preferred over completely new. This is among others due to the fact that complete changes will require new risk assessments, use of unfamiliar equipment, new service providers as well as problems related to contractual issues.

As discussed earlier in this thesis the new cement systems will never be completely ductile and although the likelihood of failure could be significantly reduced, some casing cement failures are still likely to occur also in completely new wells. Moreover, the PP&A jobs that will be conducted the next couple of decades will be performed on wells where these new and improved cement systems were not applicable. Thus, casing cement failures have most likely already occurred in many of them, and the benefit from formation barriers will be significant. Statoil has estimated the average cost savings of a formation barrier on the NCS, with the current remedial technology, to 15 MNOK per well (62). Thus, as long as the cost or detrimental effects of the methods to increase the chance of the formation providing a barrier does not exceed this, they should be implemented.

8.2 Feasibility study of suggested methods to increase chance of shales providing annular barriers for PP&A

As seen in chapter 6, there are several ways to increase the chance of shales providing annular barrier for PP&A. Here the feasibility of the suggested methods is discussed.

8.2.1 Cation exchange

As seen in section 6.1, one possible way to increase the ductility of shale sections is by exchanging the in-situ cations with cations of smaller hydrated diameter. From pure technical considerations it was found that rhodium, cesium and potassium was the ideal replacement cations. However, in addition to technical considerations also costs and possible HSE-issues play a significant part when choosing material.

Rhodium is one of the most rare elements on the Earth's crust. This is reflected by its price, currently in the same region as gold (78). Thus, since quite large quantities would be required for a large-scale cation exchange to occur, the material does not provide a good option.

Pure cesium is extremely reactive and pyrophoric and will ignite spontaneously in contact with water or air. However, in aqueous solution called cesium formate, made up by reacting cesium hydroxide with formic acid, the element is safe to handle and relatively environmentally friendly. It has moreover, due to its high density been used as a drilling and completion fluid in HPHT wells to reduce the amounts of weight materials required (79). Thus, it has proven that it can be used under the prevailing downhole conditions. However, as with rhodium, although to a far less degree, a disadvantage with the material is the high cost, currently in the region of $4,000 per barrel (79).

The last material suggested, Potassium, is a very common element with a wide variety of application areas such as for instance fertilizer, baking powder and food preservatives. Potassium based salts (e.g. KCL), has been used as a mud additive to improve hole stability the last decades (56). Moreover, in addition to the vast experience KCL is relatively cheap and does not introduce any HSE-issues. Thus, all decisive factors taken into consideration, a KCL rich fluid placed adjacent to possible shale barriers appears to be the best solution to obtain the desired cation exchange induced ductility increase. For new wells this could be obtained by using a KCL rich spacer, while for existing wells the casing will have to be perforated, and the KCL fluid circulated in place. Due to the detrimental effect of the latter, KCL treatment is mainly a good solution for new wells.

As seen in section 6.1, in addition to the positive effects, the addition of smaller ions also has some detrimental effects on the shales ability to provide a good barrier element. Thus, since there is a trade-off between positive and negative effects there is an optimum concentration that needs to be found. However, the determination of this ideal concentration is not straightforward as it will depend on parameters, such as in situ

stress, pore pressure, shale mineralogy, permeability, diffusion coefficients, strength, stiffness, borehole pressure and other drill fluid constituents (56).
Thus, the exact concentration will vary from case to case. However, due to the large possible benefit of KCL-exposure with respect to the shale formations providing a barrier, more research on the topic to obtain best practices is likely to be worthwhile and should therefore be conducted.

8.2.2 Thermal effects on mechanical behaviour of shale

Another parameter that was found to possibly increase the ductility of shale sections was temperature. However, to increase the ductility it was found that the heat induced pore pressure increase had to exceed the dissipation pore pressure rate. Thus, making the optimum rate of heating a function of permeability, thermal conductivity as well as the difference in thermal expansion coefficient between the pore fluid and solid grains.

In general heating of the formation could be obtained either by circulating high temperature fluids through the casing or using a tool that bombards the formation with electromagnetic waves. However, uncertainties both in the applied and desired rate of heating combined with the possible detrimental effects of using the wrong heat rate (see section 6.1.2), makes thermal heating to increase the ductility of shale formation difficult to apply in practice.

8.2.3 Increase creep rates

As seen in section 6.2, both creep rates and the overall strain before failure, increases with increasing deviatoric stress and temperature. As discussed in the previous section, increasing the temperature is difficult to apply in practice without risking detrimental effects such as tensile failure or increased brittleness of the formation.
The simplest way to increase the deviatoric stress at the borehole wall is to reduce the well pressure. However, too low well pressures will induce brittle failures leading disadvantageous borehole breakouts and should therefore be avoided. Ideally to maximise creep rates, the well pressure should be kept just above the lower limit for stable holes during the entire lifetime of the well. Traditionally, this has been hard to obtain because conventional weight materials settle out with time, but with new technology such as micro-barite and cesium formate this could to a higher degree be possible. Since it is hard to influence the well pressure after the casing is set, without perforating the casing, the more tailored an optimized well pressures for creep rates to increase is mainly applicable for new wells. Nevertheless, as discussed in section 6.2 even though the stress state is slightly changed, the creep rates are likely to remain in the same order of magnitude as before. Thus, with respect to PP&A, the more optimized downhole stress states could only make a difference in shales that earlier were close in creating an annular formation barrier.

8.2.4 Optimize annular gap

The maybe most efficient way to increase the chance of shales providing an annular barrier element within the time frame for PP&A is to reduce the annular gap. This can be

done either through using expandable casing strings or initially using larger casing strings than what is conventionally used. As seen in section 6.3 for 12 ¼" borehole increasing the casing size from 9 5/8" to 10 ¾" reduces the required time for creep movement to fill the annular gap from 58.7 to 33.5 years in Barnett shale. This could very well be the difference between obtaining and not obtaining a barrier within the time frame of PP&A. Thus, for wells drilled through potential shale barriers, with steady state creep rates in the region of 10^{-5} strain/day, reducing the annular gap becomes very important.

There are in general two main problems with increasing the casing size. The first one is the fact that after a hole is drilled, due to mechanisms discussed in chapter 5, the hole-size is somewhat reduced. Thus, it is impossible to put a 12 ¼" casing inside a 12 ¼" borehole. Exactly how much the hole-size is reduced varies from well to well, but to make sure that it is possible to place the casing inside the wellbore conservative standards exists. For instance typically for a 12 ¼" borehole a 9 5/8" casing is usually applied. This standardization in many ways leads to the second problem for reducing casing size. Because, even though it may be possible to estimate the hole-size reduction after a hole is drilled, to buy standardized and large scale produced casing strings is considerably cheaper than customized ones.
However, as seen substantial cost savings could be obtained through reduced PP&A complexity by using more optimized casing strings. Thus, even though initially more expensive, in the long term such an investment could still be worthwhile. Especially expandable casing strings should be considered in cases where increasing the casing size could be critical, since they do not run the same risk of getting stuck as large fixed sized casings do.

8.2.5 Shales in combination with Sandaband

As discussed in chapter 6 in wells where the shales are simply too brittle to close off the whole annular gap without loosing their integrity, they could still in combination with another sealing material such as for instance Sandaband contribute to the creation of a good annular barrier. The main benefit with radially inward moving formations in combination with Sandaband was found to be reduced required Sandaband volumes, as well as possible reductions in the Sandabands permeability.

To illustrate the possible volume savings, due to the wellbore closing in towards the casing, imagine the following simplified example. A reservoir with a pressure of 500 bars is located at a depth of 3500 TVD. To reach the reservoir the well is drilled vertically to 2500m through overburden rocks, before a 2000m section that deviates 60° from the vertical is drilled through caprock shales, as illustrated in figure 8.1. To plug such as well with Sandaband, assuming that the effect of yield stress is negligible, a hydrostatic height of 1332 meter with Sandaband ($\rho_{Sandaband}$=2150kg/m^3) is required.

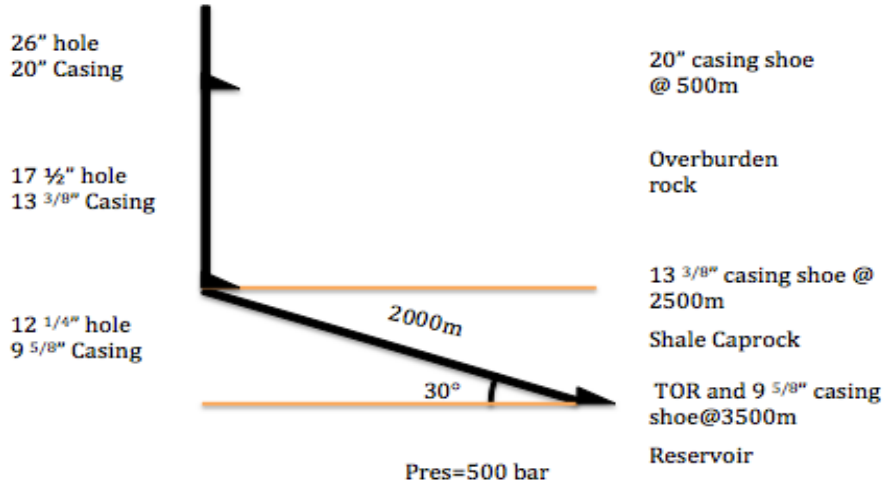

Figure 8.1 Well schematic for Sandaband plugging example

With the hole-size and casing programme illustrated in figure 8.1, without any annular gap reduction, to obtain the required pressure seal a volume of 69.7 m^3 is required. If 1/3 of the gap in the shale section is closed, the required volume is reduced to 52.4m^3, i.e. 17.3m^3 saved. Due to the high price of Sandaband this could mean significant reductions is costs. Moreover, if the deviated section was longer or more deviated the effect of reduction in gap on the required volume would be even larger. A more comprehensive list over required volumes for different reductions in gap size, as well as different deviation angles for the section drilled through the shale, can be found in table 8.2.

Table 8.2 Required Sandaband volumes for different hole-deviations (from the vertical) and reduction in annular gap size for the situation presented in Figure 8.1.

	Required volume (m^3)			
Reduced Gap (%)	Deviation (0°)	Deviation (30°)	Deviation (60°)	Deviation (85°)
0	43.8	47.8	69.7	306.3
10	41.2	44.8	64.5	277.4
20	38.6	41.8	59.3	248.6
33	35.1	37.8	52.4	210.1
50	20.8	32.8	43.8	162.1
75	24.3	25.3	30.8	90.0

As seen from the table, with respect to volume savings, the effect of the reduced gap becomes more and more important for highly deviated wells, but regardless of deviation the volume savings are in general quite substantial. Thus, through increased knowledge about downhole formations inward movements, Sandaband could become a viable option even in wells where the solution has previously been considered way too costly.

8.2.6 Shales in combination with weight materials

Another solution, that if proven sealable for all eternity, could provide and economically very favourable option in nearly vertical wells is to combine inward moving formations with settled weight materials, such as for instance barite. However, as seen in chapter 7,

conventional barite in combination with water, does not provide a good seal. Thus, for conventional settled barite to be part of a barrier at least some additives are needed. The main problems with barite as a sealing material are that the particles are too large, the distribution too well sorted and the material itself too stiff to obtain low enough permeability when compressed.
To reduce the permeability several methods could in theory be applied, such as for instance:

1. Add small, soft and non-degradable particles to the barite mixture. When compressed these particles should ideally deform plastically, hence reducing the "porosity" of the mixture. Possible materials are tin solder, lead and glass.
2. Mix conventional barite with micro barite and more coarse barite particles than what is conventionally used in the oil industry. The challenge with the solution, if proven sealable, is to make all the particles settle simultaneously so that the weight materials make up a badly sorted plug above the casing cement.
3. Apply vibration on the barite plug when settled to get better compaction. The challenge with the method, if the effect is proven significant, is to create sufficient vibration without for instance jeopardizing the integrity of the casing cement.
4. Barite in combination with oil and water emulsions. The theory is that when the settled weight material plug, consisting of settled barite and oil water emulsions, is mechanically compressed by the formation the dispersed phase droplets gets stuck in between grains on its way out during drainage. This is illustrated in figure 8.2. If this occurs, the highly deformable emulsion droplets may contribute to the seal much in the same manner as they contribute to the filter cake made during drilling. Oil in water emulsions are likely to be the best choice, as they have significantly less filter loss than water in oil emulsion muds (52).
5. Barite in combination with bentonite.
6. Barite in combination with diesel.

It must be stated that due to lack of time none of these possible solutions have been tested in this thesis. The suggested methods are therefore more suggestion for further studies, rather than anything else.

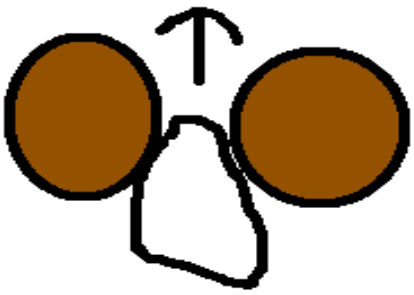

Figure 8.2 Oil droplet stuck on its way out between two grains during drainage induced by compression.

In contrary to conventional barite, micro-barite appears to be a good sealing material. However, as mentioned in chapter 7 there are some challenges related to its placement procedure since it does not settle in the same manner as conventional barite. As a consequence, alternative means of getting the material "in position", adjacent to a deforming shale zone, has to be initiated. One possible solution discussed earlier in this thesis, is to put high amounts of the material in a viscous plug pumped in front of the cement during the cement job. However, to the author's knowledge no such plug has ever been pumped. Therefore there are some uncertainties regarding it applicability, especially related to how high concentrations of the material it will be possible to place in such a viscous plug.

8.2.7 Shales in combination with immobilised Sandaband like material

As seen earlier, weight materials is not an option in highly deviated wells. However, another option that could provide an economically feasible barrier in these wells is to use a Sandaband like material (e.g. highly concentrated sand slurry) that is initially pumpable, but when placed in position becomes unpumpable. After the immobilization the theory is that the formation close in and squeeze the particles more together. Thus, in addition to possibly reducing the permeability, the formation could also induce sufficient shear stress between the sealing material and its surroundings for it to stay in position, even when exposed to large differential pressures. If the latter is obtained the volume requirements of Sandaband could be significantly reduced.

Sandabands pumpability is based on the Farris effect, which states that by mixing particles with different sizes it is possible to increase the sand concentration substantially, whilst maintaining relatively low viscosities. The effect of mixing two different sized particles on viscosity is illustrated in figure 8.3. As seen from the figure, it is possible to increase the particle concentration from 60% to far above 75%, without changing the viscosity just by changing from a monodisperse particle suspension to a bimodal suspension. Even higher concentrations for the same viscosity can be obtained by using more complex compositions (80). Sandaband consists of 70-80% by volume of quartz and the rest is water and fluidising additives to make the mixture pumpable (31).From figure 8.3 it is obvious that by either reducing the fluid content or improving the sorting, the Sandaband mixture will become unpumpable. When in position the former could be obtained either by using some sort of degradable fluidising additives, or by thermally boiling or otherwise alternating the properties of the fluidising additives, such that they become less effective in making the slurry pumpable. Improved sorting could in theory be obtained by vibration, however applying sufficient vibration where and when needed has been proven impractical (12). Thus, for vibration to become a viable option there is a need for improved vibration methods.

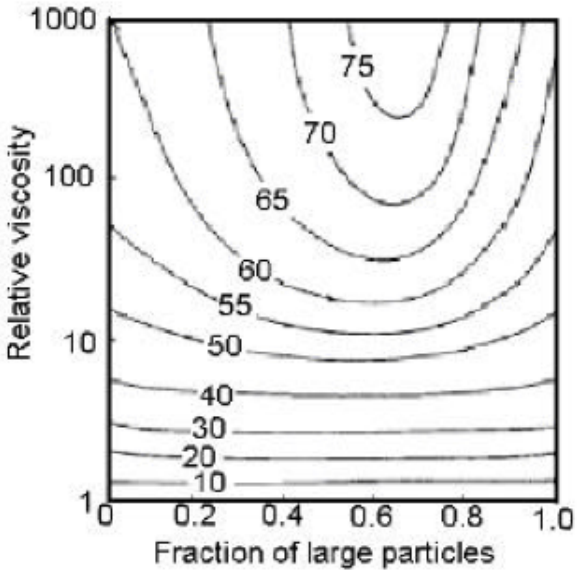

Figure 8.3 The Farris effect on a mixture consisting of two monodisperse particles sizes and a carrying fluid. Illustration shows relative viscosities as a function of the particle size fraction for different particle loading fractions (solid to fluid ratios). Coarse particles are 5 times the size of the smaller particles. After (80).

9. Conclusion

The work conducted in this thesis has revealed that even though new techniques to fix/repair lack of annular seals and new sealing materials have been developed the last decade, there still exist a huge cost savings potential by being able to use shale formation barriers to a greater extent than today. Based on a comprehensive literature study and some lab experiments the main findings are:

- Most shales have at least the potential to seal off parts of the annular gap between the formation and casing within the time frame of PP&A. Whether or not the full gap is closed is dependent on the shales flexibility and creep rates.
- Although other displacement mechanism may contribute to a greater or lesser extent, the main displacement mechanisms for the creation of annular shale formation barriers is likely to be creep
- Useful indicators of a shales creep potential is clay content and stiffness. In general soft shales containing high contents of clay and organic material have the highest creep rates.
- Smectite rich shales found between 2000 and 3000 meters appears to be most suitable for becoming annular barriers
- To increase the chance of shales providing a barrier element a potassium or cesium rich fluid should be placed adjacent to the shale formation. The most likely options are cesium formate mud or KCL salt added to the mud. The ideal concentration varies from case to case and more research is needed to determine the ideal concentrations in each case.
- Another efficient way of increasing the chance of the creation of formation barriers within the time frame of PP&A, is reducing the annular gap. This could be obtained either through increasing the casing size or through an annular fill material.
- Compressed barite in combination with only water does not constitute a good sealing material.
- Compressed micro-barite mixed with freshwater appears to constitute a practically impermeable seal.
- Increased knowledge about shale formation displacements could make Sandaband a more viable option in highly deviated wells where the solution has previously been considered too costly
- To be able to utilize formation barriers on a larger scale there is a need for improved logging tools that can “see” through more than one casing string.

Recommendations for further work

Much of the work needed to be able to on a larger scale predict the creation of formation barriers or identifying means for increasing the chance for such barriers occurring requires expensive equipment, such as for instance triaxial cells as well as core samples. With respect to future master theses such equipment and materials can be hard to obtain. Moreover, for instance accurate creep test could take several years and are therefore not suitable for a master thesis. Nevertheless, based on the equipment used in this thesis significant contributions to the field of formations as annular barriers could be obtained by identifying ideal annular fill materials that, when compressed by the adjacent formation, make up a good seal. Several tests similar to those conducted in this thesis on different materials, would be of interest. Some suggested test materials/ mixtures are:

1. Mixture consisting of barite and clay material such as for instance bentonite or kaolinite.
2. Mixture of diesel and barite to check if there is some kind of reaction making such a mixture better suited as a sealing material than just freshwater and barite.
3. Mixture of barite and oil and water emulsions. Ideally oil should be the dispersed phase, but also a comparison with water as the dispersed phase would be of interest.
4. Mixture of barite, micro-barite and water.
5. Mixture of barite and/or micro-barite with small, soft and non-degradable particles such as for instance tin solder, lead and glass.

Nomenclature

BHA – Bottom Hole Assembly
BOP – Blowout Preventer
CBL – Cement bond log
CEC- Cation Exchange Capacity
CS - Critical State
CT – Coiled Tubing
ECD – Equivalent Circulating Density
FIT – Formation Integrity Test
HCL – Hydrochloric Acid
HF – Hydrofluoric Acid
HPHT – High Pressure High Temperature
HSE – Health Safety and Environment
MD – Measured depth
LCM – Lost circulation material
LOT – Leak Off Test
LVDT – Linear Variable Displacement Transducers
LWI – Lightweight intervention
NOK- Norwegian Krones
OBM – Oil Based Mud
OLF- The Norwegian Oil Industry Association
NCS – Norwegian Continental shelf
P&A – Plug and abandonment
PP&A- Permanent plug and abandonment
PSA – Petroleum Safety Authority Norway
RPM –Revolutions per minute
TCP – Tubing Conveyed Perforation
USIT – Ultrasonic imaging tool
VDL – Variable Density Log
WBE – Well barrier element
WBEAC – Well Barrier Element Acceptance Criteria
WBM – Water Based Mud
WOC – Wait on Cement
XLOT – Extended Leak Off Test

References

1. NPD. Fakta 2012 Norsk Petroleumsvirksomhet: Norwegian Petroleum Directorate and Norwegian Minestery of Petroleum and Energy; 2012.
2. Straume M. Introduction to Plug & Abandonment Forum (PAF). OLF; 2012.
3. Sandven S. Evaluation of a method of placing cross-sectional barriers during permanent plugging of wells [Master Thesis]: University of Stavanger; 2010.
4. Nessa JO. Setting Plug & Abandonment Barriers with Minimum Removal of Tubulars [Master Thesis]: University of Stavanger; 2012.
5. Birkeland F. Final Field Permanent Plug and Abandonment- Methodology Development, Time and Cost Estimation, Risk Evaluation [Master Thesis]: University of Stavanger; 2011.
6. Njå N, O,B. P&A of Valhall DP wells [Master Thesis]: University of Stavanger; 2012.
7. Løkke-Sørensen T. Revision update, NORSOK D-010,Rev.4. 2012.
8. NORSOK. Standard D-010: Well integrity in drilling and well operations.Rev.3, August 2004. 2004. p. 61-8,130-2.
9. Holt RM. Borehole Stability during Drilling. Presented in lecture in subject TPG 4185 Formation Mechanics. Held at NTNU during the fall of 2012.
10. NORSOK. Standard D-010: Well integrity in drilling and well operations. Rev.4 Draft version 20.12.12. Standard Norge; 2012. p. 23-4,76-106,202-3.
11. Commision O. OSPAR Decision 98/3 on the Disposal of Disused Offshore Installations. 1998.
12. Nelson EB, Guillot D. Well Cementing. 2nd ed. Sugar Land,Texas: Schlumberger; 2006.
13. Skjerve K. Evaluation of sealing materials for oil and gas wells [Project Work]: NTNU; 2012.
14. DrillingFormulas.COM. Balanced Cement plug 2012 [cited 2012 01.09.12]. Available from: http://www.drillingformulas.com/balanced-cement-plug/.
15. Williams.S, Carlsen T, Constable K, Guldahl A. Identification and Qualification of Shale Annular Barriers Using Wireline Logs During Plug and Abandonment Operations. Presented at SPE/IADC Drilling Conference and Exhibtion; 17-19 march 2009; Held in Amsterdam, The Netherlands: Paper SPE 119321; 2009.
16. Vignes B. Contribution to well integrity and increased focus on well barriers from a life cycle aspect [PhD Thesis]: University of Stavanger; 2011.
17. Yudovich A, Chin LY, Morgan DR. Casing Deformation in Ekofisk. SPE 17856. 1989.
18. Dusseault MB, Bruno MS, Barrera J. Casing Shear:Causes,Cases,Cures. Presented at SPE International Conference and Exhibition; 2-6 November; Held in Bejing, China: Paper SPE 48864; 1998. p. 337-49.
19. Holt RM. Reservoir Geomechanics. Presented in lecture in subject TPG 4185 Formation Mechanics. Held at NTNU during fall of 2012.
20. Ferg TE, Lund HJ, Mueller D, Myhre M, Larsen A, Andersen P, et al. Novel Approac to More Effective Plug and Abandonment Cementing Techniques. Prestented at the SPE Arctic and Extreme Environments Conference & Exhibtion; 18-20 October 2011; Held in Moscow, Russia: Paper SPE 148640; 2011.
21. BakerHughes. Section Milling/Pilot Milling 2013 [04.03.13]. Available from: http://www.bakerhughes.com/products-and-services/completions/wellbore-intervention/casing-exits/section-milling-pilot-milling.

22. Scanlon E, Garfield G, Brobak S. New Technologies to Enhance Performance of Section Milling Operations that Reduce Rig Tiime For P&A Campaign in Norway. Presented at the SPE/IADC Drilling Conference and Exhibition; 1-3 March 2011; Held in Amsterdam, The Netherlands: Paper SPE 140277; 2011.
23. Hydrawell.no. HydraWash http://www.hydrawell.no/products/hydrawash: Hydrawell Intervention; 2013 [cited 2013 18.02].
24. Hydrawell.no. HydraArchimedes http://www.hydrawell.no/products/hydraarchimedes: Hydrawell Intervention; 2013 [cited 2013 18.02].
25. Larsen A. HydraWash-a new approach to get cement behind casing without milling: Hydrawell Intervention; 2011 [cited 2013 18.02]. Available from: http://www.norskoljeoggass.no/PageFiles/10706/4 HydraWell - HydraWash system to make Annulus Barriers.pdf?epslanguage=no.
26. di Lullo G, Rae P. Cements for Long Term Isolation-Design Optimization by Computer Modelling and Prediction. Presented at the 2000 IADC/SPE Asia Pacific Drilling Technology; 11-13 September 2000; Held in Kuala Lumpur,Malaysia: Paper SPE 62745; 2000.
27. Thiercelin MJ, Dargaud B, Baret JF, Rodriquez WJ. Cement Design Based on Cement Mechanical Response. SPE 52890. 1998:266-73.
28. Wellcem. ThermaSet-Cost Effective Oil Well Therapy 2013 [cited 2013 17.04]. Available from: http://www.wellcem.no/uploads/1/1/0/5/11057371/thermaset_brochure.pdf.
29. Wellcem. ThermaSet- the Gas Tight Solution http://www.wellcem.no/thermaset-reg.html: Wellcem; 2013 [cited 2013 16.04].
30. Wellcem. Zonal Isolation in Subsea Wells using Multi-purpose Field Vessels and ThermaSet Isolation materials SPE Bergen2008 [cited 2012 4.12]. Available from: http://bergen.spe.no/publish_files/4.2_Wellcem_E.Jorgensen.pdf.
31. Saasen A, Wold S, Ribesen BT, Tran TN, Huse A, Rygg V, et al. Permanent Abandonment of a North Sea Well Using Unconsolidated Well-Plugging Material. SPE Deepwater Drilling and Completion Conference; 28.june 2010; Galveston, Texas: SPE 133446; 2011. p. 371-4.
32. Sandaband. Non-Consolidated Plugging Material for Wellbore and Annulus. Presented at OLF P&A forum Workshop 9th of June,2011.
33. Sandaband. Sandaband 2013 [cited 2013 16.04]. Available from: http://www.sandaband.com/files/93bafb43-7a6d-4828-90a4-efe8fee065de.pdf.
34. WestGroup. SwarfPak-Ultrafast milling with accurate precision 2013 [cited 2013 15.04]. Available from: http://www.westgroup.no/products/swarfpak.
35. Skjærseth O. SwarfPak-Down Hole Swarf Deposition: P&A Forum 2012 [cited 2013 19.02]. Available from: http://www.norskoljeoggass.no/Global/Presentasjoner/PAF Workshop/12 - WeST - Odd Skj%C3%A6rseth.pdf.
36. Fjær E, Holt RM, Horsrud P, Raaen AM, Risnes R. Petroleum Related Rock Mechanics. 2nd ed. Amsterdam, The Netherlands: Elsevier; 2008.
37. Strand S. Leire: Øving i bore og brønnvæsker,UiS,2001.
38. Skalle P. Drilling Fluid Engineering: Pål Skalle & Ventus Publishing ApS; 2010.
39. Nakken SJ, Christensen TL, Marsden R, Holt RM. Mechanical behaviour of clays at high stress levels for wellbore stabiltiy applications. 1989.
40. Sachs W, Volker M. Pressure and temperature depdence of the surface tension in the system natural gas / water. Elsevier; 1994.

41. Daireaux S. Plug & Abandonment Challenge: Statoil; 2011 [cited 2013 26.03]. Available from: http://www.slideshare.net/Statoil/plug-abandonment.
42. Hosford WF. Mechanical Behaviour of Materials. Cambridge,UK: Cambridge University Press; 2005.
43. Pietruszczak S. Fundamentals of Plasticity in Geomechanics. Leiden, The Netherlands: CRC Press/Balkema; 2010.
44. Hobart S. Pre-drill Overburden Estimation. . Report No4 Knowledge systems, INC DEA Project 119. 1999.
45. Yassir N, Addis MA. Relationship between Pore Pressure and Stress in Different Tectonic Settings. In: Huffman AR, Bowers GL, editors. Pressure regimes in sedimentary basins and their prediction 2002. p. 79-88.
46. Berg S. 2D Vertical Effective Stress Modeling of the Tor Area [Master Thesis]: NTNU; 2012.
47. Skalle P. Pressure Control During Oil Well Drilling: Ventus Publishing; 2009.
48. Breckels IM, Van Eekelen HAM. Relationship Between Horizontal Stress and Depth in Sedimentary Basins. Paper SPE 10336; 1982. p. 2191-9.
49. Pasic B, Gaurina-Medimurec N, Matanovic D. Wellbore Instability: Causes and Consequences. 2007.
50. Santarelli FJ, Carminati S. Do Shales Swell? A Critical Review of Available Evidence. Paper SPE/IADC 29421; 1995.
51. Skalle P, Backe KR, Lyomov SK, Sveen J. Barite Segregation in Inclined Boreholes. Journal of Canadian Petroleum Technology Paper 97-76. 1999.
52. Skalle P. Personal Communication. 2013.
53. Zamora M. Mechanisms,Measurement and Mitigation of Barite Sag. 2009.
54. Holt RM, Fjær E, Nes OM, Alassi HT. A shaly look at brittleness. Presented at US Rock Mechanics/Geomechanics Symposium Held in San Francisco, CA: Paper ARMA 11-366; 2011.
55. Sonstebo EF, Horsrud P. Effects of brines on mechanical properties of shales under different test conditions. Balkema,Rotterdam; 1996.
56. Horsrud P, Bostrom B, Sonstebo EF, Holt RM. Interaction Between Shale and Water-Based Drilling Fluids: Laboratory Exposure Tests Give Insight Into Mechanisms and Field Consequences of KCL Contents. Presented at SPE Annual Technical Conference and Exhibition Held in New Orleans,Louisiana: Paper SPE 48986; 1998.
57. Horsrud P, Holt RM, Sonstebo F, Svano G, Bostrom B. Time dependent borehole stability: Laboratory studies and numerical simulation of different mechanisms in shale. Eurock SPE/ISRM Rock Mechanics in Petroleum Engineering Held in Delft, The Netherlands: Paper SPE 28060; 1994.
58. Yawei L, Ghassemi A. Creep Behaviour of Barnett,Haynesville, and Marcellus Shale. Paper ARMA 12-330; 2012.
59. Lavrov A. Evaluation of possible mechanisms of annular sealing in shales: Creep and Swelling. SINTEF Petroleum Research, Trondheim, 2012.
60. Gasc-Barbier M, Chanchole S, Berest P. Creep behavior of Bure clayey rock. Elsevier; 2004.
61. Fabre G, Pellet F. Creep and time-dependent damage in argillaceous rocks. International Journal of Rock Mechanics and Minining Sciences. 2006.
62. Carlsen T. Formation as barrier during P&A 2012 [cited 2013 20.02]. Available from: http://www.norskoljeoggass.no/Global/Presentasjoner/PAF Workshop/6 - Statoil -Truls Carlsen.pdf.

63. Holt RM, Kolstø MI, Potyondy D. Bound water in shale: Molecular scale simulations and experimental indications. Extended abstract, EAGE Shale Workshop,2010.
64. Mitchell J, Soga K. Fundamentals of Soil Behavior. Hobroken, New Jersey: John Wiley & Sons, Inc; 2005.
65. Xu B, Yuan YG, Wang ZC. Thermal Impact on Shale Deformation/Failure Behaviors--Laboratory Studies. Presented at the 45th US Rock Mechanics/Geomechanics Symposium; Held in San Francisco, CA June 26-29: Paper ARMA 11-303; 2011.
66. Campanella RG, Mitchell JK. Influence of temperature variations on soil behavior. Journal of the soil mechanics and foundations division, Proceedings of American Society of Civil Engineering 1968;94(No.SM3):709-34.
67. Chu MS, Chang NY. Uniaxial Creep of Shale Under Elevated Temperatures. Presented at the 21st US Symposium on Rock Mechanics (USRMS) May 27-30; Rolla, Missouri: American Rock Mechanics Association; 1980.
68. Gjedrem T, inventor; Hamsø Patenbyrå ANS, assignee. Fremgangsmåte for å hindre et fluid i å strømme i eller omkring et brønnrør ved hjelp av løsmasse. Norway 2001
69. Miller M. Barite. 2009 Minerals Yearbook: USGS; 2009.
70. Rashid S. Evaluation of Bentonite Plug for Sealing of Well Bore [Master Thesis]: NTNU; 2013.
71. Woodside-Petroleum. Management of an Underground Well Flow 2009 [cited 2013 14.05]. Available from: http://www.drillsafe.org.au/03-10_pres/drillwell_forum_mar10_woodside_mnging_an_undeg_flow.pdf.
72. Matlock W, Conn L. Miconized weight material optimizes ERD drilling: M-I SWACO; 2013 [cited 2013 14.05]. Available from: http://www.offshore-mag.com/articles/print/volume-68/issue-2/drilling-completion/micronized-weight-material-optimizes-erd-drilling.html.
73. Glover P. Porosity [cited 2013 06.03]. Available from: http://www2.ggl.ulaval.ca/personnel/paglover/CD Contents/GGL-66565 Petrophysics English/Chapter 2.PDF.
74. Saasen A, Godøy R, Breivik DH, Solvang SA, Svindland A, Gausel E, et al. Concentrated Solid Suspensions as an Alternative to Cements for Temporary Abandonment Applications in Oil Wells. Paper SPE SA 34; 2004.
75. Van Buskirk R, Loughlin M, Mody R, Mullins A, Johnson M, inventors; Baker Hughes Incorporated, assignee. Methods and apparatus for sealing and transfering force in a wellbore. USA 1997.
76. Chandler_Engineering. QX Series Pump User's Manual. 2005.
77. Weltzin T. Statfjord A PP&A 2012 [cited 2013 20.02]. Available from: http://www.norskoljeoggass.no/Global/Presentasjoner/PAF Workshop/4 - Statoil_Tore Weltzin.pdf.
78. KITCO. Rhodium Charts 2013 [cited 2013 21.05]. Available from: http://www.kitco.com/charts/rhodium.html.
79. Butterman WC, Brooks WE, Reese Jr RG. Mineral Commodity Profile:Cesium. United States Geological Survey. 2004.
80. Barnes HA, Hutton JF, Walters K. An introduction to Rheology. Amsterdam, The Netherlands: Elsevier; 1989.

81. Le Roy-Delage S, Baumgart C, Thiercelin MJ, Vidick B. New Cement systems for Durable Zonal Isolation. Prestened at the 2000 IADC/SPE Drilling Conference; 23-25 February; Held in New Orleans: Paper SPE 59132; 2000.
82. Kosinowski C. Study of Class G Cement Fatigue using Experimental Investigations. Presented at the SPE/EAGE European Unconventional Resources Conference and Exhibition;20-22 March 2012; Held in Vienna, Austria: paper SPE 153008;2012.
83. Brandl A, Cutler J, Sansil,M, Braun G. Cementing Solutions for Corrosive Well Environments. Presented at the CPS/SPE International Oil&Gas Conference and Exhibition; 8-10 June 2010; Held in Bejing, China: Paper SPE 132228; 2010.
84. Crain ER. Cementing Basics [cited 2012 5.09]. Available from: http://www.spec2000.bet/07-cementlog1.htm
85. Hayden R, Russel C, Vereide A, Babasick P, Shaposhnikov P, May D. Case Studies in Evaluation of Cement with Wireline Logs in a Deep Water Environment. Presented at the SPWLA 52nd Annual Logging Symposium; 14-18 May 2011; Held in Colorado Springs, Colorado: SPWLA; 2001.
86. Osborne MJ, Swarbrick RE. Mechanisms for Generating Overpressure in Sedimentary Basins: A Re-evaluation: AAPG Bulletin;1997.

Appendix A Reasons for casing cement failure

As briefly discussed in chapter 2, and illustrated in figure 2.6, there are many ways in which the casing cement can fail. Here a brief description of the causes for the failure modes and ways to reduce them will be discussed.

A.1 Poor bonding

One of the main reasons for casing cement failure is poor bonding between the cement and the casing and/or formation interface. This can have numerous reasons the two most likely ones being shrinkage of the cement sheath or bond failure due to induced tensile stress.

Shrinkage of the cement sheath is a problem that occurs when the cement sets and happens because the products of the hydration process have less volume than the reactants (12).

Tensile induced debonding happens when the radial tensile stress at the interface between the materials exceed the bond strength. Radial tensile stresses are typically induced during pressure or temperature decreases in the wellbore (27). The former typically occurs during completion with the introduction of light completion fluid and artificial lift equipment into the well, while the latter happens during water injection and also to some degree production starts.

To reduce and potentially avoid problems with poor bonding highly elastic and expansive cement is recommended (27) and (81).

A.2 Permeable cement sheath

The other main reason for casing cement failure is permeable cement sheath. As with poor bonding the creation of a permeable cement sheath can have several sources the most likely ones being gas intrusion during setting, mechanical failure or deterioration of the sheath due to chemical attacks.

Gas intrusion typically happens during the transition phase from cement behaving like a liquid until it becomes a solid with sufficient strength to resist formation fluids. In this period the cement looses some of its ability to transmit hydraulic pressure due to the fact that the gelling process creates adhesion forces between the cement and the surrounding pipe and borehole wall. The loss in hydraulic pressure may be sufficient to create underbalance in the wellbore leading to inflow of formation fluids that may intrude into the partly set and vulnerable cement. Such an intrusion could later on lead to a flow path in the final set cement. To avoid this right angle set cements with short transition period combined with best practices such as rotation and reciprocation of the casing string are recommended (13).

Mechanical failure of the cement sheath can happen as either shear or tensile failure (as illustrated in figure A.1) depending on the stress situation and respective strengths. These failure modes may be induced due to stress changes caused by pressure and temperature changes or other mechanical stress alterations such as casing perforations

or pipe vibration as well as changes in formation stress. The most critical situations with respect to mechanical failure may be in wells exposed to significant subsidence or tectonic activity, but also hydraulic fracturing and steam injection operations will lead to large stress increases in the cement sheath. In addition to these large stress changes, also smaller and rapid alterations in stress, can eventually lead the material to failure due to fatigue. Fatigue is likely to be the reason for many of the problems with cement and it is found that increasing the ductility of the sealing material is a better way of increasing the resistance to fatigue than increasing the strength (82).

Figure A. 1 Radial cracks in set cement induced by tensile failure as result heat from warm oil flow. After (29).

Chemical attacks are caused by aggressive formation or injection fluids and can be either expansive or dissolving in nature. Cement is exposed to expansive attacks in sulphate and magnesium containing formations. These corrosive fluids penetrate into the material and forms expanding crystals that eventually lead to an increase in internal pressure that with time ultimately will result in the formation of cracks, fractures and fragments in the solid material (83). In contradiction to an expansive attack, during a dissolving attack the fluid leach the solid material from its surface, hence if present in large enough quantities it will quickly degrade the sheath. The most severe dissolving attacks are generally found in the presence of typical reservoir stimulating fluids such as hydrochloric-(HCL) and Hydrofluoric acids(HF), but also fluids commonly and naturally occurring in the reservoir such H_2S and CO_2, have this effect on cement (83).
In general the most effective way of reducing the effect of expansive attacks is to have a low permeability cement sheath. Consequently gas intrusion and mechanical failure as discussed above will have a detrimental effect on the cements resistance towards chemical attacks. Protection against dissolving attacks can only be obtained through being inert or more commonly through a protective film.

Appendix B: WBE acceptance criteria for creeping formations

Table B.1: WBE acceptance criteria for creeping formations (10)

Features	Acceptance criteria
A. Description	The element consists of creeping formation (in-situ formation that plastically has been extruded into the wellbore) located in the annulus between the casing/liner and the borehole wall.
B. Function	The purpose of the element is to provide a continuous, permanent and impermeable hydraulic seal along the casing annulus to prevent flow of formation fluids and to resist pressures from above and below.
C. Description, construction and selection	1. The element shall be capable of providing an eternal hydraulic pressure seal 2. The minimum continuous formation interval shall be 50m 3. The minimum formation stress at the base of the element shall be sufficient to withstand the maximum pressure that could be applied 4. The element shall be able to withstand maximum differential pressure
D. Initial test and Verification	1. Position and length of the element shall be verified by bond logs: a) Two independent logging measurements/tools shall be applied. Logging measurements shall provide azimuthal data b) Logging data shall be interpreted and verified by qualified personnel and documented. c) The log response criteria shall be established prior to the logging operation. d) The minimum contact length shall be 50m with 360 degrees of qualified bonding. 2. The pressure integrity shall be verified by application of a pressure differential across the interval 3. Formation integrity shall be verified by a LOT at the base of the interval. The results should be in accordance with expected formation stress from the field model 4. If the element has been qualified by logging, pressure and formation integrity testing, logging is considered sufficient for subsequent wells. The formation interval shall be geologically homogenous and laterally continuous. Pressure testing is required if the log response is not conclusive or there is uncertainty regarding geological similarity.
E. Use	The element shall only be used in permanently abandoned wells

Appendix C: Acoustical logging tools

As mentioned in section 3.3.2 for a shale barrier to be identified two independent logging measurements have to be applied. The most common is to use the CBL/VDL and USIT log. Here the principle behind the tools and a brief description on how they can be interpreted is presented.

C.1 Cement bond log (CBL) and Variable density log (VDL)

The CBL and VDL logs are acquired with a sonic logging tool. The tool consists of an acoustic transmitter and typically two receivers, placed respectively 3ft and 5ft from the transmitter. The sonic transmitter is sending out low frequency (10-20kHz) omni-directional pulses that induce a longitudinal vibration of the casing. The data recorded at the receivers represents the averaged values over the circumference of the casing. The closest receiver (3ft) measures the first positive peak of the sonic waveform, while the second receiver (5ft) measures the full waveform. A schematic illustration of the tool and the principle of operation can be found in Figure C.1.

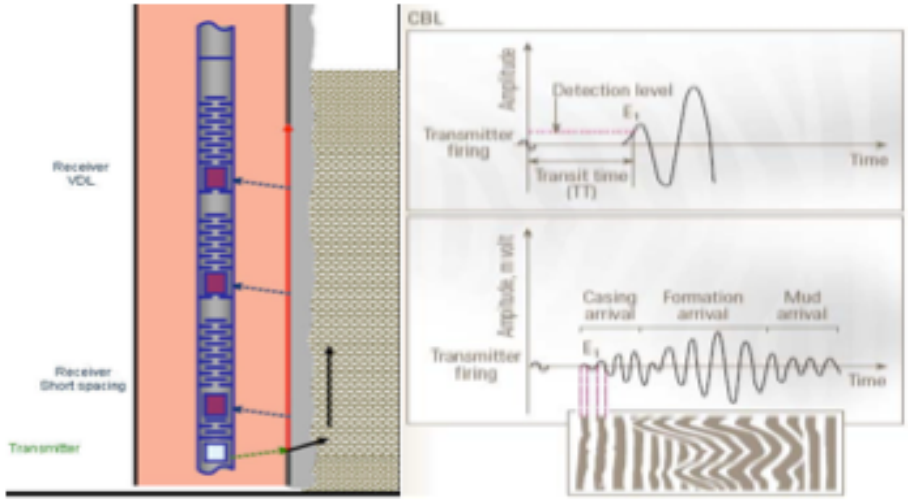

Figure C. 1 Cement bond log (CBL) tool and principle of operation. Free after (84) and (15).

Since the sonic logging tool have one transmitter and two receivers at different locations, the sound waves will travel to the receivers along various paths through the borehole fluid, pipe, annular sealing material and formation. The signal arriving at the receivers will be a composite of waves from all these paths. To present the data recorded by the receivers in the sonic tool typically a three-track log format is used.

The first track is usually the transit-time, which shows the elapsed time from the transmitter firing until arrival of the first wave. Due to shortest distance and highest velocity, the transit-time normally represents the sound wave travelling through the casing. The transit-time does not say much about the annular material and is mainly used for quality control purposes (12).
The second track displays the amplitude (in volt) for fastest travelling wave, usually the casing wave, received at the 3ft receiver and is known as the CBL log. The casing wave is the portion of the original wave that travels directly down the casing wall. The

amplitude of this wave is related to the portion being reflected back into the casing, from the casing to cement boundary. In general low values indicate a solid material in the annulus, since low values are obtained when there is a low acoustic impedance difference between the casing and the annular material (12).
The third and final track displays the results from all the received waveforms at the 5ft receiver at a certain depth vs. time and is know as the variable density log (VDL). Contrary to the CBL log, in the VDL all amplitude signals from all the paths are taken into consideration. In a perfectly bonded situation, weak casing arrivals followed by strong formation arrivals are observed. Formation arrivals can be seen on the log as a wavy chevron pattern. This because formations never are perfectly homogeneous and therefore they're acoustic properties will vary with depth. In free pipe, however the casing arrivals will be strong and appear parallel on the log while the formation arrivals will be weak if present due to the attenuation of the waves (12).

C.2 Ultrasonic imaging tool (USIT)

The USI tool consists of a high frequency transducer sending out pulses in the 200 and 700kHZ region. The frequency is adjustable and used frequencies depend on the casing thickness and amplitude decay. The transducer is housed in a rotating sub to achieve full azimuthal coverage with either 36 or 72 measurements at each depth (15).
The high frequency pulses travels from the transducer, through the fluid inside the casing to the casing wall. When the wave reach the wall, some of the energy is refracted through the casing while the majority, due to the large acoustic impedance difference, is reflected back to the transducer. The first returned pulse is used to calculate the internal radius of the casing and the eccentricity of the tool based on the signal transit times. Moreover, the magnitude of this pulse can be used as qualitative indicator of the general condition of the casing surface, such as rugosity (12).
The energy that is refracted through the casing wall travels through the casing until the boundary between the annular material and casing is reached. Once again, some of the energy is reflected and some is refracted based on the acoustic impedance difference. The time for second refracted wave can be used together with speed of sound in steel and the time for the first pulse (reflected at the inner casing wall) to determine the casing thickness.

The process of waves going through acoustic boundaries continues and the reflected portion is measured until the returning signal is too small to be detected. Moreover, in addition to measuring the reflected portion of the initial wave crossing boundaries, the fraction that is reflected inside the pipe will bounce back and forth between the pipe walls, losing energy to the surroundings at every bounce. The situation is illustrated in figure C.2.

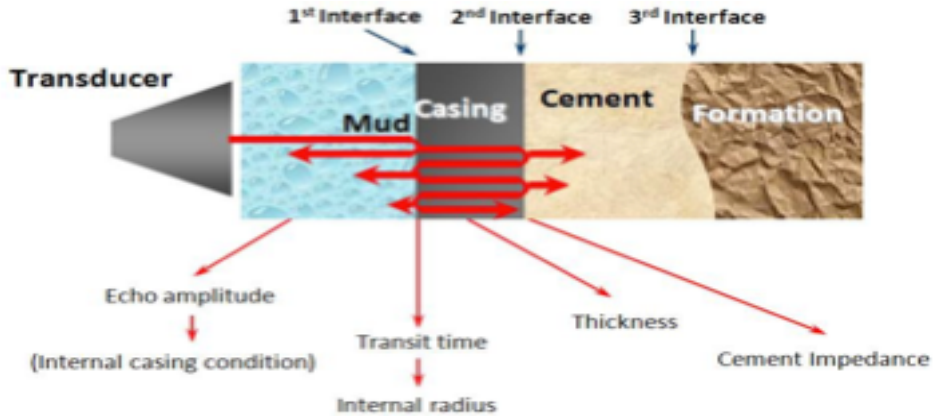

Figure C. 2 Ultra Sonic Imaging tool principle sketch. After (85).

There is found to be an exponential decay of the received echo signals, and from the decay rate information about the acoustic impedance of the annular material can be found. The measured acoustic impedance is then classified as that of a gas if it is less than 0.3MRayl, as liquid if it's between 0.3 and 2.6MRayl, or as a solid bonded material if above 2.6MRayl(12).

To interpret the measured values of the impedance, different colours are used for different values. The colour system is made using impedance thresholds that distinguish between liquids and solids. The colour system and threshold values used can be a bit different from log to log depending on company and cement system used, but it shall be stated in the heading of the log. Typically red indicates that the measured acoustic impedance levels are in the gas region, blue in the liquid region, and brown to black imply solids (12).

Appendix D: Supplementary information for behaviour models and downhole stress states.

D.1 Soil mechanical parameters for plotting

As mentioned in chapter 4 soil mechanical test are typically plotted in a q vs. p', ν vs. p' or in three dimensions in a q,p',v plot.

The q-p' plot essentially displays the maximum shear stress versus the mean effective stress. It is based on the parameter q, usually referred to as generalized shear stress and defined as (36):

$$q = \frac{1}{\sqrt{2}}\sqrt{(\sigma_1' - \sigma_2')^2 + (\sigma_2' - \sigma_3')^2 + (\sigma_1' - \sigma_3')^2} \quad (D.1)$$

And the parameter p' which is identical to the effective mean stress, thus defined as (36):

$$p' = \frac{1}{3}(\sigma_1' + \sigma_2' + \sigma_3') \quad (D.2)$$

Where σ_1', σ_2', $\sigma_3'$is the effective principal stresses as defined by eq. 4.18 with α=1. Under triaxial conditions where $\sigma'_2=\sigma'_3$, these two parameters can be given as (39):

$$q = \sigma_1' - \sigma_3' \quad (D.3)$$

And

$$p' = \frac{1}{3}(\sigma_1' + 2\sigma_3') \quad (D.4)$$

The last parameter frequently used in soil mechanics plotting is the specific volume, ν, which is defined as the total volume (grains+voids) divided by the volume of solid grain, that is (39):

$$\nu = \frac{V_{solid} + V_{void}}{V_{solid}} = 1 + e = \frac{1}{1-\phi} \quad (D.5)$$

Where φ is the porosity, and e is the voids ratio, given as:

$$e = \frac{V_{void}}{V_{solid}} \quad (D.6)$$

D.2 Reasons for abnormal pore pressures

As discussed in section 4.2.3 abnormal pore pressure could occur as the result of numerous mechanisms. Here some of these are discussed.

D.2.1 Rapid sedimentary loading

Rapid sedimentary loading, also referred to as disequilibrium compaction, is commonly observed in shales where the rate of deposition and compaction of sediments is frequently higher that the rate of fluid migration. According to the principle of effective stress, eq. 4.18, to carry the increased vertical load due to the material being buried more and more, either the effective stress or the pore pressure has to increase. In cases where fluid migration is very slow the effective stress will be more or less unaffected during burial, thus the pore pressure will have to carry most of the weight resulting in

abnormal stress. However, as time passes, the overpressure generated by this disequilibrium compaction will dissipate due to fluid movement and a normal pressure regime will be established (86).

D.2.2 Tectonics

During tectonic movements the horizontal stresses could increase significantly and studies shows that there is a strong relationship between tectonic activity and abnormally pressurized areas (45). If the formation has low permeability, assuming an undrained compressional basin, the increase in horizontal stress, σ_H, would lead to a corresponding increase in pore-pressure given by (45):

$$\Delta P_p = A(\Delta\sigma_1 - \Delta\sigma_3) + \Delta\sigma_3 \quad (D.7)$$

Where A is the Skempton's parameter A, describing the pore pressure reaction to the variation in shear stress. σ_1 and σ_3 is the maximum and minimum principal stress respectively.

D.2.3. Changes in the pore fluid

The pressure changes due to pore fluid effects are mainly related to changes in fluid volume because of thermal expansion or other physical or chemical processes. The latter two including hydrocarbon generation, diagenesis, fluid flow and buoyancy (86). Diagenesis may play a significant role in over pressuring shales, as the process of transforming montmorillonite to illite releases free water. The transition is temperature dependent, requiring temperatures in the region of 70-90°C, thus in areas with normal geothermal gradients it will not play a role until depths of 2-3km (36). In reservoir sections, typically hydrocarbon generation will be the main mechanism behind the high pressures often seen. The generation occurs in deep laying source rocks, and the created fluids flows upwards due to buoyancy. Since the flow occurs without much reduction in pressure, the fluids will carry the high pressure with them, thus over pressurizing the reservoir.

Appendix E: Effect of coring on shale sample properties

The only way to obtain direct measurements of rock strength and mechanical parameters is through rock coring. However, since the downhole conditions are very different from atmospheric conditions the properties of rock specimens may be altered during the coring and subsequent handling of the sample.
Initially a typical cored rock sample is in chemical equilibrium with its own pore fluid, located at depth of several kilometres, at an ambient temperatures ranging in the region of 50-150°C (36). When cored the rock sample is brought to atmospheric conditions in terms of stress, pore pressure and temperature. Moreover the sample is also typically exposed to drilling mud, which may or may not penetrate the core or otherwise chemically affect the specimen. Nevertheless, as a consequence of these changing surroundings, the cores will experience external and internal (pore) stress release, thermal effects as well as the potential chemical effects due to the mentioned fluid exposure.
For low permeability rocks, such as shales, due to pore pressure not being equilibrated during coring and retrieval, these changes in surroundings may alter the material properties quite significantly. First of all the lack of pore pressure equilibration will mean that as the core is retrieved it will be more and more over pressured, hence induced tensile failures are likely to occur either on a macroscopic or microscopic scale. The former could completely ruin the sample, while the latter will increase the pore space.
Moreover, due to differences in thermal expansion coefficients and compressibilities, the rock will during the coring process expand more than the pore fluid, hence furthermore increase the porosity of the sample. For shales the increase in void space can either be filled with air from surface or vaporized water (50). The former is obtained simply by the sample being exposed to air at surface, while the vaporisation occur due to a cavitation process. The latter is caused by the fact that shales have a very low permeability, thus downhole fluids are not “allowed” to enter unless they have a very low viscosity. As a consequence, due the increase in void space as the sample is brought closer to surface, the pore pressure will decrease and eventually it may reach such low levels that the pore water vaporizes.
Nevertheless due to these differences in volumetric expansions during coring and retrieval, the shale is likely to be incompletely saturated when it reaches the surface. Due to the extremely small pore sizes in shales, such a diphasic saturation will give rise to extremely high capillary pressures (see chapter 3), making them extremely sensitive to contact with wetting fluids such as water, which will be practically speaking sucked into the sample. This can furthermore lead to a complete disintegration of the sample through tensile fractures, or simply a large swelling like volumetric expansion.